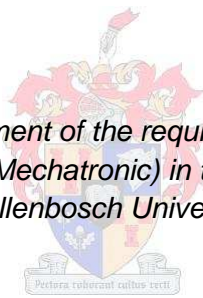


Design of an Impedance Guided Intra-Arterial Catheter

Paul Schwartz

Thesis presented in partial fulfilment of the requirements for the degree of Master of Science in Engineering (Mechatronic) in the Faculty of Engineering at Stellenbosch University



Supervisor: Prof C Scheffer

March 2013

DECLARATION

By submitting this thesis electronically, I declare that the entirety of the work contained therein is my own, original work, that I am the sole author thereof (save to the extent explicitly otherwise stated), that reproduction and publication thereof by Stellenbosch University will not infringe any third party rights and that I have not previously in its entirety or in part submitted it for obtaining any qualification.

Date:

Copyright © 201H Stellenbosch University
All rights reserved

[Type text]

Abstract:

This thesis entails the stages of the development of an arterial catheter capable of being guided by the impedance of human tissue. Such a device would be desired in cases where it is not possible to locate the artery of a patient using anatomical landmarks. This design thus aims to improve the accuracy of first time placement of arterial catheters. The thesis entails the literature study done in order to initiate the development of said device, followed by preliminary concept design and evaluation. The thesis also contains a description of all experimental phases, done on in vitro tissue samples, in vivo samples in living porcine subjects and in vivo samples in living human patients. Experiments were performed to determine if any repeatable noticeable difference in tissue impedance could be identified and utilized in the hope of guiding this device using acquired differences in tissue impedance. The different stages of development for the prototype used in these tests are also described in detail. In addition, the results of the different tests are presented, which prove that there is a significant difference between blood tissue impedance and the surrounding tissue types encountered, allowing for guidance of the proximal tip of the arterial catheter, based on the tissue impedance measured. Finally, the thesis entails a description of further work which could be performed if this concept were to be considered as a marketable product.

Abstrak:

Hierdie tesis behels die verskillende stappe in die ontwerp van 'n kateter wat deur middel van die verskillende impedansie vlakke van biologiese weefsel gelei kan word in die menslike liggaam. Sò 'n toestel sal behulpsaam wees in gevalle waar plasing nie gedoen kan word met die behulp van anatomiese landmerke nie. Hierdie ontwerp mik dus om die akkuraatheid van die plasing van kateters te verbeter. Die tesis behels die literatuur studies benodig om sò 'n toestel te ontwerp, gevolg deur voorlopige konsep ontwerpe en die evaluasie van hierdie konsepte. Die tesis behels ook die verskillende eksperimentele fases van die projek; eksperimente op in vitro weefsel monsters, in vivo diere toetse en in vivo kliniese toetse op menslike weefsel. Al hierdie eksperimente is gedoen om te bepaal of enige herhaalbare, waarneembare verskil in weefsel impedansie geïdentifiseer kan word en dus gebruik word met die hoop om diè teoretiese kateter te lei met behulp van diè verskil in weefsel impedansie. Die verskillende stappe van die ontwerp van die prototipes gebruik in hierdie eksperimente word ook in detail beskryf. Die resultate van die verskillende eksperimente word ook aangebied, wat bewys dat daar 'n beduidende verskil is tussen die impedansie van bloed weefsel en die impedansie van die aanliggende weefsel tipes, wat dus impliseer dat die proksimale punt van die kateter gelei kan word deur die gemete impedansie by die punt van die toestel, gebaseer op die resultate wat gevind is. Laastens behels die tesis ook 'n beskrywing van toekomstige werk wat gedoen kan word indien die konsep ontwikkel word tot 'n bemerkbare produk.

Acknowledgements

The author thanks the following people for their contributions towards this thesis:

Prof C Scheffer, for his general guidance, assistance and advice during the entire course of this project.

Prof PR Fourie, for his insight, advice and enthusiasm regarding several aspects of the project.

Prof AR Coetzee, for his assistance and advice with the animal testing and clinical testing of the project.

Mr. BC Reeve and Ms. EL Cesare for their patience and assistance with the editing of this report.

All BERG (Biomedical Engineering Research Group) colleagues for their advice during the course of this project.

Table of contents

1.	Introduction.....	1
2.	Motivation and scope	3
3.	Literature review.....	3
3.1.	Background	4
3.2.	Impedance measurement.....	6
3.3.	Physiology	8
3.4.	Electrical impedance tomography	10
4.	Design specifications.....	12
5.	Concept design	14
5.1.	Mechanical concepts: housing and handle	14
5.2.	Mechanical concepts: electrode positioning.....	16
5.3.	Electronics concepts: user feedback.....	21
5.4.	Electronics concepts: impedance measurement	22
6.	Preliminary design.....	26
7.	Preliminary experimentation.....	30
7.1.	Experimental design.....	30
7.2.	Experimental procedure	31
7.3.	Results & conclusion	32
8.	Experimental prototype design.....	39
8.1.	Mechanical design.....	39
8.2.	Electronics design	41
9.	Animal testing.....	44
9.1.	Experimental design & protocol	44
9.2.	Experimental procedure	45
9.3.	Results & conclusion	46
10.	Final prototype design.....	50
10.1.	Mechanical design.....	50
10.2.	Electronics design	51
10.3.	Programming.....	57
10.4.	Prototype testing	61
11.	Clinical trials	63
11.1.	Experimental design & protocol	64

11.2.	Experimental procedure	66
11.3.	Results and conclusion	67
12.	Potential future work.....	79
13.	Conclusion.....	81
14.	References	84
	Appendix A: Additional graphs and tables	87
	Appendix B: Extracts from protocol for animal testing	107
	Appendix C: Extracts from protocol for clinical testing.....	110

List of figures

Figure 1-1: Arterial catheter, needle and cannula assembled	1
Figure 1-2: Disassembled arterial catheter, with needle (top) and cannula (bottom)	1
Figure 3-1: Fully disassembled catheter	4
Figure 3-2: Separate-guidewire and Integral-guidewire techniques	6
Figure 3-3: Anterior view of the forearm, showing the radial artery	8
Figure 3-4: Anterior view of the thigh, showing the femoral artery	9
Figure 3-5: Frequency dependence of relative permittivity and specific conductivity of a heterogeneous material such as biological tissue	9
Figure 3-6: Neighbouring method of EIT in a cylindrical volume	11
Figure 3-7: EIT image of heart and lungs model.....	11
Figure 5-1: An early concept showing the handheld device (left), the needle of the arterial catheter (middle) and the cannula (right)	14
Figure 5-2: An early concept diagram, showing 4 electrodes placed on the exterior of the catheter	16
Figure 5-3: Diagram depicting AC voltage source (V_i), voltage over the tissue (V_L), reference resistor (Z_S) and tissue impedance (Z_L)	23
Figure 6-1: Diagram depicting the connections between the electronics, the signal generator and the oscilloscope	27
Figure 6-2: Impedance magnitudess accuracy tests in first prototype.....	28
Figure 6-3: Impedance phase accuracy tests in first prototype	29
Figure 7-1: Arterial wall tissue impedance magnitude box and whisker chart.....	35
Figure 7-2: Arterial wall tissue impedance phase box and whisker chart.....	35
Figure 7-3: Comparative impedance magnitude chart, with tissue type averages and standard deviations	36
Figure 7-4: Comparative impedance phase chart, with tissue type averages and standard deviations	36
Figure 7-5: Tissue impedance magnitude at 30 kHz box and whisker plot	38
Figure 8-1: Silver electrode wound around cannula	40
Figure 8-2: Modified arterial line, disassembled	40
Figure 8-3: Diagram of animal testing setup	41
Figure 8-4: Impedance magnitudes accuracy tests in second prototype.....	42
Figure 8-5: Impedance phase accuracy tests in second prototype	43
Figure 9-1: Modified arterial catheter being inserted into the femoral artery	46
Figure 9-2: Blood impedance magnitude box and whisker plot	47
Figure 9-3: Blood impedance phase box and whisker plot	48

Figure 9-4: Relative frequency distribution chart of impedance magnitudes of blood, muscle and fat tissue.....	48
Figure 10-1: Prototype arterial catheter tip without cannula	51
Figure 10-2: Prototype arterial catheter tip	51
Figure 10-3: Power supply schematic.....	53
Figure 10-4: AC signal generator schematic.....	54
Figure 10-5: Signal converting schematic.....	55
Figure 10-6: Control panel of prototype	57
Figure 10-7: Diagram of components.....	57
Figure 10-8: Flowchart of programming code	58
Figure 10-9: Theoretical case for turning point errors.....	60
Figure 10-10: Demonstration of prototype being used.....	63
Figure 11-1: Theoretical expected model, showing impedance magnitude over time.....	65
Figure 11-2: Graph illustrating the impedance magnitude of time in subject 3.....	68
Figure 11-3: Graph illustrating the impedance magnitude of time in subject 4.....	69
Figure 11-4: Graph illustrating the impedance magnitude of time in subject 6.....	69
Figure 11-5: Graph illustrating the impedance magnitude of time in subject 7.....	70
Figure 11-6: Graph illustrating the impedance magnitude of time in subject 8.....	70
Figure 11-7: Graph illustrating the impedance magnitude of time in subject 9.....	71
Figure 11-8: Graph illustrating the impedance magnitude of time in subject 10.....	71
Figure 11-9: Expected model overlaid with impedance magnitude over time of subject 3	73
Figure 11-10: Expected model overlaid with impedance magnitude over time of subject 4	73
Figure 11-11: Running window average, with different window sizes (a: original, b: $W = 3$, c: $W = 5$, d: $W = 7$)	76
Figure 11-12: Overlaid graph of plots at crossover point	78
Figure A.1-1: Skeletal muscle tissue impedance magnitude box and whisker chart.....	87
Figure A.1-2: Skeletal muscle tissue impedance phase box and whisker chart.....	87
Figure A.1-3: Fat tissue impedance magnitude box and whisker chart.....	88
Figure A.1-4: Fat tissue impedance phase box and whisker chart	88
Figure A.2-1: Skeletal muscle impedance magnitude box and whisker plot.....	89
Figure A.2-2: Skeletal muscle impedance phase box and whisker plot.....	89
Figure A.2-3: Fat impedance magnitude box and whisker plot.....	90
Figure A.2-4: Fat impedance phase box and whisker plot.....	90
Figure A.3-1: 0,5 k Ω , 0° Tests impedance magnitude error graph	91
Figure A.3-2: 0,5 k Ω , 0° Tests impedance phase error graph	91

Figure A.3-3: 5 k Ω , 0° Tests impedance magnitude error graph	92
Figure A.3-4: 5 k Ω , 0° Tests impedance phase error graph	92
Figure A.3-5: 10 k Ω , 0° Tests impedance magnitude error graph	93
Figure A.3-6: 10 k Ω , 0° Tests impedance phase error graph	93
Figure A.3-7: 0,5 k Ω , 30° Tests impedance magnitude error graph	94
Figure A.3-8: 0,5 k Ω , 30° Tests impedance phase error graph	94
Figure A.3-9: 5 k Ω , 30° Tests impedance magnitude error graph	95
Figure A.3-10: 5 k Ω , 30° Tests impedance phase error graph	95
Figure A.3-11: 10 k Ω , 30° Tests impedance magnitude error graph	96
Figure A.3-12: 10 k Ω , 30° Tests impedance phase error graph	96
Figure A.3-13: 0,5 k Ω , 60° Tests impedance magnitude error graph	97
Figure A.3-14: 0,5 k Ω , 60° Tests impedance phase error graph	97
Figure A.3-15: 5 k Ω , 60° Tests impedance magnitude error graph	98
Figure A.3-16: 5 k Ω , 60° Tests impedance phase error graph	98
Figure A.3-17: 10 k Ω , 60° Tests impedance magnitude error graph	99
Figure A.3-18: 10 k Ω , 60° Tests impedance phase error graph	99
Figure A.4-1: Patient 3 impedance phase over time.....	100
Figure A.4-2: Patient 4 impedance phase over time.....	100
Figure A.4-3: Patient 6 impedance phase over time.....	101
Figure A.4-4: Patient 7 impedance phase over time.....	101
Figure A.4-5: Patient 8 impedance phase over time.....	102
Figure A.4-6: Patient 9 impedance phase over time.....	102
Figure A.4-7: Patient 10 impedance phase over time.....	103

List of tables

Table 3-1: Resistivity of biological tissue in humans and in cows	10
Table 5-1: Advantages and disadvantages of housing and handle concepts	15
Table 5-2: Advantages and disadvantages of electrode placement concepts.....	18
Table 5-3: Ideal electrode placement concepts in different scenarios.....	20
Table 5-4: Advantages and disadvantages of different feedback concepts	21
Table 5-5: Advantages and disadvantages of impedance measuring concepts	25
Table 7-1: Expected resistance values based on theory	31
Table 7-2: Averages and standard deviations of tissue impedance magnitude at different frequencies.....	33
Table 7-3: Averages and standard deviations of tissue impedance phase at different frequencies.....	34
Table 10-1: Values used for testing of final prototype.....	64
Table 11-1: Extract of combined probability table	75
Table 12-1: ATmega2560 package dimensions	79
Table A.4-1: Probability table of $ Z _T < Z _H$	104
Table A.4-2: Probability table of $ Z _T > Z _L$	105
Table A.4-3: Combined probability table, including average probability	106

Nomenclature

[C]	Capacitance
[C _R]	Real capacitor value used for testing
[C _T]	Theoretical capacitor value needed for testing
[F]	Frequency
[F _{Cal}]	Frequency calibration factor
[I]	Current
[R]	Resistance
[R _R]	Real resistor value used for testing
[R _T]	Theoretical resistor value needed for testing
[SF _Z]	Impedance magnitude scaling factor
[SF _θ]	Impedance phase scaling factor
[V]	Voltage
[V _L]	Voltage over load
[V _i]	Total voltage over system
[V _{xmax}]	Maximum voltage for calibration on channel x (x is either 0 or 1)
[V _{xmin}]	Minimum voltage for calibration on channel x (x is either 0 or 1)
[X]	Reactance
[Z]	Impedance
[Z _L]	Load impedance
[Z _S]	System reference impedance
[Z]	Impedance magnitude
[Z _{EEPROM}]	Impedance magnitude saved to EEPROM
[Z _{max}]	Max impedance magnitude saved
[Z _T]	Threshold between high level impedance magnitudes and low level impedance magnitudes
[Z _H]	High level impedance magnitude values
[Z _L]	Low level impedance magnitude values

$[W]$	Window width in running average window algorithm
$[\theta]$	Phase angle
$[\theta_{\text{EEPROM}}]$	Phase saved to EEPROM
$[\theta_{\text{max}}]$	Max impedance phase saved
$[\theta_{\text{NP}}]$	New, corrected phase shift
$[\theta_{\text{P}}]$	Phase shift
$[\theta_{\text{P}}]$	Previous phase shift measurement
$[\rho]$	Resistivity
$[\sigma]$	Conductivity
$[\sigma_{\text{s}}]$	Standard deviation
$[\tau]$	Period

1. Introduction

In the medical industry, intra-arterial catheters are widely used apparatus that have become essential to medical practitioners worldwide. Intra-arterial catheters (more commonly known as arterial catheters, arterial lines or A-lines) are most commonly used in intensive care procedures and anaesthesia. They are flexible catheters which are inserted into patients' arteries (usually the radial-, brachial-, femoral-, ulnar- or dorsalis pedis-arteries [1]). They are most commonly used in order to measure blood pressure and oxygen saturation in real time during anaesthesia [2]. The apparatus generally consists of a lubricated stainless steel hypodermic needle enveloped by a thin flexible tube (known as a cannula), which are not permanently fixed together. Figure 1-1 illustrates the two main components of a typical arterial catheter, with the needle and cannula assembled. It also illustrates the location of the proximal end and the distal end of the arterial catheter.



Figure 1-1: Arterial catheter, needle and cannula assembled

Figure 1-2 below shows the arterial catheter from Figure 1.1, but now disassembled to show the cannula, the needle and their relation to each other.



Figure 1-2: Disassembled arterial catheter, with needle (top) and cannula (bottom)

In general, the needle portion is removed after the entire arterial catheter has been successfully placed inside of the lumen of the patient's artery, while the cannula remains placed inside the artery. The placement of the cannula inside the artery of a patient allows open access to the patient's bloodstream and thus allows the arterial catheter to be used for multiple purposes, including real time blood pressure and oxygen saturation measurement, obtaining arterial blood gas measurements, frequent blood samples and monitoring the response of vasoactive drugs [1-3]. The introduction of medical tools used inside the patient's arteries (such as the tools required to install coronary artery stents) can also be achieved through the catheterization of certain arteries or veins [4].

In general, the placement of an arterial catheter is a simple procedure which is performed regularly by trained professionals. However, there are cases where there are difficulties with locating an artery. This can be caused by a variety of conditions, such as collapsed arteries or low blood pressure. In these cases, the insertion of arterial lines can be traumatic for the patient if the insertion is done incorrectly.

In situations like these, it would be ideal to have a device which could indicate where the proximal tip of the arterial catheter is and display feedback to the personnel administering the arterial catheter. This way, the personnel would know where the needle is within the patient's body (at the area of insertion) and would indicate when the proximal end is fully located inside the lumen of the artery, thus guiding the insertion process.

With this idea in mind, Prof PR Fourie approached the University of Stellenbosch's Biomedical Engineering Research Group, South Africa, with the request for such a device to be investigated. Additionally, he proposed that the device could utilize the difference in electrical impedance of different human tissue as a means to determine where the proximal end of arterial catheter is located. This project is thus based on the design of such an impedance guided intra-arterial catheter.

This report contains the motivation and the scope for the project, followed by a section dedicated to the research that has been done in order to develop the device. The report includes the specifications that were received and generated, the early concept generation and the evaluation of said concepts. This is followed by incremental design advancements and experimental phases (preliminary in vitro tissue sample testing, in vivo live animal testing and in vivo live human testing), with suggestions of changes which can be made in order to further the design into a marketable product thereafter and finally a conclusion, summarizing the thesis.

2. Motivation and scope

As mentioned earlier, under certain circumstances the insertion of an arterial catheter can be difficult, due to the lack of a visible artery or biological landmarks. In cases such as these, a hypothetical device that could determine where the proximal end of the arterial catheter is and which tissue surrounds it could be of value, as it would be capable of guiding the placement of the arterial catheter. A guided arterial line would allow for more accurate placement and improve the chances of successful first time placement, reducing human error and potential patient discomfort. In current practice, ultrasonic guidance of arterial catheters is used in cases when blind placement is insufficient, but the equipment required for ultrasonic placement is both cumbersome and expensive. It would thus be ideal to have a cheaper, simpler form of guidance for the placement of arterial catheters.

If the device were to be highly successful, it could make it possible for lesser skilled clinical personnel to effectively and safely use it and thus allow for arterial lines to be placed in circumstances when experienced medical doctors are unavailable. In addition to this, it would also reduce trauma caused by repeated insertions of arterial lines, by reducing the chances of an unsuccessful placement.

The scope of the thesis entails the research and development of an impedance guided intra-arterial catheter, starting with research required for the project, developing and evaluating concepts, early prototype designs, experimental phases and ending in the final prototype to be tested on humans for the final proof of concept.

The goals of this project are thus to conceptualize a design capable of measuring the impedance inside of the human body when an arterial catheter is being placed. In addition to this, to conclude whether or not it is possible to differentiate between different types of living human tissue based only on its impedance is another goal. This leads to the final goal: to determine whether it is possible to guide an arterial catheter based on this difference in tissue impedance. If this is the case, this thesis would lay down the ground work for a cost-effective alternative form of guidance for arterial catheters.

3. Literature review

An overview of the literature review is presented here. It is divided into the following sections:

- Background
- Impedance measurement
- Physiology

- Electrical impedance tomography (EIT)

The first section highlights the required knowledge of arterial catheters for the purpose of this thesis, thus dealing with information on the structure of these arterial catheters, the materials they are composed of, existing methods of guidance and methods of insertion. The second section handles the measurement of electrical impedance, including calculations required to measure an unknown impedance and what is required to do so, as well as investigating the effects of introducing the electrical signal required to the human body. The third section gives a brief overview of the required knowledge of human physiology for this project and thus includes the types of tissue which could be encountered, as well as some known electrical properties of human tissue. The fourth section discusses electrical impedance tomography, a current technique where electrical impedance is used for medical diagnostics.

3.1. Background

As mentioned in Chapter 1, arterial catheters consist of two main parts: the pre-lubricated needle and the cannula. The additional parts, the filter, the case and the cap case are found in most commercially available arterial lines, as illustrated in Figure 3-1.

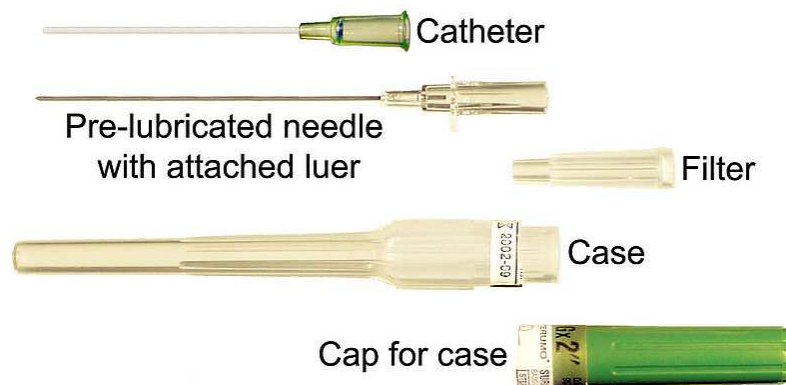


Figure 3-1: Fully disassembled catheter (William Rafti, April 2005, 'Catheter disassembled')

When introduced to a patient's body, the catheter, needle and filter are all assembled, while the case and case cap are removed prior to insertion. When successfully placed into the artery, arterial pulsatile blood will flow through the needle (granted that the patient has a normal to high blood pressure), into the luer (a chamber at the distal end of the device). In cases where the patient has a low blood pressure, this pulsatile blood return may be very slow to appear.

Due to the nature of arterial catheters, biocompatibility of the materials used is highly important, as the materials need to be exposed to the human tissue. These materials must be inert so the human body has no adverse immunological reaction to foreign matter [5]. The materials used for the cannula are generally silicones, silicone composites, polyvinyl chloride (PVC), latex rubber [6], teflon or polyethylene [7], while the needle is made from stainless steel alloys and usually lubricated with silicone to permit easier passage into the cannula [8].

Traditionally, placement of arterial catheters is done either with the aid of ultrasonic guidance [9,10] or with no form of guidance ('blind' placement), utilizing anatomical landmarks [2] to determine where to place the arterial catheter. Ultrasonic guidance is typically used on patients when vessel palpitation is difficult to locate (due to obesity or small vessels) [11]. The improved success rate of ultrasonic guidance over blind placement has been tested and has shown a 71% increased success rate of first time arterial catheterization [12]. The equipment used for ultrasonic guidance are 'Doppler-Smart' needles, which cost \$40-70 per needle¹ [13], in comparison to standard arterial catheters which cost roughly \$5 per needle (price obtained from conversation with Prof AR Coetzee, April 2012). Additionally, the ultrasound machines cost \$17,000-140,000 (prices obtained from Absolute Medical Equipment, www.absolutmed.com, July 2012). Ultimately, the implementation of ultrasonic guidance is expensive, both in terms of the initial investment of the machines and in terms of the continuous expenditures on the specific needles and equipment maintenance.

There are three different methods of arterial catheterization, namely: separate-guidewire, integral-guidewire and direct puncture.

The separate-guidewire technique (also known as the Seldinger technique) utilizes an arterial catheter which is placed and advanced into the body until a pulsatile blood return is observed. Once this happens, the needle is removed while the cannula remains in the artery. A guidewire is then advanced through the cannula, allowing for the cannula to be advanced deeper into the artery, after which the guidewire is removed [14, 15].

The integral-guidewire technique utilizes a similar principle as the separate-guidewire technique, except the guidewire is inseparable from the arterial catheter. The guidewire is placed within the needle of the arterial catheter and once a pulsatile blood return is observed, the guidewire is advanced through the needle, into the artery, by means of an advancement tab on the unit. The cannula is then advanced deeper into the artery, after which the guide wire and the needle are removed [16]. The differences between the separate-guidewire technique and the integral guidewire technique can be seen in Figure 3-2.

The direct puncture technique utilizes an arterial catheter without any guidewire. The unit is placed and advanced into the body until a pulsatile

¹ Price as of 1998. More recent pricing could not be found.

blood return is observed. Once the blood return is observed, the cannula is advanced by hand and the needle is removed [17, 18].

In all three of these techniques, the arterial catheter is placed at an angle of between 30° and 45°, using the administrator's dominant hand, while the nondominant hand gently palpates the patient's artery. The return of pulsatile blood is a visual acknowledgement that the needle has breached the lumen of the artery [18]. However, it does not indicate that the cannula has entered the lumen, which is why it needs to be advanced with or without the aid of a guidewire.

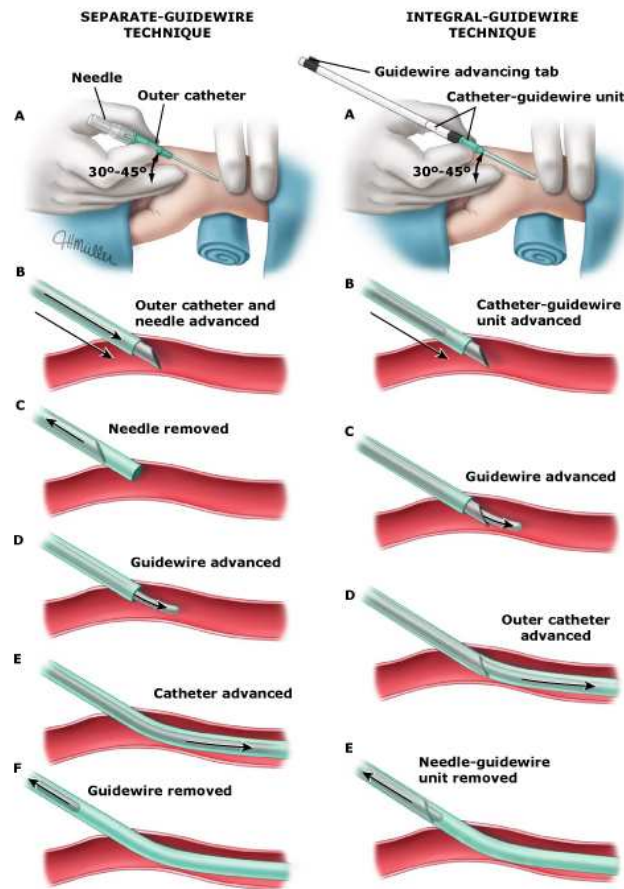


Figure 3-2: Separate-guidewire and integral-guidewire techniques [11]

3.2. Impedance measurement

Electrical impedance is the measure of the resistance opposing an alternating current in a system when an alternating current (AC) is applied [19]. It can be seen as the complex version of direct current (DC) resistance. It is described in eq. 3-1:

$$Z = R + iX \quad (3-1)$$

Where R is the real component, X is the imaginary component and i is the imaginary number (the square root of negative one). Z can also be written as:

$$Z = |Z|\angle\theta \quad (3-2)$$

Where θ is

$$\theta = \tan^{-1}\left(\frac{X}{R}\right) \quad (3-3)$$

And $|Z|$ is

$$|Z| = \sqrt{R^2 + X^2} \quad (3-4)$$

Utilizing the above properties, Ohm's Law and basic circuit analysis, an unknown impedance can be measured and calculated in a system with known parameters and an AC voltage used to excite the impedance.

Such calculations require the knowledge of how complex division works. Complex division is done by multiplying the numerator and the denominator by the complex conjugate of the denominator. In the case below

$$Z = \frac{a+bi}{c+di} \quad (3-5)$$

the complex conjugate of the denominator is

$$\overline{c+di} = c - di \quad (3-6)$$

and thus, from eq. 3-5 and eq. 3-6

$$Z = \frac{(a+bi)(c-di)}{(c+di)(c-di)} \quad (3-7)$$

Solving the above leads to

$$Z = \frac{(ac+bd)+i(bc-ad)}{c^2+d^2} \quad (3-8)$$

Thus, eq. 3-8 is required to calculate measured impedance.

During impedance measurements of tissue, a voltage will have to be applied over the tissue. This, in turn, will lead to an electrical current passing through tissue. These applied currents could be dangerous to biological tissue in living organisms and could possibly lead to death. Currents of 100 - 300 mA result in myocardial fibrillation [20] (which can be fatal), currents above 15 mA will cause the loss of muscle control, currents above 5 mA are perceived as painful and currents below 1 mA are below the perception threshold in humans [21]. It would thus only be acceptable if the currents subjected to the patients are below 5 mA at all times.

3.3. Physiology

The expected types of tissue that could be encountered by the proximal tip of an arterial catheter are [22, 23]:

- Skin
 - Epidermis
 - Dermis
 - Subcutaneous tissue
- Skeletal muscle
- Fat
- Arterial wall
 - Tunica externa
 - Tunica media
 - Tunica intima
- Arterial blood

During a flawless insertion, the arterial catheter should not be expected to encounter any skeletal muscle. However, in cases where the catheter is not placed accurately, it is possible to encounter skeletal muscle tissue. Figures 3-3 and 3-4 show the positioning of the radial artery in the forearm and the femoral artery in the leg, respectively. Typical insertion for the radial artery is done near the wrist, while insertion in the femoral artery is done near the groin, both in areas where the artery is not covered by skeletal muscle.

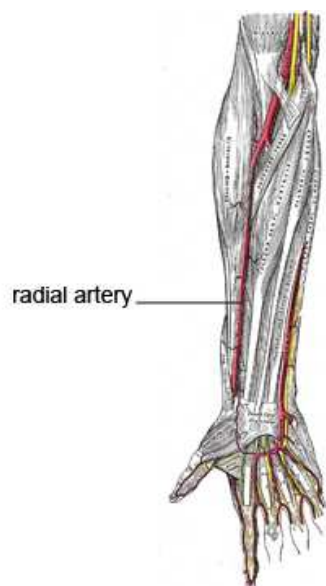


Figure 3-3: Anterior view of the forearm, showing the radial artery (Image adapted from [22])

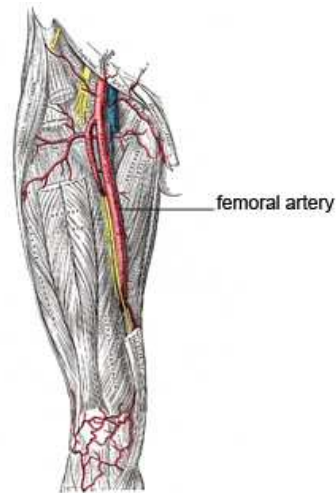


Figure 3-4: Anterior view of the upper thigh, showing the femoral artery (Image adapted from [22])

Concerning the electrical qualities of biological tissue, it has been shown to have frequency dependant rising conductivities [24, 25], as seen in Figure 3-5 below. This figure illustrates both the relative permittivity and the specific conductivity of biological tissue as a function of the electrical frequency applied.

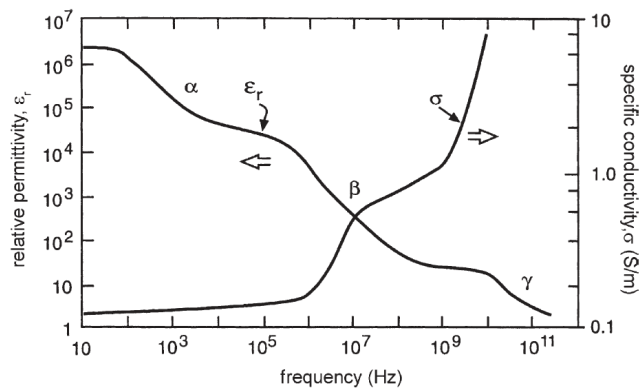


Figure 3-5: Frequency dependence of relative permittivity and specific conductivity of a heterogeneous material such as biological tissue [24]

Furthermore, with the knowledge that conductivity is inversely proportional to resistivity, or:

$$\sigma = \frac{1}{\rho} \quad (3-9)$$

As well as knowledge of Pouillet's Law

$$R = \rho \frac{l}{Area} \quad (3-10)$$

and combining eq. 3-9 and eq. 3-10, to give

$$R = \frac{l}{\sigma \cdot Area} \quad (3-11)$$

it can thus be seen that the resistance of biological tissue should decrease at higher frequencies, based on the increase in conductivity with frequency and the inverse proportionality of resistance and conductivity. This increase in resistance should be most apparent after roughly 10 kHz, based on Figure 3-5. This behaviour is expected, as it is understood that current passes easier through biological tissue at higher frequencies, thus causing lower tissue impedances at higher frequencies [26].

Tests have been conducted, which illustrate the resistivity of biological tissue. Using this data, the measured impedance values can be compared, to verify the functionality of the device designed. Table 3-1 below indicates the resistivity levels of different biological tissue [27].

Table 3-1: Resistivity of biological tissue in humans and in cows [27]

	Resistivity in human (Ω-cm)	Resistivity in cows (Ω-cm)
Blood	137 - 363	81 - 272
Skeletal Muscle	240 (Longitudinal) 675 (Transverse)	300 (Longitudinal) 700 (Transverse)
Fat	1100 - 2180	2000 - 3850

From the above table it can be seen that human and mammalian tissue resistivity seems to be similar. This would imply that performing tests on animals would be accurate for this thesis. Tests were later performed on porcine specimens instead of bovine, as it was simpler to obtain these specimens. The assumption was made that the difference between bovine and porcine specimens would not be of such a magnitude that it would hinder the research.

3.4. Electrical impedance tomography

Electrical impedance tomography (EIT) is a medical imaging method used to visualize sections of the human anatomy. In this method, an array of electrodes are attached around the circumference of the section to be imaged. Electric current is applied between two adjacent electrodes, while voltage is measured in the remaining electrode pairs. This is repeated by applying the current to different adjacent electrodes and measuring the voltage over the new remaining electrode pairs. Using these measurements and several reconstruction algorithms, visualizations of the changes in resistivity through the section being imaged can be made [28 - 30].

There are various methods of performing EIT, governed by the order and position in which current is applied to the section as well as in the order and position in which voltage measurements are taken. One such method, the Neighbouring Method [28], is shown in Figure 3-6.

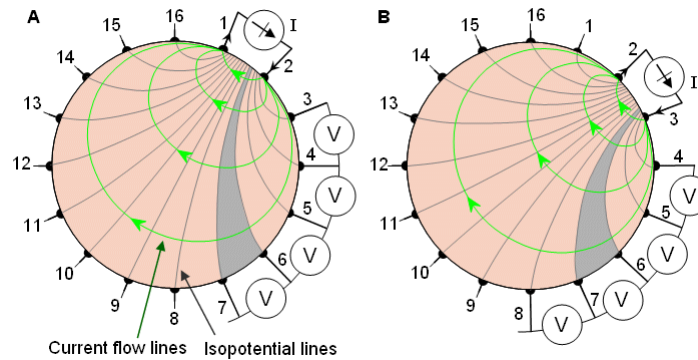


Figure 3-6: Neighbouring method of EIT in a cylindrical volume [28]

Figure 3-6 illustrates two steps in the neighbouring method. In the first step, seen in Figure 3-6a, current is applied over electrodes 1 and 2, while voltages are measured between electrode pairs 3 to 4, 4 to 5, up to and including 15 to 16. Each of these measurements represent the impedance in the area between the voltage measuring electrodes and the current source (as seen in the grey area between electrodes 6 and 7 in Figure 3-6). In the second step, as seen in Figure 3-6b, current is applied over electrodes 2 and 3, while the voltages are measured between electrode pairs 4 to 5, 5 to 6, up to and including 16 to 1. This process is repeated n times (where n is the amount of electrodes) and each step produces $n - 2$ results.

Once all of these measurements have been taken, reconstruction algorithms are used to construct an image of the electrical impedance distribution across the cross section of the anatomy. An example of such an image can be seen in Figure 3-7.

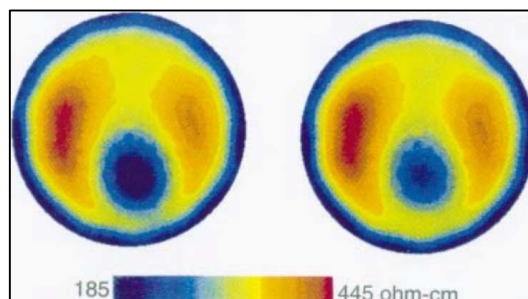


Figure 3-7: EIT image of heart and lungs model [29]

Figure 3-7 illustrates two experimental images generated using EIT, both from a test tank which contained a model heart and two model lungs. The tank itself was filled with salt water, while the lung and heart models were made from agar, using different quantities of salt to control the resistivity of the models. In the second image, a smaller sized heart model was used, to simulate the changes in volume of the heart during the different stages of the heart's cycle [29].

EIT poses several problems and constraints which need to be overcome before it can be considered as a clinically useful device. The reconstruction problem (described in detail in the work done by M. Cheney, D. Isaacson and J.C. Newell [29]) is both ill-posed and nonlinear, which makes the development of fast, accurate algorithms difficult. The device also requires a large amount of electrodes and rapid measurements, in order to obtain a high level of accuracy. Even with a large amount of electrodes, the complications caused by the reconstruction problem make it unlikely that EIT will have a resolution similar to CT or MRI. On the other hand, EIT is a cheaper, non-invasive method of imaging and presents information about the electrical properties of biological tissue, which cannot be obtained with CT or MRI [29, 30].

4. Design specifications

In order for the impedance guided intra-arterial catheter to achieve the goals mentioned earlier, it will have to adhere to certain specifications. These specifications were developed by combining the specifications mentioned by two medical practitioners (Prof PR Fourie, paediatrician, and Prof AR Coetzee, anaesthesiologist) and combining their specifications with those generated with the aid of the research done. This chapter shows the specifications by Prof Fourie, followed by the specifications from Prof Coetzee and then illustrates the engineering specifications that were derived.

From the literature study done, it can be seen that the device requires at least two electrodes for the measuring of impedance and an AC signal which can excite the impedance in order to measure it. It also requires equipment capable of measuring this excited impedance, as well as equipment that can analyse the gathered data and either store it or present the appropriate feedback.

The device requested by Prof PR Fourie is an arterial catheter that is guided by the impedance of human tissue at the proximal tip of the needle. The device needs a simple, understandable form of feedback to the operator of the device, in an easy to read location. The device must be affordable and easy to manufacture. The device has to be safe to use and thus all parts that will be inside the patient need to be biologically compatible. Furthermore, if any parts are to be reused, they need to be constructed and assembled in such a way that they are easy to clean, with a high surface finish on the exterior as to avoid dirt and coagulated blood build-up. In order for the device to be used and tested on

humans, the final prototype must run on batteries and not electricity from a wall socket.

After consulting Prof AR Coetzee, the head of anaesthesiology and critical care of Tygerberg Hospital, South Africa, a few further specifications were added. Firstly, the centre of gravity of the handheld portion of the device must be at the proximal end of the operator's fingers, allowing the needle's tip to naturally lean towards the patient's skin. Secondly, the bottom part of the handheld device needs to be as flat as possible, as to not obstruct the movement of the device when the arterial line advanced into the body at the angle of insertion.

From the above mentioned specifications from the two doctors and the literature, the following engineering specifications were generated:

Electronic specifications of device:

- Final prototype must be battery powered
- Must generate an AC signal to excite impedance
- Must have either an integrated circuit (IC) capable of measuring impedances or an analogue to digital (A/D) converter to measure the voltages in order to calculate the impedances
- Must have a microprocessor to evaluate data received and compare it to pre-set known tissue impedance values
- Must have a visual form of feedback, ideally small and simple
- The current applied to the human tissue needs to be at a safe level (below 5 mA at all times) and voltage regulators need to be included to prevent any current leakages

Mechanical specifications of device:

- Device must be modular, allowing the electronics to be reused, while the needle and cannula are disposed of after use
- Handheld device should be small and comfortable to hold
- Centre of gravity in the handheld device needs to be at the proximal end of the user's fingertips
- At least two conductive points at the tip of the needle, to measure voltages at the proximal tip
- All parts and modifications to the needle and cannula need to be biologically compatible
- Exterior of the device needs to have a smooth surface finish

The above specifications were those used when designing the final prototype of the device, however, not all specifications were used in early testing of the prototypes.

5. Concept design

Utilizing the specifications mentioned in the previous chapter, a set of concepts were generated. The concepts were divided into four sections. The first two sections are dedicated to the mechanical concepts and the last two sections to the electronic concepts. The mechanical concepts encompass the enclosure for the electronics (along with the handle for the device) and the positioning and fixing of the electrodes on the cannula. The electronics concepts involve the method in which the impedance would be measured as well as the method of feedback to the user. In each of the following subsections, the concepts are first discussed and then compared and evaluated.

5.1. Mechanical concepts: housing and handle

Below are two concepts generated, based on the housing of the electronics, as well as the handle for the device. These concepts were generated as a whole, due to the ability to integrate the two concepts as one design.

The first concept of the enclosure is a handheld modular device, which can attach to the end of an arterial catheter, combining the electronics enclosure with the handle for the device. Embedded on the top section of the device is the preferred method of feedback. Inside the device is all the electronics required for the device to operate. The electronics are positioned in such a way that the centre of gravity is located towards the proximal side of the device. An early concept diagram can be seen in Figure 5-1.

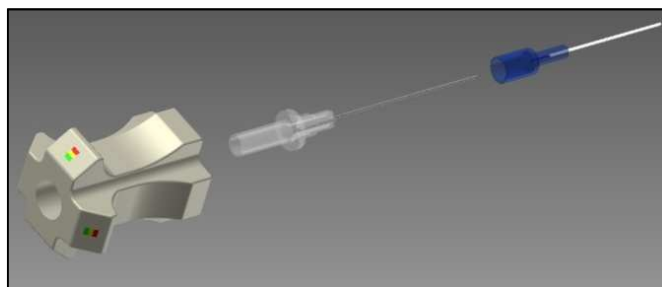


Figure 5-1: An early concept showing the handheld device (left), the needle of the arterial catheter (middle) and the cannula (right)

The second concept for the enclosure is a small enclosure separate from the handle. This implies that the enclosure either has to communicate wired or

wirelessly with the electrodes at the end of the arterial catheter. This means that a separate handle has to be developed and then attached to the end of the arterial catheter. The feedback methods can thus be placed in either the separate enclosure or inside the handle of the device. Though a handle on the device is not entirely necessary when there is a separate enclosure housing all of the electronics, it will serve as a protected interface point for the electrodes to connect with the electronics from the separate housing. However, if wireless communication methods are used, the handheld device will be required as to contain and protect the wireless communication apparel as well as the battery power required for said apparel.

For the above-mentioned concepts, the following table of advantages and disadvantages was constructed.

Table 5-1: Advantages and disadvantages of housing and handle concepts

	Advantages	Disadvantages
Single handle, housing all electronics	Smallest design Least cumbersome Less parts, should be easier to manufacture	Electronics will need to be kept very small Unable to use larger batteries
Separate external enclosure and handle (wired communication)	Allows for larger batteries to be used Doesn't require the electronics to be minimized as much Simpler design than wireless	Most cumbersome design Wires could hinder insertion
Separate external enclosure and handle (wireless communication)	Allows for larger batteries to be used Less cumbersome than wired	Will require batteries and wireless apparatuses in both handle and separate enclosure Requires minimization of electronics in order for wireless module and batteries to fit in handle, making the external housing redundant Wireless communication could receive interference from other medical devices

From Table 5-1, it can be seen that the wireless communication separate enclosure concept is the least ideal, offering few advantages above the single handle housing concept, aside from the option for larger batteries. The electrical interference from ECGs and diathermies could interfere with measurements, thus lowering the accuracy of the device, which is unacceptable. The single handle housing concept boasts impressive advantages which comply with the specifications set out in the previous chapter, while requiring very small electronics designs in order to fit everything in this housing. Granted that the electronic components can be fit in such a small space, this concept would be ideal. However, if this is not possible, the separate wired external enclosure concept would then be used.

5.2. Mechanical concepts: electrode positioning

The actual arterial catheter will require certain modifications, to accommodate the need for electrodes required to take measurements. Below are two concepts (and two deviations from these concepts), surrounding the placement, positioning, fixing and insulation of these electrodes.

The first concept can be seen in Figure 5-2. Embedded into the cannula are n electrodes, extending all the way across the length (either straight or wrapped helically) of the cannula, equally spaced apart. These electrodes are exposed at the proximal end of the cannula and are thus conductive at the tip. The electrodes are also exposed at the distal end, to be connected to the electronics inside the housing or the handle. Another electrode is coupled to the hypodermic needle of the arterial catheter, which forms the grounding electrode for the system.

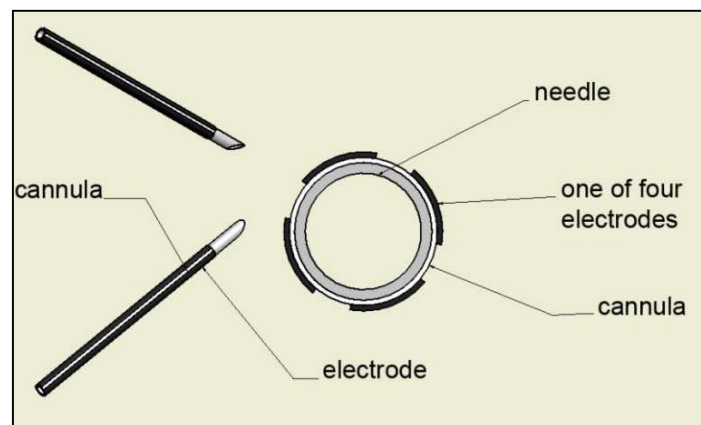


Figure 5-2: An early concept diagram, showing 4 electrodes placed on the exterior of the catheter

The n electrodes on the cannula, equally spaced around the circumference of the cannula, allow for n sets of measurements in n directions for increased accuracy and more information about the variety of tissue surrounding the tip. Each of the outer electrodes, along with the grounded needle allow for the measurement of the voltage over the tissue at the tip of the arterial catheter. This placement of the electrodes is similar to that in the work done by Takafumi, *et al.* [31], but used for a different purpose. Placing these electrodes on the exterior of the cannula will add thickness to the exterior of the catheter, which is not ideal. Introducing these electrodes during the cannulas manufacturing process will enable the electrodes to be embedded inside the cannula, with the only exposed points at the tapered proximal end and at the distal end. This will result in the added thickness being avoided and a more acceptable design being achieved.

A minor deviation from the above concept would be to not use the hypodermic needle as a grounding electrode and instead dedicate one of the electrodes on the catheter as a grounding electrode. This would allow for measurements to be taken independently from the hypodermic needle, allowing for more flexibility in terms of placement techniques (as described in Chapter 3.1).

The second concept is to place all of the electrodes in or around the hypodermic needle. The main advantages of this concept is that there would be no added thickness to the catheter, which would not hinder insertion, as well as the advantage of having all electrodes removed along with the needle, instead of them remaining in the patient's artery for the same duration as the catheter.

One way in which to achieve this is to embed insulated electrodes onto the outer surface of the hypodermic needle and remove the insulation at the proximal and distal tips, allowing for conductance (and thus, the ability to take measurements) at the tip of the needle. Another way (which was employed at a later stage in this thesis) is to use an insulated wire and feed it through the inner hollow area of the hypodermic needle and loop it 180° back at the proximal tip and then feed it back to the distal portion of the catheter, through the area between the needle and the cannula of the catheter. Removing the insulation on this wire at the proximal tip will thus allow this wire to serve as an electrode, along with the needle, enabling two electrodes in the device. A picture of a prototype of this concept can be seen in Figures 10-1 and 10-2.

Using the above mentioned concepts, the Table 5-2 was generated to compare the advantages and disadvantages of the concepts.

Table 5-2: Advantages and disadvantages of electrode placement concepts

	Advantages	Disadvantages
Electrodes on cannula of catheter, needle as grounding electrode	<p>Easiest to manufacture professionally and easy to manufacture by hand for prototyping purposes (in the case of one electrode on the exterior)</p> <p>Capability of having multi-directional measurements</p> <p>Easiest to insulate</p>	<p>Could add thickness to the catheter if not professionally manufactured</p> <p>Electrodes present in bloodstream for the duration of catheterization</p> <p>Measurements cannot be taken if needle is withdrawn</p>
Electrodes on cannula, including grounding electrode	<p>Easy to manufacture professionally</p> <p>Capable of multi-directional measurements</p> <p>Capable of taking measurements independent of the position of the needle, allowing more flexibility in terms of insertion techniques</p> <p>Easy to insulate</p>	<p>Difficult to place multiple electrodes on the exterior by hand for prototypes</p> <p>Electrodes present in bloodstream for the duration of catheterization</p> <p>Could add thickness to the catheter if not professionally manufactured</p>
Electrodes on the exterior of the hypodermic needle	<p>All electrodes are removed after successful placement</p> <p>No added thickness to the catheter material</p>	<p>Difficult to fix and insulate electrodes on the hypodermic needle</p> <p>Difficult to manufacture for prototyping purposes</p> <p>Measurements cannot be taken if needle is withdrawn, restricting insertion techniques that can be used</p> <p>Tightens the interface between the needle and the catheter</p>

<p>Electrode fed through central channel of the needle and back between needle and cannula</p>	<p>All electrodes are removed after successful placement</p> <p>No added thickness to the catheter material</p> <p>Easy to manufacture by hand for prototyping purposes</p> <p>No fixing of electrodes to surfaces, thus no adhesives required</p>	<p>Measurements cannot be taken if needle is withdrawn, restricting insertion techniques that can be used</p> <p>Tightens the interface between the needle and the catheter, causing the removal of the hypodermic needle from the catheter to be less smooth</p> <p>Less open space in the open channel in the needle, increasing resistance for the pulsatile blood return</p>
---	--	--

From Table 5-2, it can be seen that placing all of the electrodes on the exterior of the hypodermic needle is the least ideal concept, as it offers very few advantages in comparison to its competitors, while having disadvantages that could cripple the device's reliability. Additionally, the difficulty in placing electrodes on the stainless steel needle would make manufacturing difficult and prototyping even more difficult.

It would appear that from a prototyping point of view, the concept with the electrode fed through the central channel of the needle would be the safest to implement, as it requires no form of adhesive to fix electrodes to the surface of either the catheter or the needle, while also removing all of the components added to the arterial catheter after successful placement. This, however, comes at the price of some restrictions in terms of operation (as mentioned earlier), making this concept less ideal for a mass produced marketable product.

The concept with the electrodes on the exterior of the cannula of the catheter with the needle serving as the grounding electrode would function better as a design used in prototypes, allowing for a simple and cheap method of testing and taking measurements, at the expense of some restrictions in operation. This concept is easier to implement than the previously mentioned concept, but at the cost of long-term safety. Unlike the 'electrode through the central channel' concept, utilizing this concept during in vivo human testing would expose the human bloodstream to the electrodes for the entire duration of catheterization and if the electrodes were fixed with a form of adhesive (which would be the case if this concept was prototyped), the patient's bloodstream would also be exposed to this adhesive. The risk of the electrodes breaking and the adhesive affecting the bloodstream are risks that cannot be taken. Thus, in shorter tests when measurements of select tissue types need to be done, this concept would be more viable, but tests where the catheter would

remain inside the patient's bloodstream for prolonged periods of time, the previous concept would be more viable (both only in the case of testing using self-made prototypes, instead of professionally manufactured products).

From the marketable, mass production point of view, it would appear that the concept with all of the electrodes (including the grounding electrode) on the cannula of the catheter would be the most ideal. This decision was made because it would be simple to manufacture this (introduce the electrodes in the forming process of the cannula and expose them when tapering the proximal tip of the cannula) and it offers the most operational flexibility, allowing any insertion technique without hindering impedance measurements. If manufactured properly, most of this concept's disadvantages become irrelevant and if the electrodes are properly placed and are made from a biologically compatible material (such as gold or silver), their prolonged exposure to the human bloodstream would not be a problem.

To summarize, Table 5-3 illustrates in which cases which concept would be best suited.

Table 5-3: Ideal electrode placement concepts in different scenarios

	Prototype for experiments with prolonged exposure to bloodstream	Prototype for experiments with no prolonged exposure to bloodstream	Professionally manufactured device
Electrodes on cannula, needle as grounding electrode		X	
Electrodes on cannula, including grounding electrode			X
Electrode fed through central channel of the needle and back between needle and cannula	X		

5.3. Electronics concepts: user feedback

The device being designed will require a form of feedback to the user to put the measurements to use. This form of feedback will have to be simple, yet capable of relaying as much information as possible. Overcomplicated feedback will hinder the small and simple design specifications for the device, but an oversimplified form of feedback would be inadequate. Below are three concepts that were generated as forms of feedback:

The first concept is the use of sound as a feedback method. This concept is based on simplicity, with different sounds being played depending on the impedance levels measured, with a distinguishable sound playing once placement has been successfully concluded.

The second concept is the use of LEDs, ideally RGB LEDs, capable of displaying multiple colours. This allows different coloured visual feedback to be given, depending on the impedance levels encountered. The colours used will have to be chosen wisely, as to not hinder users who are colour blind. Using a pulse width modulator with these RGB LEDs will enable a large spectrum of colours to be used, allowing for a large resolution of feedback and also allowing the device to cater for those who suffer from colour blindness. This can be done by avoiding the use of colours associated with colour blindness (most commonly red and green).

The third concept is the inclusion of a screen, which could either display the position of the proximal tip of the arterial catheter with the aid of pictures or words. Using pictures will be less than ideal as it would take up a lot of space and energy and may be overcomplicating the feedback. Displaying feedback in the form of words (the main idea is to display the name of the tissue type associated to the current impedance measured) will be less complicated than generating a picture, but will still be more complicated than the previous two concepts. Table 5-4 list the advantages and disadvantages of the three concepts generated above.

Table 5-4: Advantages and disadvantages of the different feedback concepts

	Advantages	Disadvantages
Sound feedback	Does not require the operator to look at the device Very simple	Binary feedback, unless varying tone or frequency of sound Varying tone or frequency would make distinguishing sounds relative and thus harder to form constructive feedback from device External noise could impede effectiveness

<p>LED feedback</p>	<p>Simple to implement and use</p> <p>Can give a wide range of feedback, especially if used with a pulse width modulator</p> <p>Capable of multidirectional measurement feedback, if more than one RGB LED is used</p> <p>Low power use</p>	<p>Requires the operator to look at the device (peripheral vision would be enough though)</p> <p>Requires the operator to remember which colours are associated with which tissue types</p> <p>Needs to be designed around colour blind users</p>
<p>Screen feedback</p>	<p>Most informative form of feedback</p>	<p>Most complicated and cumbersome form of feedback</p> <p>Requires the operator to look at the device (and read constantly, if written feedback is given)</p> <p>High power consumption</p>

From Table 5-4, it was decided that LEDs would provide the ideal form of feedback. It gives a good balance between simplicity, power efficiency and information. Though it does require the operators to learn which colours are associated to which position of the arterial catheter, this should not be too difficult and would not hinder the insertion process as much as having to read a screen during insertion. While the sound feedback is simpler and does not require the operator to look anywhere else other than the point of insertion, the relative differences in sound could lead to confusion and external noise could drastically hinder the feedback obtained.

5.4. Electronics concepts: impedance measurement

As stated in the specifications section, a series of electronics will be required in order to measure and excite the impedance in the human tissue. All concepts will require the use of a microprocessor to store, compare and analyse measured data. Below are three different concepts which were generated to excite and measure the impedance of human tissue.

The first concept involves using a dedicated IC, made with the sole purpose of measuring electrical impedances. These ICs are small, quick, accurate and power efficient, but require more programming to allow them to be flexible for larger testing operations.

The second concept involves using an oscilloscope and a signal generator, while the third concept involves building a set of electronics capable of generating an AC signal and then using an A/D converter to measure multiple points in all the measured channels to calculate the impedance measured. Both these concepts would function on the same mathematical principles, described below.

The aforementioned electronics will include an AC signal source and a reference resistor (Z_S), which will be used in the calculations of the impedance of the tissue measured (Z_L). The electronics will measure voltages over V_L and V_t using either the oscilloscope or the A/D converter, depending on the concept used. These parameters can be seen in Figure 5-3 below.

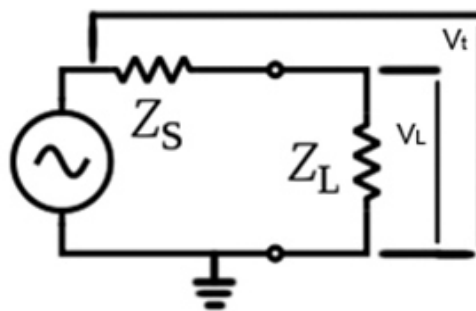


Figure 5-3: Diagram depicting AC voltage source (V_t), voltage over the tissue (V_L), reference resistor (Z_S) and tissue impedance (Z_L)

The process of calculating the impedance starts by recalling Ohm's Law (but bearing in mind that V_t , V_L , I and Z_L are complex numbers):

$$V = IR \quad (5-1)$$

thus

$$V_L = IZ_L \quad (5-2)$$

From Figure 5-3 and eq. 5-1:

$$V_t - V_L = IZ_S \quad (5-3)$$

Substituting eq. 5-2 into eq. 5-3 and rearranging give

$$Z_L = \left(\frac{V_L}{V_t - V_L} \right) Z_S \quad (5-4)$$

However, because V_L is a complex number, complex division is required to determine Z_L . Utilizing eq. 3-8, the complex division can be written as:

$$\left(\frac{V_L}{V_t - V_L}\right) = \frac{(ac+bd)+i(bc-ad)}{c^2+d^2} \quad (5-5)$$

where

$$a = \text{Re}(V_L) \quad (5-6)$$

$$b = \text{Im}(V_L) \quad (5-7)$$

$$c = (\text{Re}(V_t) - \text{Re}(V_L)) \quad (5-8)$$

$$d = (\text{Im}(V_t) - \text{Im}(V_L)) \quad (5-9)$$

However, because the angle between V_L and V_t is relative, the phase of V_t can be considered as 0. With this in mind, $\text{Im}(V_t)$ thus becomes 0, leading to

$$d = -\text{Im}(V_L) \quad (5-10)$$

Substituting eq. 5-6 to eq. 5-10 into eq. 5-5 leads to

$$\text{Re}\left(\frac{V_L}{V_t - V_L}\right) = \frac{(\text{Re}(V_L) \cdot (\text{Re}(V_t) - \text{Re}(V_L)) + \text{Im}(V_L) \cdot (-\text{Im}(V_L)))}{\text{Re}(V_t)^2 - 2\text{Re}(V_t)V_L + \text{Re}(V_L)^2 + \text{Im}(V_L)^2} \quad (5-11)$$

And

$$\text{Im}\left(\frac{V_L}{V_t - V_L}\right) = \frac{(\text{Im}(V_L) \cdot (\text{Re}(V_t) - \text{Re}(V_L)) + \text{Re}(V_L) \cdot (-\text{Im}(V_L)))}{\text{Re}(V_t)^2 - 2\text{Re}(V_t)V_L + \text{Re}(V_L)^2 + \text{Im}(V_L)^2} \quad (5-12)$$

Substituting eq. 5-11 and eq. 5-12 into eq. 5-4, one then gets

$$\text{Re}(Z_L) = \text{Re}\left(\frac{V_L}{V_t - V_L}\right) \cdot Z_S \quad (5-13)$$

and

$$\text{Im}(Z_L) = \text{Im}\left(\frac{V_L}{V_t - V_L}\right) \cdot Z_S \quad (5-14)$$

Finally, substituting eq. 5-13 and eq. 5-14 into eq. 3-3 and eq. 3-4, one finds

$$|Z| = \sqrt{\text{Re}(Z_L)^2 + \text{Im}(Z_L)^2} \quad (5-15)$$

and

$$\theta = \tan^{-1}\left(\frac{\text{Im}(Z_L)}{\text{Re}(Z_L)}\right) \quad (5-16)$$

Which, when substituted into eq. 3-2 leads to the impedance, as

$$Z_L = \sqrt{\text{Re}(Z_L)^2 + \text{Im}(Z_L)^2} \angle \left(\tan^{-1}\left(\frac{\text{Im}(Z_L)}{\text{Re}(Z_L)}\right)\right) \quad (5-17)$$

Equations 5-11, 5-12, 5-15, 5-16 and 5-17 thus give an easy method for determining Z_L , with Z_S as a known value and V_L and V_t being easily measured. For the oscilloscope/signal generator concept, a computer linked to the oscilloscope will be able to perform these calculations (with the aid of

software, such as Matlab, Scilab or Microsoft Excel), whereas the concept using designed electronics will require the calculations to be done using a microprocessor.

Below is a table, illustrating the advantages and disadvantages of each concept.

Table 5-5: Advantages and disadvantages of impedance measuring concepts

	Advantages	Disadvantages
Dedicated IC and microprocessor	Very small, simple design High accuracy Energy efficient	The ability to modify variables can be complicated and will require additional components High cost and lead time on these ICs
Oscilloscope, signal generator and PC	Easy to change variables Simple to set up High accuracy	Bulky Does not comply with the battery powered specification Expensive components
Custom made electronics and microprocessor	Can be customized according to specific requirements Design can be small when designed with surface mounted chips	Design can require external housing if not using surface mounted chips Accuracy is dependent on the quality of design

From Table 5-5, it can be seen that each concept has its merits, but are highly dependent on the requirements for the situation. It can be seen that once the device has been finalized and that the operating parameters have been established, the dedicated impedance measuring IC would be the ideal choice, due to the small size, high accuracy and low power usage.

Contrarily, the use of the oscilloscope, signal generator and PC could not be used in the final device (or on living human subjects) due to the concept not adhering to the battery-powered specification set out in the previous chapter. However, this concept would be ideal for the first phase of testing, when the operating parameters would be changed rapidly, thus offering the most experimental flexibility.

Finally, the custom made electronics offer a smaller design (capable of being much smaller if made using surface mounted components), while still offering flexibility for experimental purposes.

It was thus decided to use the oscilloscope, signal generator and PC for preliminary tests. The custom made electronics would be used for more advanced tests. It is recommended that the dedicated impedance measuring IC be used for a final, marketable product.

The above sections give an overview of the concept development and evaluation during the project. While some concepts are clearly better than others, it was found that several concepts are situational, leading to some concepts functioning better for the experimental phases of the project, while other concepts are more viable for a final product. It is because of this that certain concepts were used during the experimental phases and then changed or developed into different concepts for later experimental phases in the project.

6. Preliminary design

The preliminary design of the device was intended for the first phase of experiments, which were aimed to investigate any fundamental differences in impedance between different types of tissue and to conclude if a simplified version of the concept would work. It was thus decided to use the simplest and most flexible of the concepts generated in the previous section.

For the purposes of the first phase of experimentation, two stainless steel needles (diameter of 0,6 mm) were used, fixed 0,5 mm apart by soldering both to a plate. This was performed to simulate the electrodes placed on the exterior of the catheter. Both needles were covered in a thin layer of resin over all but the last 1 mm of both tips of the needles, to allow only the proximal and distal tips of the needles to be conductive. One needle was used as the ground electrode and the other was used to carry the AC signal. Soldered onto the latter needle was a 10 k Ω potentiometer, serving as a reference resistor, but allowing for modifications to be made to its resistance value where needed. The exposed area of both needles were calculated (assuming a cylindrical shape for the needle) as 0,0188 cm².

A signal generator (Topward Function Generator 8110) was attached to the conductors leading from the needles, as well as a PC oscilloscope (Velleman PCSU1000), allowing for measurements of V_t and V_l to be taken, as seen in Figure 5-2. Figure 6-1 illustrates a schematic of this setup.

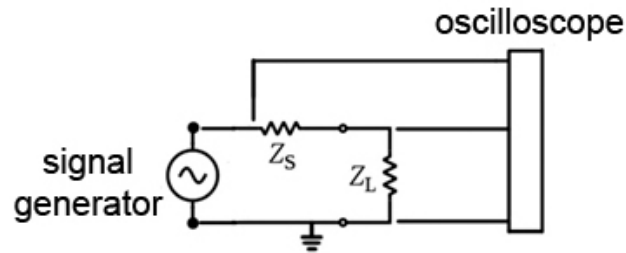


Figure 6-1: Diagram depicting the connections between the electronics, the signal generator and the oscilloscope

The PC oscilloscope was interfaced with a laptop (Dell XPS1640) running MS Excel 2010 as well as PCLabSE2000 4.04 and outputted the A/D measurements taken on both channels to Excel via the PCLab software. In MS Excel, the data was used to calculate the impedance of the tissue tested. This was done by analysing the two data sets read (one for V_t and one for V_L) to find the peak voltages of both data sets and then determining the gap between the two peaks and converting that into a relative phase angle. With the amplitudes of V_t and V_L as well as the relative angle between the two and the value of the reference resistor, it was possible to calculate the impedance, as explained in Chapter 5.

In order to validate the accuracy of this prototype, tests were conducted using three different resistance levels. The system was calibrated (described in Chapter 7.2) prior to the accuracy tests. The first series of tests were done with a 0,5 k Ω resistance, the second series with a 5 k Ω resistance and the last set with a 10 k Ω resistance. With each level of resistance, 10 measurements were taken, after which all the equipment would be switched off, disconnected, reconnected and then switched on again, before the 10 tests would be repeated. This cycle would be repeated 5 times. Measurements were taken with a peak to peak voltage of 10 V, centred around 0 V, with a frequency of 100 kHz. All of this data was then saved to MS Excel, after which this software was used to calculate the averages and standard deviation of each test. The averages were then subtracted from the actual value of the resistance, to give the average error. This was also done for the phase measured, with an actual value of 0° in all of the tests. Below are two figures with four graphs, indicating the results of these accuracy tests.

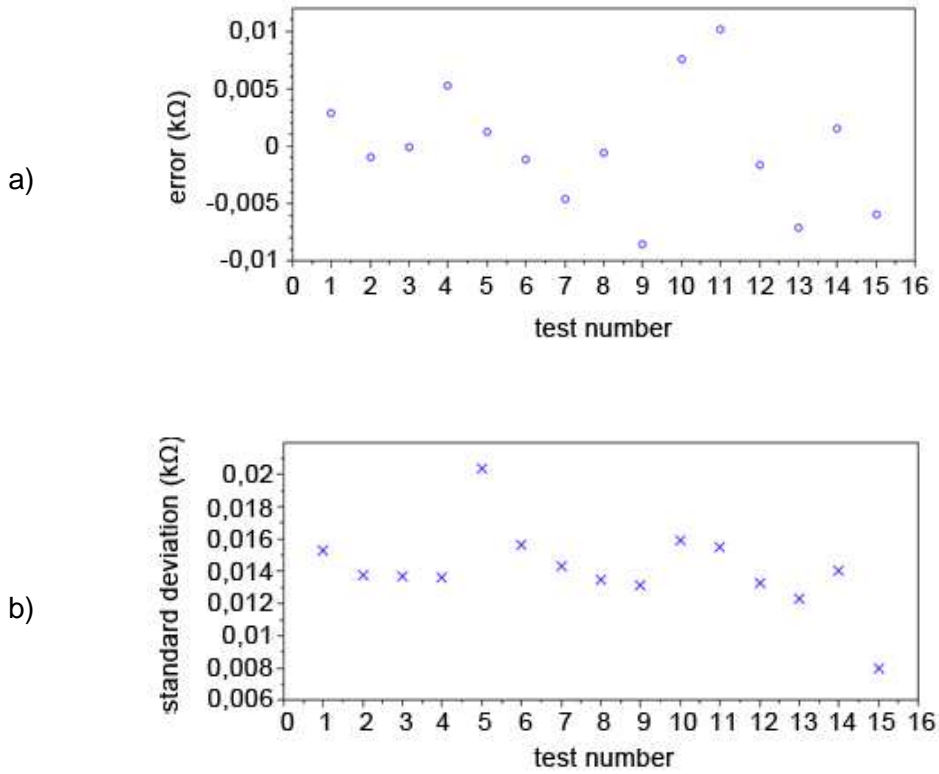


Figure 6-2: Impedance magnitude accuracy tests in first prototype

Figure 6-2 shows two graphs (referred to as 6-2a and 6-2b), with 6-2a indicating the average error in each set of tests and 6-2b showing the standard deviation in each set of tests. The x-axis represents the test number, where test numbers 1-5 are the repeated tests at 0,5 kΩ (with Z_S set to 1 kΩ), tests 6-10 are the repeated tests at 5 kΩ (with Z_S set to 5 kΩ) and tests 11-15 are the repeated tests at 10 kΩ (with Z_S set to 10 kΩ). These results indicate a very low error margin on the higher value impedance measurements. The value of this error remains the same for lower value impedances, but result in a higher percentage error. The similarities in the error would imply that the resolution of the PC oscilloscope is the cause of these inaccuracies. Furthermore, the results also indicate that the repeatability of the system is not a problem, showing very similar standard deviations for all but tests 5 and 15.

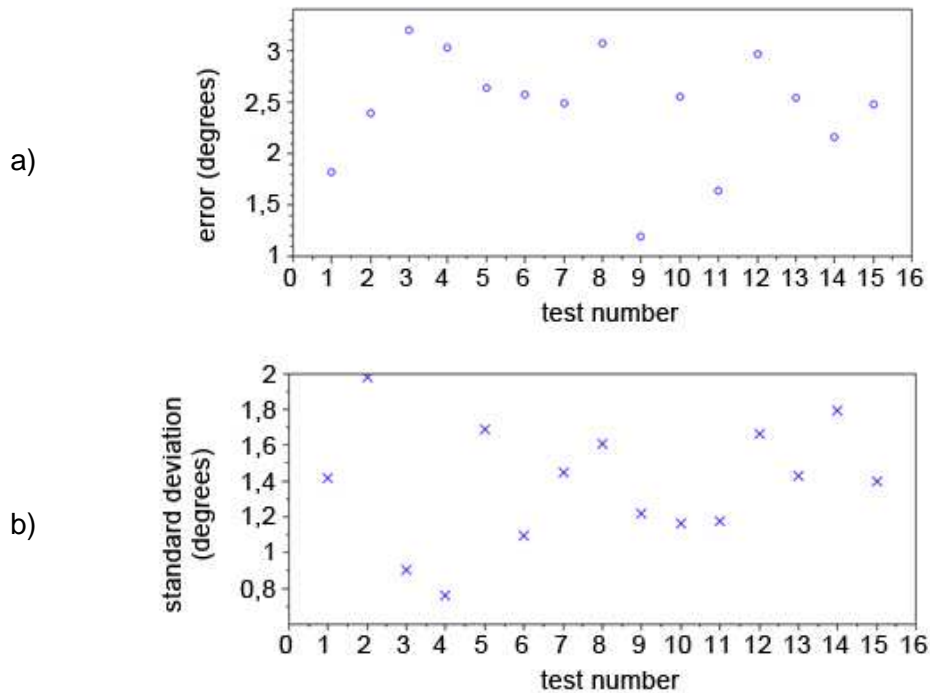


Figure 6-3: Impedance phase accuracy tests in first prototype

Figure 6-3 is constructed in a similar fashion as Figure 6-2, except these two graphs (6-3a and 6-3b) illustrate the average error and standard deviation of the impedance phase. For tests 1-15, the impedance phase should remain 0° . It can be seen that there is a moderate error margin, with the majority of the average error values being close to $2,5^\circ$. The implication of a $2,5^\circ$ error on such a measurement as in these test would lead to an inaccurate calculation of a reactance in the system with the value equal to 4,36 % of the resistance calculated (based on eq. 3-2 and eq. 3-3). It was decided that, although not ideal, this error would not be catastrophic and would not jeopardise the experiments.

Figures 6-2 and 6-3 also illustrate the repeatability of the system. It can be seen in Figure 6-2a that there is some disparity between the average errors in the different tests, while this is less apparent in Figure 6-3a. This scatter is most prominent in Figure 6-2a in tests 11-15 but in these tests, this percentage error is very low (maximum average error percentage is 0,1 %), which was deemed acceptable. It was thus decided that experimentation would commence with this setup.

7. Preliminary experimentation

Utilizing the prototype described above, a preliminary series of experiments were performed. This chapter is divided into three sections. The first section (the experimental design) includes the goals of the experiment, the settings used, on what subjects the experimentation would take place and what could be expected in terms of accuracy. The second section (the experimental procedure section) describes the preparatory steps taken for the experiment, how the system was calibrated, how the measurements were taken and how the variables were changed. The final section includes the results obtained from the experiments, how the results were processed, the interpretation and implications of the results and comparisons with the theory discussed in Chapter 3.

7.1. Experimental design

The goals of the preliminary experiments were to determine whether or not there is a fundamental difference of the impedance in different kinds of biological tissue. Additionally, the tests were done at varying AC frequencies, allowing comparisons to be made between different tissue impedances at different frequencies and thus allow for a decision to be made regarding which frequency is to be used in the final prototype. Furthermore, these experiments would give valuable feedback on the functionality of the concept used.

The experiments would be successful if a discernible difference was found between the tissue types at one or more selected frequencies and if it was found that the device was capable of measuring the impedance as planned. If the experiments were successful, the development of the prototype could be furthered and more experiments could be done.

The experiments were done with the prototype described in Chapter 6, where details regarding the prototype's components and accuracy can be found. Testing was done on samples of dead porcine tissue. The tissue types selected for these sets of experiments were fat, skeletal muscle, skin and arterial wall tissue. Blood tissue was meant to be tested on, but due to reasons explained later, fewer tests were performed on blood tissue.

All tissue types were received from an abattoir (Winelands Pork, Western Cape, South Africa), from pigs slaughtered on the day of collection. Arterial wall tissue was found on the aorta attached to the heart of the pig, while fat and muscle tissue samples were found in loin chops. Skin samples were obtained from the exterior rinds of the above mentioned meat samples. Fresh blood was obtained from the abattoir as well. The experiments were performed on the same day as the collection of the samples.

All experiments were performed in a laboratory, at room temperature. The waveform generated by the signal generator was chosen to be an 8 V peak-to-peak sinusoidal wave, centred around 0 V. The frequencies at which the measurements were taken were chosen to be 500 Hz, 1, 5, 10, 20, 30, 40,

50, 60, 70, 80, 90 and 100 kHz. 100 measurements per tissue type per frequency were taken.

These experiments were performed on dead tissue at room temperature and these would not be the conditions when using the device on patients. An assumption was made that there would be a difference in impedance, based on whether or not the tissue is alive or dead, due to cellular activity (or the lack thereof) and the temperature of the tissue. However, it was also assumed that if there was a discernible difference between all of the mentioned tissue types while dead and at room temperature, there would still be a discernible difference if the tissue were alive and at body temperature. Thus, the inaccuracies expected would be caused by the inaccuracies in the measuring system (described in Chapter 6), the difference in tissue temperature and the fact that the tissue experimented on was not living tissue.

Utilizing the values in Table 3-1, eq. 3-10, the exposed area of the specimen ($0,0189 \text{ cm}^2$) and the length of the sample (0,1 cm), Table 7-1 of expected results was generated (assuming similarities in bovine and porcine tissue). The values measured in the experiments were the impedance magnitude and phase, where the expected values here represent the electrical resistance and thus these values cannot be directly compared. However, the impedance magnitude can be compared to the expected resistance if the impedance phase is small (implying that the impedance consists mainly of resistance and very little reactance).

Table 7-1: Expected resistance values based on theory

Tissue	Resistivity ($\Omega\text{-cm}$)	Expected resistance ($\text{k}\Omega$)
Blood	81 - 272	0,428 - 1,439
Skeletal muscle	300 - 700	1,587 - 3,704
Fat	2000 - 3850	10,58 - 20,37

7.2. Experimental procedure

For this phase of experimentation, the prototype double needle probe was connected to the signal generator and the PC oscilloscope. The value of Z_S was set to $2 \text{ k}\Omega$ and was verified using a MY62 digital multimeter, with $0,05 \text{ k}\Omega$ tolerance. The signal generator was set to a zero amplitude, which was then verified using the PC oscilloscope. If it was not measured as 0 V , the PC oscilloscope would be recalibrated (after disconnecting the probes from the oscilloscope) and if the inaccuracy remained, the DC offset on the signal generator was altered until a zero reading was measured on the oscilloscope (with a tolerance of $0,05 \text{ V}$). This was followed by switching the

signal generator to the desired frequency and amplitude, followed by verifying this waveform with the PC oscilloscope and correcting it with the amplitude and frequency settings on the signal generator. Once the waveform was verified to be correct (within a tolerance of 0,05 V and 0,05 kHz) the calibration process was complete.

The probe was then inserted into the tissue and once it was firmly placed, the program was set to run, taking measurements and then calculating a single impedance measurement, as described in Chapter 6. Once the process was completed and the impedance value was calculated, the probe was removed and reinserted into another region of tissue, where another measurement was taken.

After 100 measurements were taken of a specific frequency, the frequency was set to the next frequency to be tested with, the results were saved, the waveform parameters verified again using the PC oscilloscope (as described above) and once that was completed, another 100 tests were conducted on the tissue, as detailed above. Once 100 measurements were taken per frequency, the tissue type was removed, the needles were cleaned using detergents and testing would begin on a different tissue type in the same manner as described above.

7.3. Results & conclusion

From the experiments, a few important things were noted. Firstly, it was difficult to measure the impedance of blood outside of a living body, due to the rapid coagulation of blood. The few successful tests that were conducted on blood did indicate that blood has a much lower impedance than the rest of the tissue types tested, with the highest value measured nearing 0,8 k Ω . It was decided that more measurements would be taken on blood by means of in vivo experiments on living organisms. However, it was still noted that this measured value for blood correlates to the expected theoretical values, established in Tables 3-1 and 7-1. Secondly, it was immediately noted that the dermis and epidermis layers of skin tissue measured substantially higher than the rest of the tissue at all frequencies. It was decided that further testing on skin tissue would be trivial and was thus ignored. Testing on skeletal muscle, fat and arterial wall tissue proceeded as explained and was met with satisfying results.

It was found that the experimental prototype worked sufficiently for the purpose of the experiments. Furthermore, valuable data was collected regarding the impedance of the biological tissue examined. Two tables, containing the average values and standard deviations for each tissue type per frequency can be seen below. Table 7-2 indicates that fat tissue has the highest average impedance magnitude, followed by the arterial wall and then skeletal muscle. Table 7-3 indicates that the difference in impedance phase is far less distinguishable than the impedance magnitude.

Table 7-2: Averages and standard deviations of tissue impedance magnitude at different frequencies

Frequency (kHz)	Muscle		Fat		Arterial Wall	
	Magnitude (k Ω)		Magnitude (k Ω)		Magnitude (k Ω)	
	\bar{x}	σ_s	\bar{x}	σ_s	\bar{x}	σ_s
0,5	1,62	0,14	17,38	5,89	4,46	0,64
1	1,41	0,23	16,21	5,70	3,74	0,33
10	0,92	0,15	14,85	4,93	2,92	0,29
20	0,68	0,12	12,91	5,97	2,68	0,31
30	0,68	0,17	11,43	3,66	2,55	0,36
40	0,62	0,12	11,03	3,30	2,56	0,28
50	0,61	0,19	9,71	2,61	2,55	0,45
60	0,62	0,13	8,56	2,61	2,58	0,34
70	0,63	0,14	9,15	2,03	2,62	0,35
80	0,58	0,08	8,25	1,82	2,57	0,29
90	0,64	0,11	7,58	1,96	2,67	0,34
100	0,60	0,08	7,60	1,53	2,43	0,29

Table 7-3: Averages and standard deviations of tissue impedance phase at different frequencies

Frequency (kHz)	Muscle		Fat		Arterial Wall	
	Phase (°)		Phase (°)		Phase (°)	
	\bar{x}	σ_s	\bar{x}	σ_s	\bar{x}	σ_s
0,5	33,97	2,49	10,81	5,26	15,18	4,97
1	31,30	2,93	9,59	4,33	13,34	3,21
10	28,18	3,92	13,44	7,68	13,59	6,36
20	27,74	5,61	16,17	6,95	10,07	4,34
30	18,66	3,19	15,99	4,85	8,40	2,82
40	16,17	3,33	21,59	5,70	8,65	3,72
50	14,28	3,45	23,48	5,78	8,61	2,65
60	14,48	2,29	24,79	6,56	8,99	3,42
70	12,85	2,53	31,75	8,11	10,85	3,34
80	12,63	2,14	34,08	7,26	11,13	2,89
90	10,92	3,92	33,89	9,60	10,49	3,09
100	11,15	1,80	37,87	8,40	11,02	2,80

Box-and-whisker charts for the aorta wall impedance magnitude and phase can be seen below, in Figures 7-1 and 7-2, while similar box-and-whisker charts for skeletal muscle and fat tissue can be found in Appendix A.1. It can be seen that the impedance magnitude lowers as the frequency is increased and that (after 30 kHz) the values stabilize and remain consistent. It can also be seen that the phase average results remain consistent, though there are much larger error bars present than in the impedance magnitude graphs.

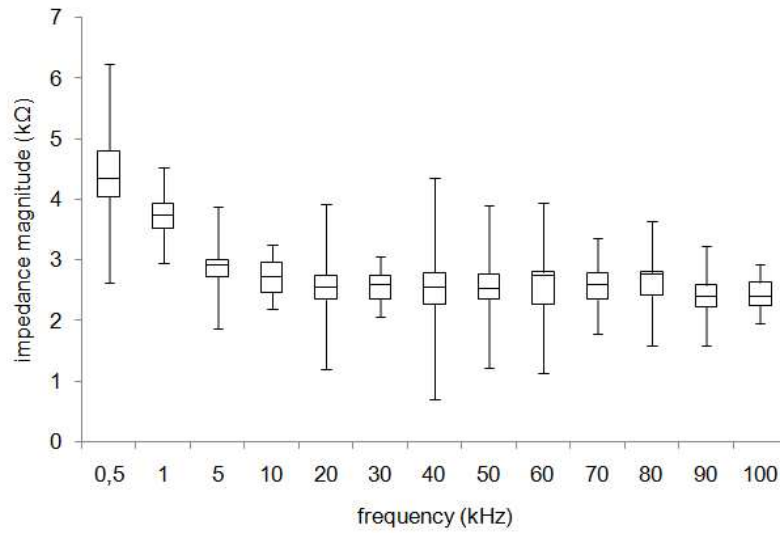


Figure 7-1: Arterial wall tissue impedance magnitude box and whisker chart

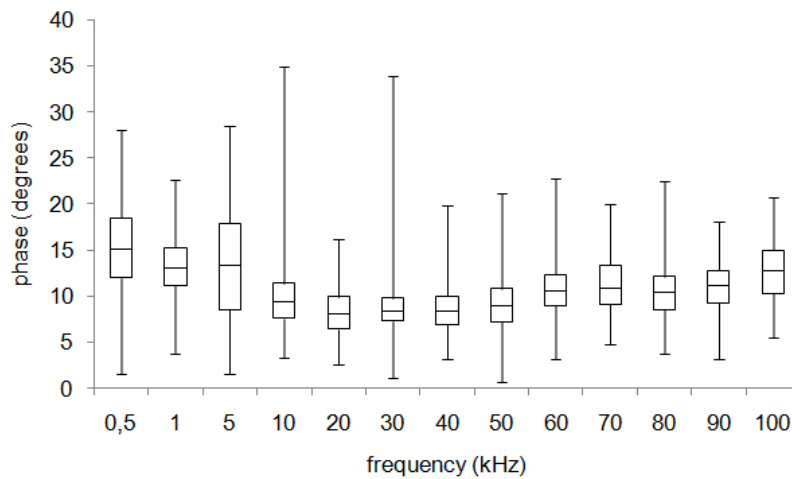


Figure 7-2: Arterial wall tissue impedance phase box and whisker chart

Furthermore, Figures 7-3 and 7-4 comparing the average values and standard deviations for each tissue type at each frequency can be seen. The hatched section on these charts illustrates the area encompassed by the average plus the standard deviation and the average minus the standard deviation. The lines running through these hatched areas indicates the average values.

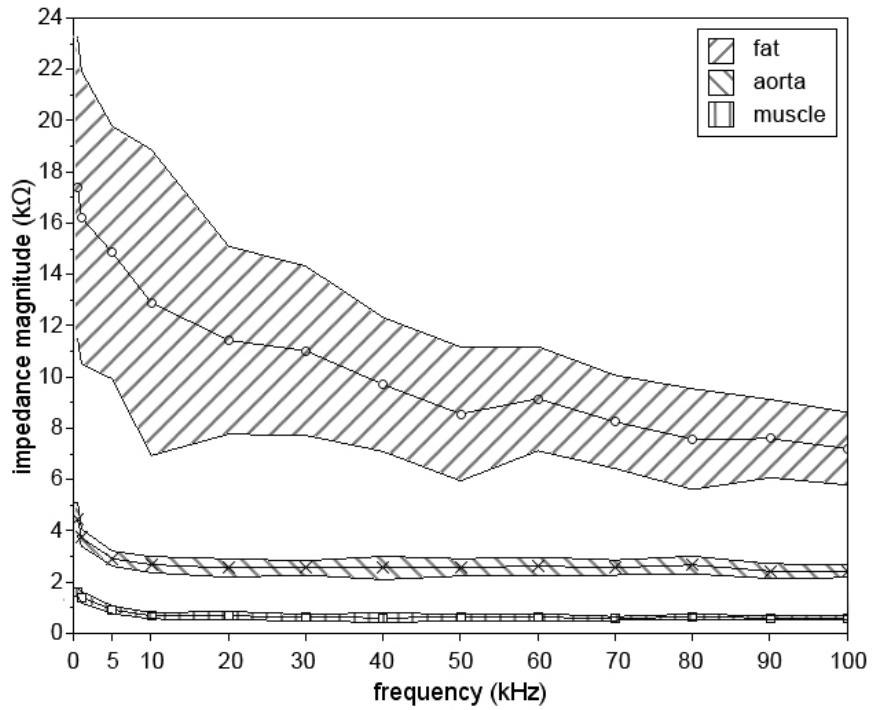


Figure 7-3: Comparative impedance magnitude chart, with tissue type averages and standard deviations

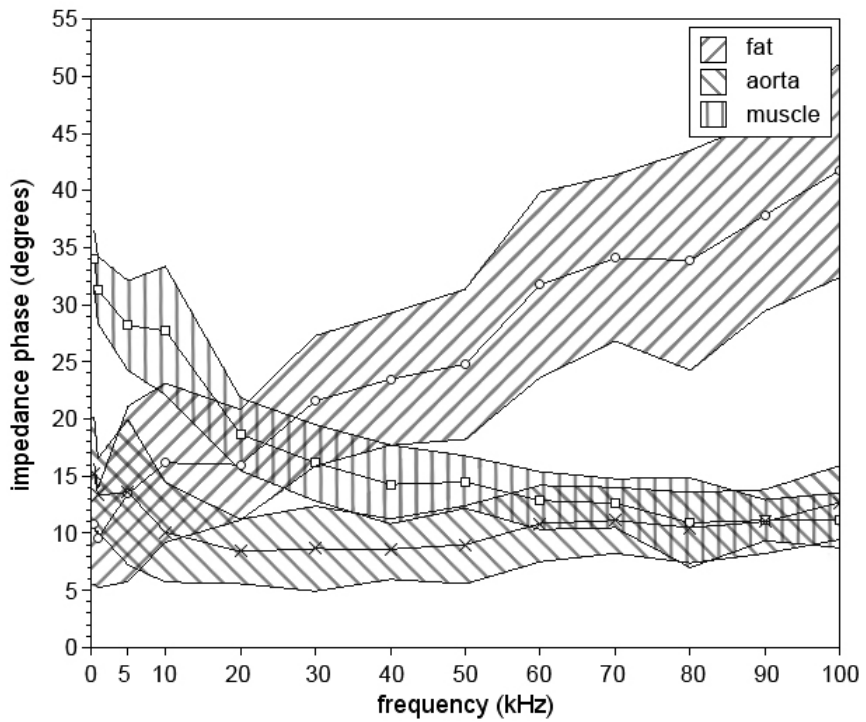


Figure 7-4: Comparative impedance phase chart, with tissue type averages and standard deviations

The averages, standard deviations and first and third quartile statistical calculations were made using MS Excel, due to the raw data being stored in Excel. Plots were drawn using Scilab.

Tables 7-1 and 7-2, along with Figures 7-1 through to 7-4 (and additional Figures A.1-1 to A.1-4, found in Appendix A.1) give a graphical summarization of the results obtained regarding arterial wall, skeletal muscle and fat tissue over the different frequencies tested on. It can be seen from Figures 7-1, 7-2 and A.1-1 to A.1-4 that there is a fair amount of scatter in the distributions, but that the 1st and 3rd quarters are in most cases close to the average, which would imply that this observed scatter is probably caused by anomalies in the measurements and not by variances in the tissue. Figures 7-1, A.1-1 and A.1-3 all indicate that the impedance magnitude of the three tissue types progressively decrease as the frequency is lowered, up until about 10-20 kHz, where they seem to stabilize. It is assumed that the high deviation in fat tissue is attributed to the varying moisture content in the tissue.

It is made clear in Figure 7-3 that the average values (along with the standard deviations) measured for the tissue types have a distinct difference between each other at certain frequencies, indicating that the tissue types are discernible when evaluating the impedance magnitude. Furthermore, it can be seen that (at lower frequencies) the impedance magnitude of fat and skeletal muscle tissue correlate well with the expected theoretical resistance, while their impedance magnitude lowers as the frequency is increased, as expected (explained in Chapter 3.3 and seen in Figure 3-5). The correlation between the expected values and the measured values, as well as the parallels between the theoretical and measured frequency dependant behaviour of the impedance, imply that the prototype used measured the impedance magnitude of biological tissue correctly and accurately.

Figures 7-2, A.1-2 and A.1-4 indicate a less predictable pattern for the behaviour of the impedance phase for the different tissue types, with fat tissue rising as the frequency is increased, while skeletal muscle tissue decreases slightly until it stabilizes at roughly 20 kHz. Arterial wall tissue seems to have no clear tendencies as the frequency increases. Figure 7-4 further illustrates that the phase of the tissue types is a lot less predictable than the impedance magnitude and it would not be viable to judge the tissue type based solely on its phase.

Blood tissue, as mentioned above, proved difficult to test and few measurements were taken, but not enough to provide any meaningful information. Skin tissue was seen to be above 50 k Ω in all tests and at all frequencies and thus it was decided that further investigation would not be necessary. Additionally, due to the nature of the device, it would be obvious when the arterial line has passed through the skin and thus the impedance values of skin would not be as important as that of the other tissue types tested.

The frequency dependence relative to the impedance magnitude illustrated in Figure 7-3 allowed for the decision to be made to do further experimentation

at only 30 kHz. From the test results, it can be seen that at 30 kHz the impedance magnitudes offer enough information to allow identification and categorization of tissue types. 30 kHz was also chosen as it is a low frequency, close to the 20 kHz stabilization point. For the future development of the concept, a lower frequency would be ideal, as it would require a lower sampling rate in the final concept's A/D converter, which would lower the requirements for the final product. The figure below illustrates box and whisker plots of the different tissue magnitudes at 30 kHz, to illustrate how distinguishable the impedance magnitude is at this frequency.

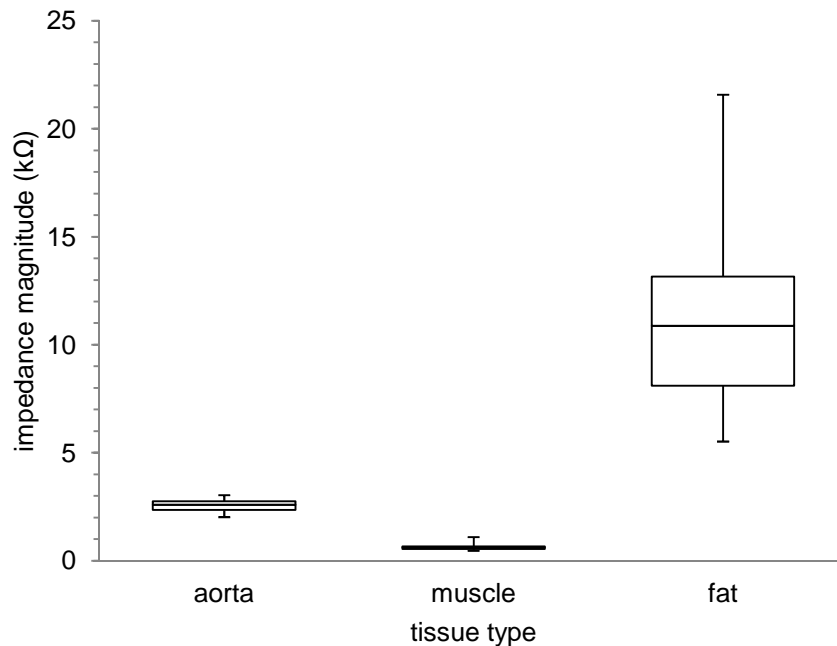


Figure 7-5: Tissue impedance magnitude at 30 kHz box and whisker plot

Figure 7-5 illustrates that there is a clear difference between the measured impedance magnitude values at 30 kHz, which implies that this frequency is suitable for future testing.

The most important implication of the results is that Figures 7-1 through to 7-5, along with Figures A.1-1 through to A.1-4 indicate that it is possible to distinguish between the different tissue types by measurement of their impedance. These results thus suggest that the concept of an impedance guided intra-arterial catheter could be viable.

As mentioned earlier, the assumption was made that if different dead tissue types at room temperature have an apparent difference, it would be highly possible that the same would apply for living tissue at body temperature. To validate this hypothesis, the next phase of experimentation would be to

perform tests on living organisms. This would be to observe the difference between living tissue and dead tissue and, more importantly, to verify whether or not there is a difference in impedance in the different kinds of living tissue and if it would be enough of a difference to make an accurate decision on which tissue type it is. Thus, the next step in the project would be to further the design, to allow for the next phase of experimentation.

8. Experimental prototype design

It was shown in the previous chapter that the preliminary prototype design was functional and achieved what it was expected to do. The next phase of experimentation would require further development of the prototype in terms of the mechanics of the arterial line, as testing would now be done on live animals and would thus have to be approved by the animal research ethics committee. This iteration of the design would thus utilize a concept that would be safe for the testing on animals in the aim to take safe, easy impedance measurements for short duration in living animal tissue.

This chapter is divided into two sections. The first section handles the development of the mechanical aspects of the design, while the second section handles the development of the electronic aspects of the design. After the second section, there is an overview of the accuracy and reproducibility of the system.

8.1. Mechanical design

The pair of stainless steel needles used in the previous experiments would no longer be sufficient, due to the regulations of the Animal Research Ethics Committee. For the next set of experiments, the concept utilizing the electrode on the outside of the cannula with the grounding needle was employed. It was thus decided to create modified arterial catheters for the purpose of the animal testing phase.

Silver wire was wound helically around the cannula and was fixed to the exterior of the cannula with a non-toxic epoxy resin, serving as both an adhesive and as a form of electrical insulation. This silver wire (uninsulated, 99,99% purity, diameter of 127 μm , purchased from A-M systems) would serve as one of the electrodes of the prototype. The last 0,5 mm of the silver wire at the proximal end of the cannula was not covered in the resin, allowing the tip to be conductive. Additionally, the distal end of the wire was also kept uninsulated and was bonded to copper wire with silver conductive paint. This copper wire was fed to the electronics. Figure 8-1 below illustrates the silver wire, wound around the cannula, prior to insulation.

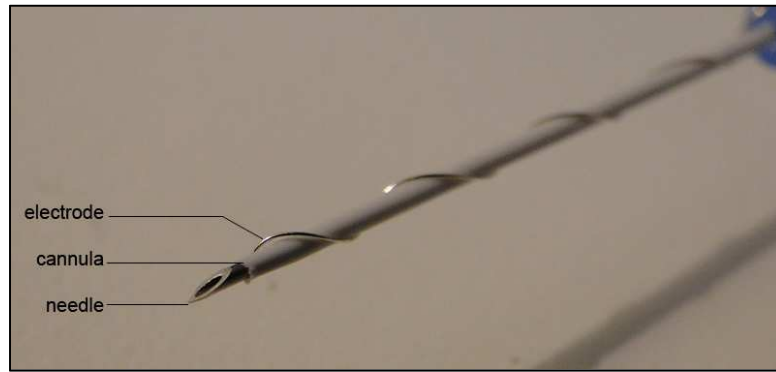


Figure 8-1: Silver electrode wound around cannula

Another copper wire was bonded with silver conductive paint to the hypodermic needle of the arterial line and would eventually serve as the grounding electrode for the prototype. The copper wire attached to the outer electrode was attached to a 10 k Ω potentiometer and the other terminal of this potentiometer was coupled to more copper wire, which would lead to the electronics. The copper wire from the needle of the arterial line would also lead to the electronics. The estimated distance between the two electrodes was measured to be 1,75 mm. Figure 8-2 shows one of the modified arterial catheters used in the animal testing phase, with the red cable connected to the needle and the black cable connected to the silver wire wound around the cannula.

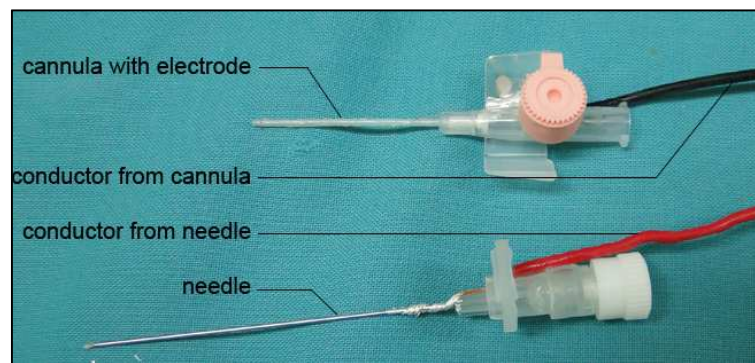


Figure 8-2: Modified arterial line, disassembled

Figure 8-3 illustrates a diagram depicting the connections between the oscilloscope, the signal generator, the laptop, the potentiometer, the electrode on the cannula and the needle.

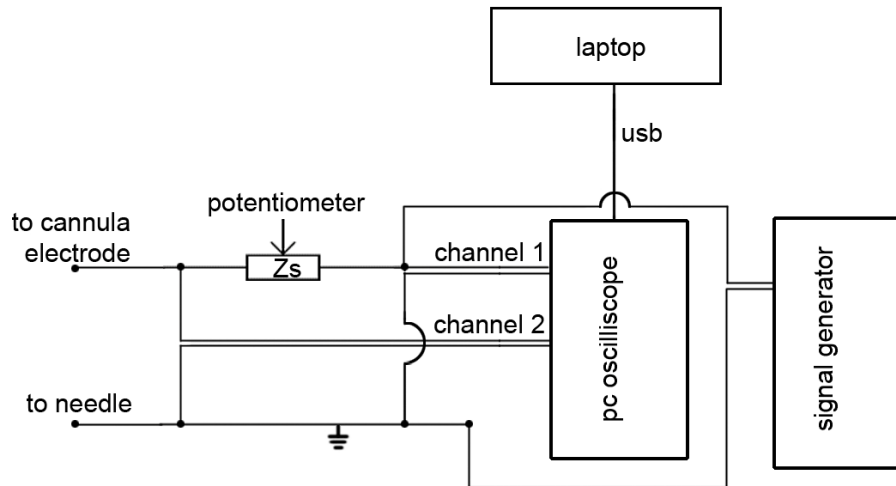


Figure 8-3: Diagram of animal testing setup

This prototype of the arterial catheter was very similar to the concept chosen for the final end product and verifying the functionality of this design would thus be crucial in the upcoming experiments.

8.2. Electronics design

The electronics of the prototype were kept similar to that used in the previous experimental phase, to allow for flexibility of design changes (if required) and modifications. For these tests, the frequency was kept constant at 30 kHz, as explained in Chapter 7.3. The value of the potentiometer would also be altered (along with the value for Z_s in the impedance calculation algorithm), in order to set it to a reasonable average of all the tissue types that would be measured.

It was decided to keep the minimum value for Z_s at 1 k Ω . This, along with the peak amplitude of 4 V of the signal generator meant a maximum current of:

$$I_{max} = \frac{V_{max}}{Z_{smin}} \quad (8-1)$$

This was calculated as a maximum current of 4 mA, which adhered to the safety specifications set.

The changes to the electronics were very slight, as further changes to the electronics were left for the final prototype design, granted that the current prototype proved to be successful in the animal testing phase. Thus, the components used in this device were identical to those described in Chapter 6. The programming for the interface with the device was slightly

modified, however. Where the previous version of the program would calculate one impedance measurement when the program was prompted to, the newer version would take 100 measurements in sequence, as it would not be allowed to repeatedly remove and reinsert the arterial catheter into a living animal's tissue, as per request of the Animal Research Ethics Committee.

The testing to determine the accuracy of this current prototype was repeated in a similar fashion as the previous prototype, as described in Chapter 6. Testing was once again done on a 0,5 k Ω , a 5 k Ω and a 10 k Ω load and the system was calibrated prior to testing, in the same method described in Chapter 7.2. The frequency was set to 30 kHz, the voltage was set to 8 V peak to peak, centred around 0 V and the value for Z_S was kept at 4 k Ω for all of these tests. In these tests, 50 measurements were taken per test, instead of 10. Due to the similarity in the electronics used, it was not expected to see any large changes in the accuracy, as it was assumed that the changes in the mechanical design of the device would have little effect on the accuracy. It was assumed, however, that the larger amount of measurements (50 instead of 10) would produce more representative results for statistical processing and could thus eliminate anomalies from the measurements. The results are presented in the same way as the results shown in Chapter 6, with Figure 8-4 presenting the impedance magnitude accuracy results.

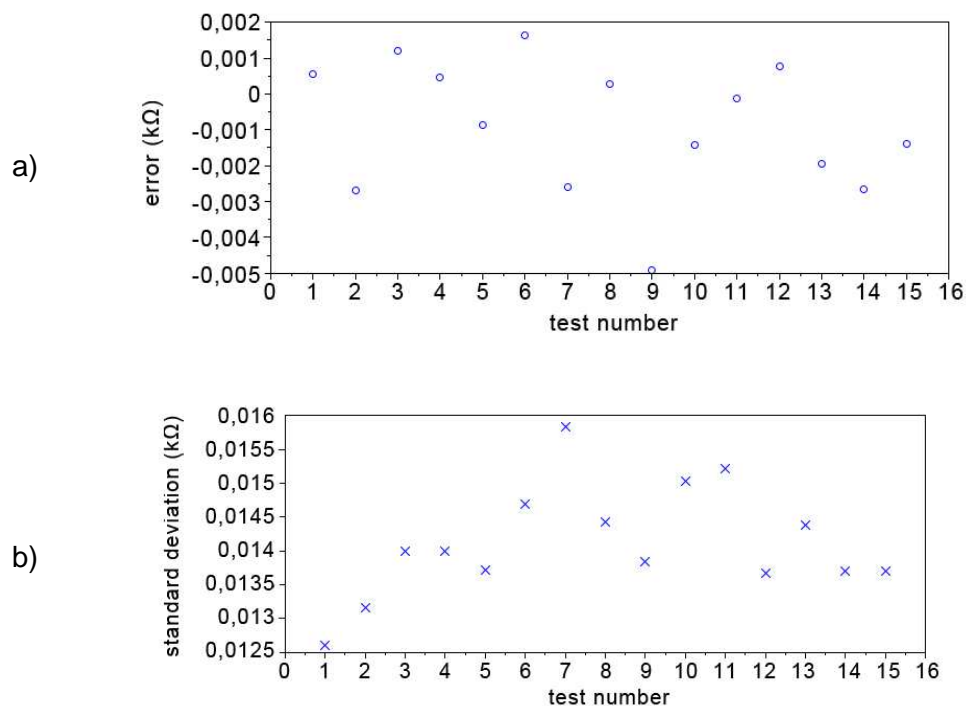


Figure 8-4: Impedance magnitude accuracy tests in second prototype

The results presented in Figure 8-4 indicate slightly more representative results than those achieved in the previous prototype accuracy testing phase. As with the previous accuracy tests, tests 1-5 indicate correlate to the 0,5 kΩ tests, while tests 6-10 correlate to the 5 kΩ tests and finally tests 11-16 correlate to the 10 kΩ tests. It can be seen that the average error is lower in Figure 8-4a than in Figure 6-2a. Figure 8-5 shows the phase test results and indicates a very slight improvement in accuracy.

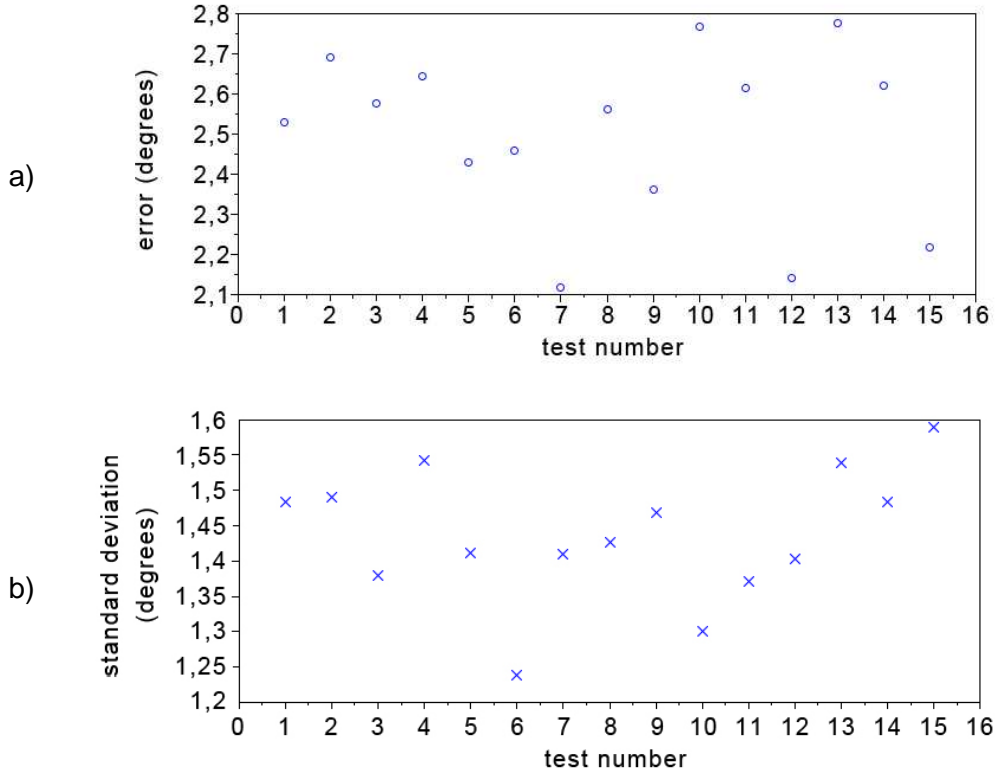


Figure 8-5: Impedance phase accuracy tests in second prototype

This increase in accuracy shown in the above figures could be attributed to the larger sampling size used in the software, which allowed for more accurate average values to be calculated. Figure 8-4 illustrates an amount of scatter present in all of the tests, suggesting that the low impedance (<1 kΩ) repeatability could contribute to a minute error (the maximum average error seen would attribute to a 6% error). The value of this error would remain similar through all impedance magnitude levels, causing a smaller percentage error in higher impedances. This problem could be attributed to the resolution of the PC oscilloscope. It was decided that these inaccuracies were not detrimental and that testing would continue.

9. Animal testing

The decision to perform animal testing was made in order to gain information about the impedance of living tissue and to see whether the discernible difference measured in dead tissue could be measured in living tissue. This chapter is divided into three sections. The first being the experimental design and protocol section, which details the goals of the experiments, the subjects used, the settings used and details as to the protocol sent to the Animal Research Ethics Committee. The second section would detail the experimental procedure, including the preparation for the experiments, the calibration of the system and the changing of variables. Finally, the results and conclusion will deal with the data gathered, the processed results, how the results were processed, the interpretation of the results, the comparison between these results and the previous results and the implications of these findings.

9.1. Experimental design & protocol

The goals of the animal testing would be to determine whether or not the updated mechanical prototype would be a valid design for in vivo use and to determine if a substantial difference between the impedance of living tissue is present. Additionally, the results would be compared with the results obtained from the previous set of experiments, to see the correlation between the impedance of living and dead tissue. For these experiments, the care and wellbeing of the animals would be of critical importance, in order to adhere to moral and ethical standards.

It was decided that the animal testing would be performed on pigs, as they are anatomically similar to humans (this assumption is based on the popular use of pig tissue in xenotransplantation [32]) and are more abundant than other choices (such as baboons [33]). Smaller animals, such as guinea pigs or rats, would not be suitable for these experiments as their size would not be appropriate in the context of the arterial catheters used. Male and female pigs would be experimented on, with a weight of approximately 25 kg each. Five pigs were chosen for experimentation, as a pilot study. If the experiments were found to be inconclusive, more tests would be performed on an appropriate amount of pigs, based on the data gathered from the tests. A low number of pigs were chosen for the first study, as the experimentation on live pigs was very expensive.

The components and setup used for these tests are described in full in Chapters 6 and 8. The tissue types to be measured in these experiments would be blood, skeletal muscle, fat and arterial wall tissue. The signal generator in these tests would be set to produce a 8 V peak to peak sine wave, centred around 0 V, set at 30 kHz. The value of Z_S was set to be close to the average expected value of the tissue to be tested.

A full protocol was sent to the Animal Research Ethics Committee as application for animal testing and extracts of the protocol can be seen in

Appendix B. The first and second protocols were denied by the ethics committee, due to the committee requiring further clarification on various elements of the application. Due to the timing of the monthly ethics committee meetings, it took five months to acquire approval for the animal testing.

It was decided that the values from Table 3-1 could not be used to derive a theoretical expected model, as seen in Table 7-1. This decision was made due to the decrease in impedance magnitude at higher frequencies, which would cause these theoretical values to be much higher than the measured values. It was thus decided that a comparison with such a model would not be valuable.

9.2. Experimental procedure

The animals were to be transported to the Central Animal Research unit at the Faculty of Health Sciences, University of Stellenbosch, where they were kept in pens in accordance to the standard procedures of the aforementioned faculty. The person in charge of the animal transport and care during this time would be Mr. Noël Markgraaff, the animal house manager of the faculty.

The animals were to be hosted in a controlled environment prior to receiving anaesthetics, as to reduce physiological stress, which could potentially contaminate experimental results. After being anaesthetised, the animals would be unconscious and moved to a surgical theatre for the procedure.

It was decided by Prof AR Coetzee, head of anaesthesiology and critical care of Tygerberg Medical Campus, that the pigs be anaesthetised using:

- 2-5 mg/kg ketamine in a single dose, administered intravenously
- 2-4 mg/kg thiopentone in a single dose, administered intravenously and
- 1-2% halothane, inhaled during the procedure via the circle breathing circuit.

Once the anaesthetised animal would reach the operating theatre, the trachea would be intubated and oxygen and air would be biventilated. Normal saline would be infused at a rate of 5 ml/kg per hour.

After the completion of the above preparations, small incisions would be made in the thighs of the pigs, deep enough to expose the femoral arteries.

Once this was completed, the experimental prototype was set up and calibrated, as described in Chapter 7.2. After calibration was completed and the signal generator was set to 30 kHz (within a 0,05 kHz tolerance) and a 8 V peak to peak voltage, centred around 0 V (within a 0,05 V tolerance), the oscilloscope probes were connected to the wiring from the modified arterial

catheter. Once this was done and all software was verified to be ready, the arterial catheter was placed into the target tissue type.

Once placed, 100 impedance measurements were recorded from the target tissue and the modified arterial line was removed. After the completion of the measurements for one tissue type, the modified arterial line was cleaned with detergent and measurements were taken from the next tissue type. Once all target tissue types were measured, the experiment was concluded and all equipment was disconnected and switched off. Figure 9-1 shows the insertion process during the testing.



Figure 9-1: Modified arterial catheter being inserted into the femoral artery

It was decided by Prof Coetzee to euthanize the animals after the procedure, using 20 mmol KCl while the animals were still under anaesthetics. After euthanasia, the animal carcasses were disposed of in accordance to the standards of the Faculty of Health Sciences.

9.3. Results & conclusion

The results of the animal testing experiments were mostly successful, with useable results in most instances. A major problem that was found in these tests was that the in vivo measurement of arterial wall tissue was highly awkward and inaccurate, due to the thinness of the arterial wall and the displacement of the blood vessels as the arterial line would puncture it. Because of this, the measurements obtained from the arterial wall tests were ignored due to the possibility of large inaccuracies.

Furthermore, it was noted that the amount of blood on and around tested tissue played a large role in the measured impedance of tissue types. Blood soaked fat, for example, would have much lower impedance than fat tissue that has not been contaminated with blood. Thus, due to exceptionally high blood contamination in the fat tested on the third pig, the values were exceptionally low and these data sets were also thrown out.

Despite these complications, meaningful results were obtained from the experiments. It was noted that the mechanical design described in Chapter 8.1 functioned as planned, granted that the silver wire at the proximal tip of the arterial line was bent at a 180° angle, as to avoid having the tip of the silver wire piercing any tissue and potentially breaking the exposed tip of the wire.

Below are two box and whisker plots (Figures 9-2 and 9-3) and a relative frequency distribution chart (Figure 9-4), illustrating some of the results gathered. All data gathered in MS Excel was then processed using Excel's *quartile* and *average* functions, as well as its Data Analysis toolbox and histogram function to produce the data for the frequency distribution chart.

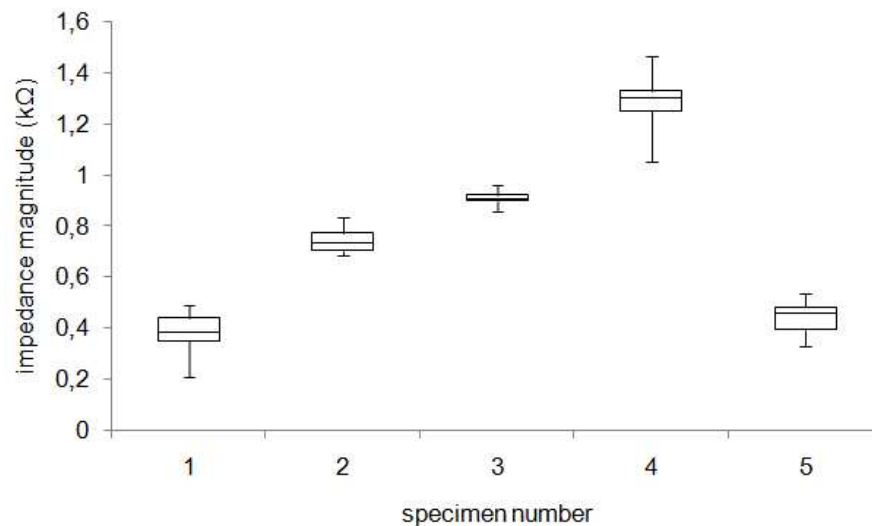


Figure 9-2: Blood impedance magnitude box and whisker plot

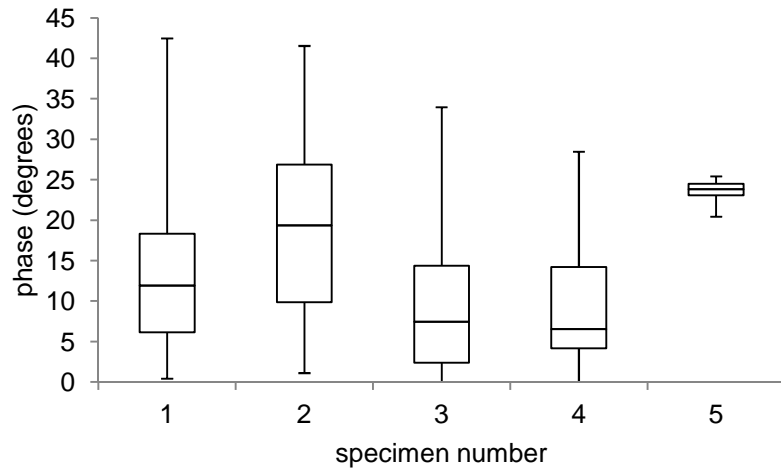


Figure 9-3: Blood impedance phase box and whisker plot

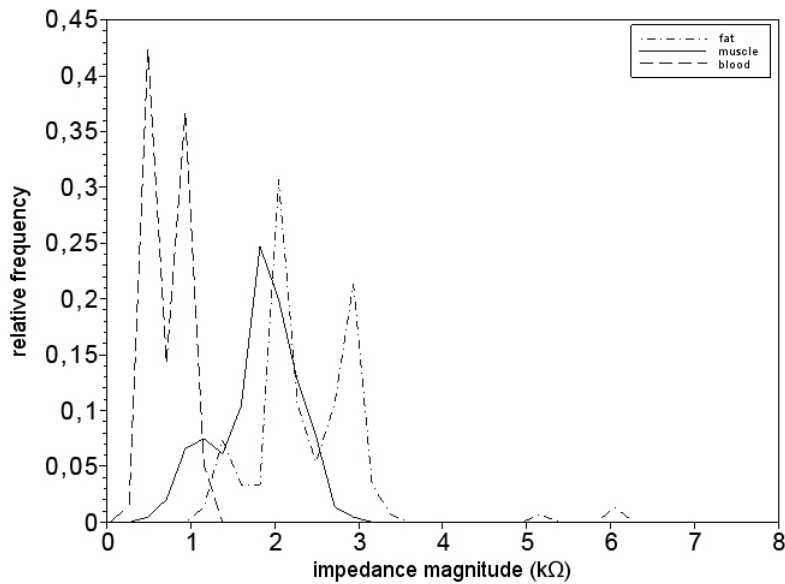


Figure 9-4: Relative frequency distribution chart of impedance magnitudes of blood, muscle and fat tissue

Figures 9-2 through 9-4 and Figures A.2-1 through A.2-4 illustrate the information gathered from the testing. From Figures 9-3, A.2-2 and A.2-4 it can be seen that the phase measurements for the living tissue types were highly sporadic and unreliable. Figure A.2-1 shows that, aside from specimen #1, that there is consistency in the skeletal muscle impedance magnitude measurements.

Figure A.2-3 requires some explanation regarding the large difference in trends between the first three specimens and the last specimen. During the testing, it was found that the fat tissue that has been contaminated with blood showed an impedance slightly higher than muscle tissue. However, during the testing on specimen #4, care was taken to allow for testing on a dry section of fat, in the neck of the animal, which yielded the results indicated for specimen #4 on Figures A.2-3 and A.2-4.

Most importantly, however, is Figure 9-4, which shows the frequency of the occurrence of impedance magnitude values for the three tissue types, excluding the dry fat anomaly described above (it is assumed that the fat surrounding the arteries where an arterial catheter would be placed would not be the same dry fat found in the neck of the specimen). What the figure implies is that there is a fairly distinct difference in impedance magnitude between blood tissue and skeletal muscle tissue, while the difference in impedance magnitude between fat and skeletal muscle is less apparent.

It was also noted that the fat measurements taken in living animals was a lot more varied (but typically lower) than those taken in dead tissue samples. This was assumed to be due to the higher moisture content in living fat tissue. Furthermore, it was seen that impedance of skeletal muscle tissue measured slightly higher in living tissue samples than in dead samples. This could be attributed to the activity in living muscle tissue and the possibility of the structure of dead muscle tissue having deteriorated somewhat, causing less electrical resistance.

It was also noted during all of the experiments that the introduction of the modified arterial catheter and the AC signal had no physiological effects on the pigs. The heart rate, oxygen saturation and blood pressure of the specimens were monitored and no changes were found during the introduction of the AC signal.

Despite a number of problems during the animal testing phase, it was noted that the concept used in the modified arterial catheters was successful and could be developed further. It was also noted that it is possible to distinguish between different tissue types based on the impedance measured; however, the impedance gap separating the different tissue types is not as large as hoped for, leaving some accuracy to be desired. However, the detectable difference between blood tissue and other biological tissue was found to be highly apparent, meaning that the device would still be capable of determining when it is placed into the bloodstream with high accuracy.

It was decided after these experiments to do a final set of tests on living human specimens. The animal testing proved the prototype used to be functional. It also proved that the introduction of the AC signal to be safe, allowing for use on humans. Furthermore, it would be ideal to determine if human tissue shows the same results seen in the tests on animals. If the results were found to be similar, it would prove that an impedance guided arterial catheter could be a viable design for future human testing.

10. Final prototype design

The design of the final prototype was based on all of the design specifications stated in Chapter 4 and the results obtained from the animal testing phase. The final prototype would have to be designed in such a way as for it to be compliant to HREC (Human Research Ethics Council) regulations. This would mean for certain changes to be made to the prototype used in the animal testing phase.

The biggest difference between the procedure of the animal testing and the clinical trials would be that the testing during clinical trials would have to be done as per normal in medical practice. Thus, the arterial line would be inserted once, through the skin and into an artery and all measurements would have to be taken in that time span, unlike the animal testing, during which the arterial line could be inserted into target tissue types for specific tissue measurements.

This chapter is divided into four sections. The first being centred around the mechanical design of the prototype, the second section focusing on the electronics used in the design, the third focusing on the programming used and the fourth section discusses how the accuracy of this prototype was tested and verified.

10.1. Mechanical design

The major requirement for the electrodes on the arterial line for clinical trials would be that there could be no surface roughness on the cannula (roughness would cause the artery to spasm) and that the outer diameter of the cannula not be increased (to permit easier passage). This meant that using a nontoxic resin to bind the silver electrodes to the outside of the cannula would no longer suffice, as it added significantly to the thickness of the cannula and could cause a rough surface finish. With the appropriate equipment, the silver wire could be embedded into the cannula, or the cannula could be manufactured with the silver wire inside of it, but producing such cannula for the purpose of the clinical trials was not feasible. Therefore, a different design would have to be used.

It was decided to use the following design concept: An insulated silver wire (PFA insulated, 99,99% purity, coated diameter of 139,7 μm , purchased from A-M systems) would be fed through the central channel of the needle, until it would stick out at both ends of the needle. The silver wire exposed at the proximal end of the needle would then be bent 180° back, causing the silver wire to lie on top of the needle. The cannula would then be slid over the needle and the wire, tensing the wire and holding it in place. This would mean that the insulated silver wire would, at the proximal tip of the needle, leave the central channel of the needle and then loop back on the outside of the needle, underneath the cannula, thus leaving a small bent section of silver wire at the proximal tip of the

needle. Using a sharp blade, the insulation on the silver wire could be scraped off at the described bend of the silver wire, creating an exposed portion of the silver wire at the proximal end of the arterial line. This would thus serve as an electrode for measuring the impedance of the tissue, without adding any thickness to the cannula. This design is shown in Figures 10-1 and 10-2 below and illustrate the placement of the mentioned silver wire. This design is based on one of the concepts generated in Chapter 5-2.

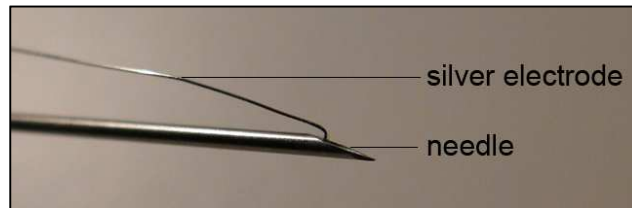


Figure 10-1: Prototype arterial catheter tip without cannula

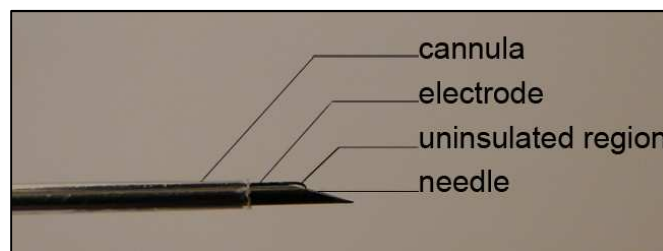


Figure 10-2: Prototype arterial catheter tip

A further advantage of this design would be that all modified components would be removed from the patient's body as soon as the needle is withdrawn from the cannula (versus the modified components only being removed once the cannula is removed). The disadvantages of this design would be that no measurements could be taken if the needle was withdrawn into the cannula and that the added effective thickness of the needle meant that the needle would be slightly harder to withdraw from the cannula.

10.2. Electronics design

The electronics used in the previous experiments would not be used. A smaller electronic setup was designed and used, in order to minimize the design. It was planned to use an IC capable of measuring impedances (the AD5933), but when working with the device, technical problems

arose, which necessitated the purchase of more of these ICs. Due to time and financial constraints, this was not feasible and the electronics described below were used instead.

The electronic design entailed a design that generated an AC signal, centred around 0 V and apply it to the unknown tissue. The signal measured over the tissue was then converted, to be read by an analogue to digital (A/D) converter, capable of reading values between 0 V and 5 V. The signal was analysed by the microprocessor and finally, the desired output was given. The electronic design was split up into the following sections:

- Power supply
- AC signal generation
- Signal converting
- Signal processing
- Control panel

The Arduino Mega 2560 [34, 35] was chosen as a development board for its strong microprocessor and A/D sampling capabilities. It would perform the signal processing and be responsible for the control of the system. The ICL8038 [36] was chosen to generate the AC signal at 30 kHz and would require both a +12 V and a -12 V voltage supply in order to produce a 5 V peak-to-peak signal, which would oscillate around 0 V. AD741 operational amplifiers (op-amps) [37] would be required to add a DC offset of 2,5 V to the return signal, to set the range of the input signal to 0 to 5 V, allowing it to be read by the A/D converter.

The Arduino Mega2560's A/D converter can sample at different rates. Changing the sampling rate is done by defining the value of a prescaler which is used to calculate the sampling rate as follows [35]:

$$ADC_{\text{Sample Rate}} = \frac{\text{Clock Speed}}{\text{Prescaler} \cdot 13} \quad (10-1)$$

The value of the prescaler is set to 2^n , where n is an integer between 1 and 7. This allows for different sampling rates to be obtained (calculated as 9,6 ksps to 615 ksps, using the Arduino's clock speed as 16 MHz) by setting the value of the prescaler in the code. However, raising the sampling rate of the A/D converter lowers the accuracy of the converter. Based on the Arduino Mega 2560 datasheet [35], accuracy is acceptable when the prescaler is set as 16, 32, 64 or 128 (the latter being the default setting). Aiming for both accuracy and a high enough sampling rate, the prescaler value was chosen as 16, which gives a maximum sampling rate of 76 ksps.

The power supply, based on the above specifications, would be required to produce the following voltages, for use in the system:

- +12 V
- -12 V
- +2,5 V
- Ground

Additionally, voltage regulators (LM7812 [38] for +12 V rails, LM7912 [39] for -12 V rails, LM7805 [38] for +5 V rails and LM136 [40] for the 2,5 V rails) would be required in order to maintain the voltages at a safe level. It was decided to allow the device to work off of either battery power or from a DC power source. The DC power source would not be used during the clinical trials, but would be used during testing and debugging of the device. Two 9 V batteries were connected in series to give a total of 18 V supply voltage when set to battery mode. Figure 10-3 illustrates a schematic of the power supply used.

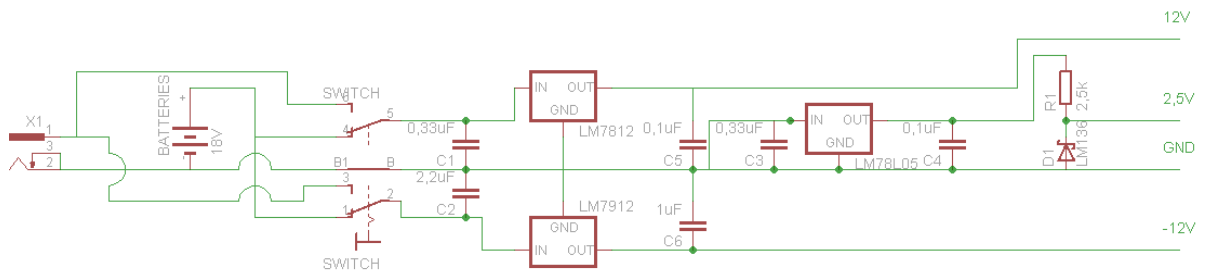


Figure 10-3: Power supply schematic

The AC signal generation portion of the device would be centred around the ICL8038, a programmable waveform generator, capable of producing triangle, square or sine waves at a set frequency. The frequency is determined by the values of R_1 , R_2 and C_1 , as seen in Figure 10-4 and is calculated as (if $R_1=R_2=R$):

$$F = \frac{0,33}{RC_1} \quad (10-2)$$

The derivation for eq. 10-2 can be found in the data sheet for the ICL8038 [36]. Figure 10-4 below illustrates the schematics for the portion of the device used to generate the signal required.

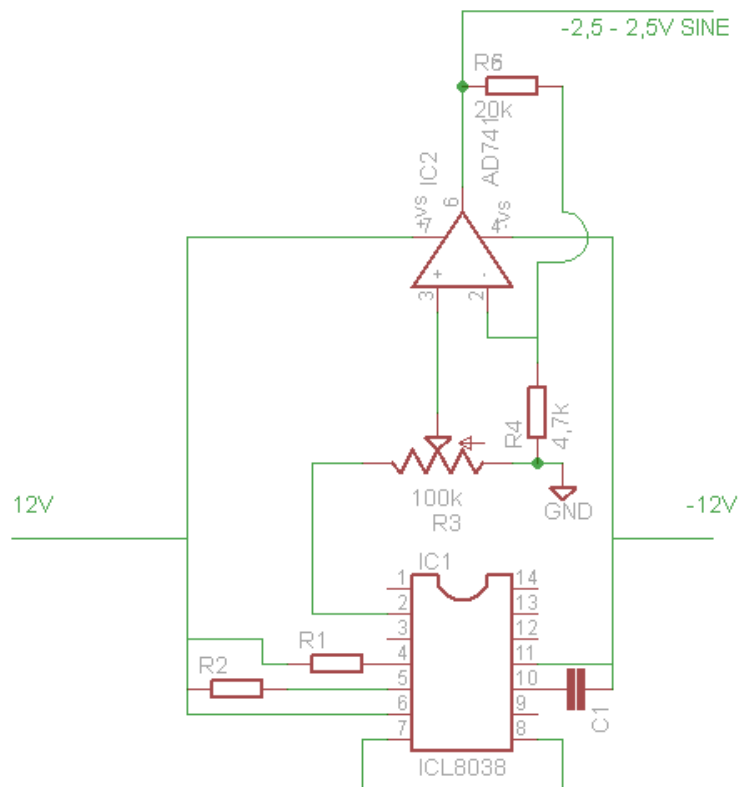


Figure 10-4: AC signal generator schematic

The signal converting portion of the device takes the two return signals (one from measuring the total voltage, or V_t from Figure 5-3, the other measuring the voltage over the load, or V_L from Figure 5-3) and convert them for processing by the A/D converter. The signals would have a maximum voltage of 2,5 V and a minimum of -2,5 V, while the A/D converter could read a minimum of 0 V and a maximum of 5 V. Thus, two op-amps were used as adder op-amps, adding the 2,5 V supplied from the power supply. Buffer op-amps (AD741) were also added, both on the output of the signal generator IC and at the inputs to the adder op-amps, as otherwise the impedance of the components would contaminate the results measured. Figure 10-5 illustrates the schematic for the portion of the device responsible for the converting of the signals before they would reach the microprocessor.

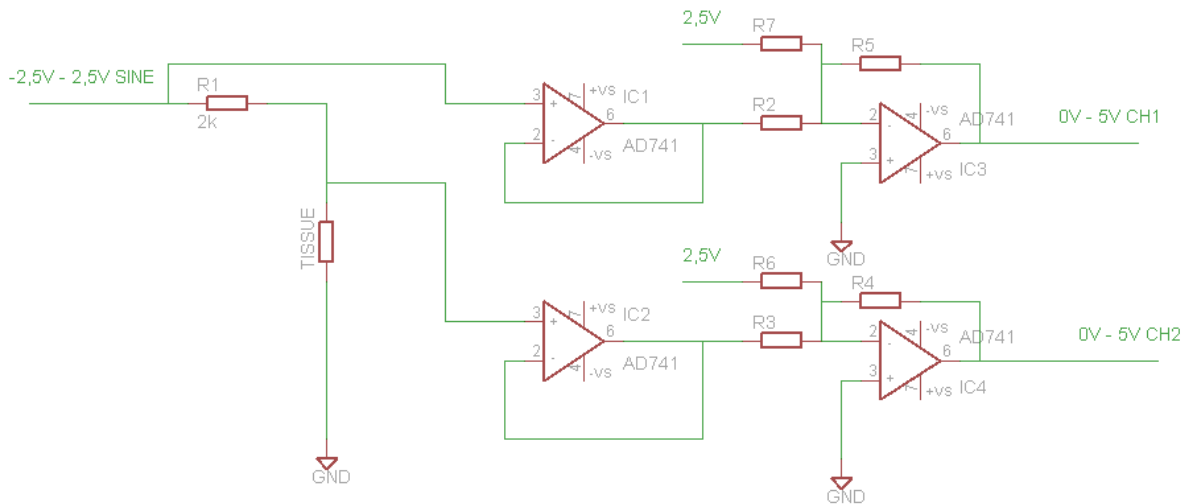


Figure 10-5: Signal converting schematic

The signal processing is handled by the Arduino Mega2560. The Mega2560 uses two A/D converter channels for the processing of the signals. Utilizing the control panel (described below) and the programming (described in Chapter 10.3), the Mega2560 can convert the incoming signal to the impedance values measured. It is capable of storing said measurements on a built in EEPROM on the Mega2560, which can then later be accessed.

The control panel incorporated the following parts:

- An ON/OFF switch
- A three-way toggle switch
- A single button
- An RGB LED
- A USB port
- A DC input port

The ON/OFF switch was used to switch the device between using its battery or a DC input. If there is no DC input, switching it to DC input would function as OFF.

The three-way toggle switch was used to set the mode of operation of the device. The three modes are:

1. Record

2. Standby

3. Return

The record mode enables the device to save measurements onto the EEPROM. The built in EEPROM has space for 512 8-bit values. The record mode thus scales the measurements and then saves impedance magnitude values in the first 256 bytes on the EEPROM (0 – 255) and the impedance phase values in the last 256 bytes (256 - 511). Once all 512 bytes on the EEPROM have been filled, recording stops and a flag is set to prevent accidentally overwriting recorded data.

The standby mode produces the AC signal and take measurements, but does not save any measurements. It is used when the device is switched on, before recording starts. Once recording ends, it switches back to standby.

The return mode reads the values from the EEPROM and writes them to a PC, through the USB interface of the device. The data returned is scaled back to counteract the scaling done by the recording mode and is transmitted through the serial interface. The data is transmitted in such a way that the 256 impedance magnitude values are transmitted first, then the corresponding 256 phase values.

The button can be used to erase all data on the EEPROM, setting all values in the EEPROM to zero.

The RGB LED is able indicate the process of recording, returning and erasing data and flashes a corresponding colour during the different processes, to allow the operator to know when recording, returning or erasing is complete.

The USB input is used to upload the programming code to the Mega2560, to power the device when measurements are returned and to transmit the returned data from the Mega2560 to the operator's computer.

The DC input was used during testing and debugging of the device, when strictly using batteries was not required. Figure 10-6 shows a picture of the control panel described. Figure 10-7 shows a diagram of all of the above components when connected to each other as described.



Figure 10-6: Control panel of prototype

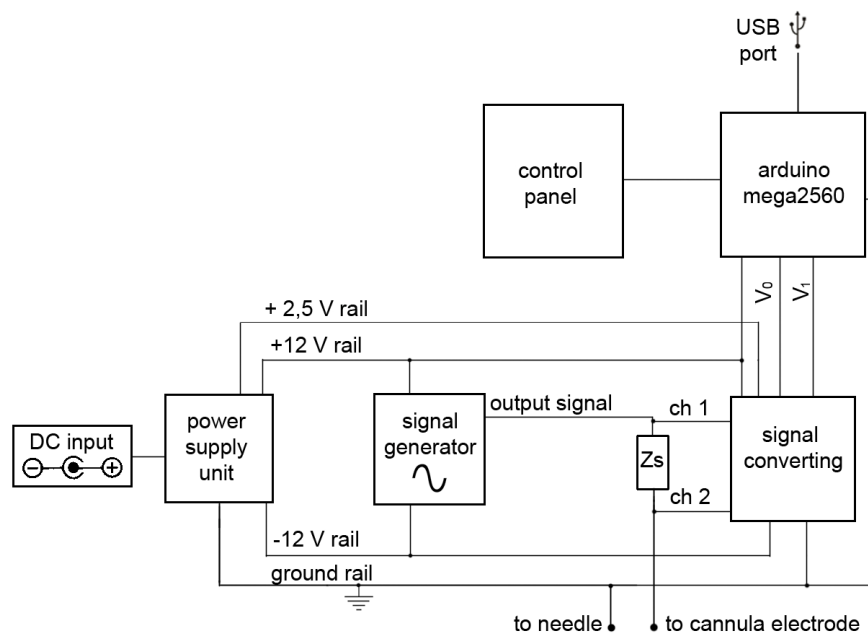


Figure 10-7: Diagram of components

10.3. Programming

The programming of the Mega2560 was required to take accurate measurements on the two used A/D converter channels and use those measurements to calculate the impedance measured. It needed to perform calibrations prior to measurements, take measurements, determine the relative phase shift between the two channels, calculate the impedance and then act depending on what settings were set on the control panel. The

main program is a looping code, which follows the flowchart seen in Figure 10-8.

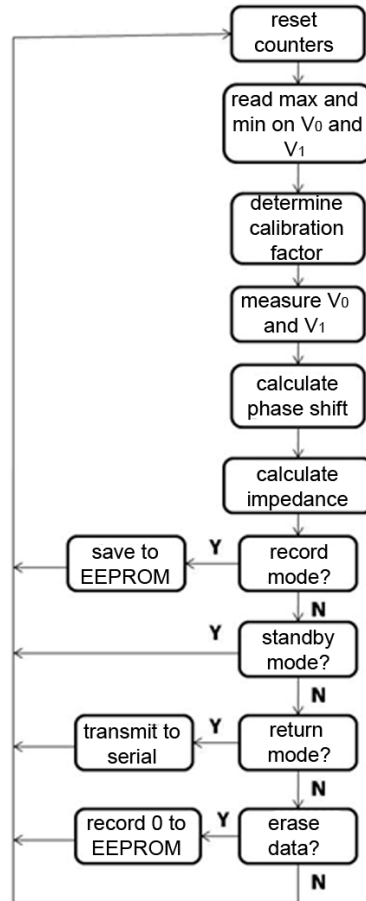


Figure 10-8: Flowchart of programming code

The first step in the code is to clear all variables and counters that need to be cleared. These include variables for previous measurements and counters for loops throughout the code.

The second step is to determine the maximum and minimum voltages read on channels V_0 and V_1 . These are required to calibrate the measurements. The values measured would be between 0 and 1023 (corresponding to 0 V and 5 V, respectively), with the theoretical middle point at 512 (2,5 V). Measurements are then processed by subtracting 512, to shift the measured values back to a range from -512 to 512 (from -2,5 V to 2,5 V), which is then used for calculations. However, if this assumed middle point is not at exactly 512, then future calculations could be inaccurate. Thus, to calibrate the system, $V_{x\max}$ and $V_{x\min}$ (the respective maximum and

minimum measurements read on channel x) are used to determine the real middle point before calculations, as follows:

$$F_{\text{Cal}} = V_{\text{xmin}} + \frac{(V_{\text{xmax}} - V_{\text{xmin}})}{2} \quad (10-3)$$

F_{Cal} , the calibration factor, is then used to accurately shift the measured values to the -512 – 512 range.

Once the maximum and minimum voltages are read and the calibration factor calculated, the next step is to measure one measurement per channel with a known time delay between the two measurements. With a known frequency of 30 kHz, the period of the signal can be determined using:

$$\tau = \frac{1}{F} \quad (10-4)$$

Which leads to $\tau = 33,34 \mu\text{s}$. Using the Mega2560's micro function, the time difference (in microseconds) can be measured in between two points in the programming code. Using this, it was possible to determine the time delay between two A/D measurements. That time delay was calculated to be $16 \mu\text{s}$. Thus, adding a second time delay to set the delay between the measurement of V_0 and V_1 equal to $\tau = 33,34 \mu\text{s}$ would allow the measurement of V_1 to be taken a full 360° after the measurement of V_0 . This required time delay was easily calculated as $17,34 \mu\text{s}$. Using the Mega2560's delay function, the measurement of V_1 could thus be delayed for the calculated amount.

After the measurements are taken for V_0 , $V_{0\text{max}}$, V_1 and $V_{1\text{max}}$, it is possible to determine the phase angle of both points using:

$$\theta_x = \sin^{-1}\left(\frac{V_x}{V_{\text{xmax}}}\right) \quad (10-5)$$

With the values for θ_0 and θ_1 known, it is possible to determine the relative phase shift between the two signals, by using:

$$\theta_p = |\theta_0 - \theta_1| \quad (10-6)$$

However, when the two phases occur over either the 90° or the 270° turning points in the sinewave, a mathematical error would occur. Figure 10-9 illustrates two conditions where this error would take place.

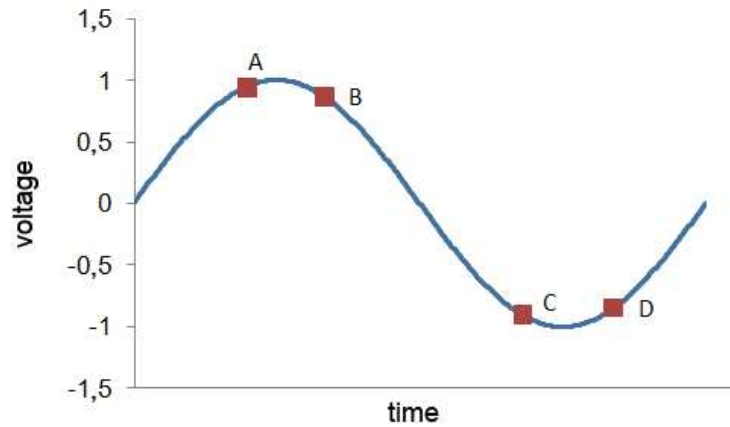


Figure 10-9: Theoretical case for turning point errors

The two conditions in Figure 10-9 show where the first channel measurements are taken at points A or C, followed by the second channel measurements on points B or D. In both these cases, the position of B and D relative to the turning point of the wave would be ambiguous, unless B is smaller than A and D is larger than C (these conditions indicate that points B or D have crossed over the turning point of the wave). However, if B is larger than A, or D smaller than C, an inaccurate measurement would be taken. The code was thus programmed to compare the phase value obtained to the previous value measured, in the case that the first measurement is either larger than 70° or smaller than -70° . If it is found that this new value differs with more than 10° from the previous measurement, this new value for the phase is calculated as:

$$\theta_{NP} = \frac{(\theta'_{p} + \theta_p)}{2} \quad (10-7)$$

This correction would not entirely eliminate this error, but it would reduce the error sufficiently.

Once the phase shift has been calculated, the Mega2560 can calculate the impedance magnitude and phase. Using eq. 5-6 to eq. 5-16, the impedance magnitude and the phase are calculated and available.

The final steps depend on the status of the buttons and switches on the control panel. If the device is in standby mode, no action would be taken and the loop would restart. If the device is in record mode, the impedance magnitude and phase would be scaled to an 8-bit value, by the following equations:

$$|Z|_{EEPROM} = \frac{|z|}{SF_{|z|}} \quad (10-8)$$

$$\theta_{\text{EEPROM}} = \frac{\theta}{SF_{\theta}} \quad (10-9)$$

Both scaling factors were determined by choosing the maximum amount to be saved for both impedance magnitude and phase. These values were chosen by the operator of the device, prior to testing. The scaling factors were thus calculated by:

$$SF_{|z|} = \frac{|z|_{\text{max}}}{2^8} \quad (10-10)$$

$$SF_{\theta} = \frac{\theta_{\text{max}}}{2^8} \quad (10-11)$$

Using eq. 10-8 to eq. 10-11 and selecting the maximum recorded values for the impedance magnitude and phase, it is possible to then scale the values to be written into the EEPROM. After the values are written, a counter increments and the loop would restart.

If the device is in return mode, it would enter a loop, during which it reads each value stored on the EEPROM and, using eq. 10-8 and eq. 10-9, it reverses the scaling done during the recording phase. The data is then transmitted via USB and the Arduino software interface to a PC for analysis and storage. Once all values are read, converted and transmitted, the loop restarts.

If the device is in erase mode, it enters a loop, during which every address in the EEPROM is set to 0. Once all addresses in the EEPROM are set to 0, the loop restarts.

10.4. Prototype testing

Before the designed prototype could be used in clinical trials, it would first have to be tested for its accuracy. In order to test the prototype, 1% tolerance resistors and ceramic capacitors were coupled in series to the measuring terminals of the prototype. The device was then set to record (as described in Chapter 10.3) and, once the recording was done, it was set to return the values measured. These values measured were then used to determine the accuracy of the system, by comparing the values recorded to the theoretical value of resistor/capacitor setup.

The scaling factor (mentioned in Chapter 10.3) were used with:

$$|Z|_{\text{max}} = 20 \text{ k}\Omega$$

$$\theta_{\text{max}} = 90^{\circ}$$

Which led to:

$$SF_{|z|} = 0,078125$$

$$SF_{\theta} = 0,3515625$$

These scaling factors also represent the resolution of the prototype and thus represent the minimum error that could be expected from the system.

To determine the accuracy of the system, it was decided that testing would have to be done using the values seen in Table 10-1. A total of nine tests were performed, testing a combination of levels of impedance phase and magnitude. Each test was repeated ten times, to measure the reproducibility of the prototype, to obtain a better idea of the accuracy of the system.

Using eq. 3-1 to eq. 3-4, the required theoretical resistor and capacitor values were calculated. However, some of these values were rounded to nearby available values of resistors and capacitors available for purchase. The actual used values were then used to determine the true expected values of the impedance magnitude and phase ($|Z|'$ and θ' respectively). All of these values are shown in Table 10-1 below.

Table 10-1: Values used for testing of prototype

Test	$ Z $ (k Ω)	θ (°)	R_T (k Ω)	C_T (μF)	R_R (k Ω)	C_R (μF)	$ Z '$ (k Ω)	θ' (°)
1	0,5	0	0,5	N/A	0,5	N/A	0,5	0
2	5	0	5	N/A	5	N/A	5	0
3	10	0	10	N/A	10	N/A	10	0
4	0,5	30	0,433	21,22	0,432	22	0,495	29,16
5	5	30	4,33	2,122	4,32	2,2	4,95	29,16
6	10	30	8,66	1,061	8,64	1	10,14	31,56
7	0,5	60	0,25	12,25	0,25	12,2	0,502	60,10
8	5	60	2,5	1,225	2,5	1,22	5,02	60,10
9	10	60	5	0,613	5	0,68	9,26	57,02

The results of the prototype testing can be found in Appendix A.3. Figures A.3-1 through A.3-18 show bar graphs of the impedance magnitude and phase errors (both average and maximum error) over the ten repeated tests run per test setup. The results were robust, especially in terms of the impedance magnitude results. The impedance phase accuracy was not as good as the previous prototypes, but this was due to the inaccuracies at

certain stages in the waveform, as illustrated in Figure 10-7. However, it could be seen that the repeatability of the prototype was acceptable, with the average impedance magnitude error being below 0,1 k Ω in most cases. The average impedance phase error was found to be below 4° in the first six tests and below 7° in the last three tests. This level of accuracy was deemed acceptable.

Finally, the signal generated by the ICL8038 was also tested, using the Velleman PCSU1000 Oscilloscope's waveform parameters function. This calculated the waveform's frequency to be 30,7 kHz, the maximum voltage to be 2,58 V and the minimum voltage to be -2,43 V.

Figure 10-10 illustrates a photo taken to demonstrate the finished prototype in use. It can be seen that all of the electronics are contained within the housing, exposing only the control panel and the wires connected to the prototype arterial catheter.

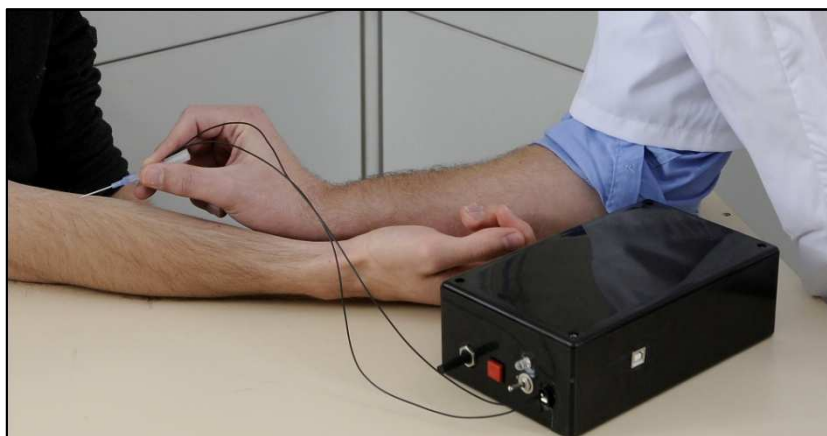


Figure 10-10: Demonstration of prototype being used

11. Clinical trials

The process for the clinical trials is explained in this chapter and is divided into three sections. The first section explains the experimental design and protocol, detailing the goals of the experiment, information on the protocol submitted, the components used, how the system was calibrated, the exclusion criteria for the trials, the way in which data was captured, the expected results and how the results were processed. The second section, the experimental procedure section, covers the preparatory steps for the experiments and the format of the experimentation. The third section, the results and conclusion, covers the data gathered, the processed data, comparisons between the

expected model and the actual results, interpretation of the processed results and discussions based on the results.

11.1. Experimental design & protocol

The clinical trials phase was the final phase of testing for the prototype arterial catheter. The goals were to determine whether or not the design of the prototype is sufficient for use by medical practitioners as well as determining whether or not the impedance values measured in living human tissue would indicate a discernible difference that would allow for the prototype arterial lines to be guided by said impedance difference. Additionally, feedback was obtained from the medical practitioners who would use the device, to identify any problems with the device, in terms of usability.

To perform the clinical trials, approval from the Stellenbosch HREC committee would first be required. A full clinical trial protocol was submitted to the HREC committee in March 2012 and, despite the proposal necessitating revisions twice, was approved in July 2012. Extracts from the final protocol can be found in Appendix C.

The prototype used was the prototype designed for the clinical tests, as described in Chapter 10, which includes all of the components, how the system was calibrated and the expected accuracy of the device.

The clinical trials were performed at Tygerberg Hospital, under the supervision of Prof AR Coetzee, head of the Department of Anaesthesiology. The testing was done on patients at the hospital who required the insertion of an arterial line. These patients were asked for their participation in the clinical trials and the modified arterial line was used if they would give their consent. The exclusion criteria for subjects would be the declination of consent or any patients with any of the following conditions: congenital heart disease, cardiomyopathy, cardiac ischaemia/infarct/unstable angina, torsade de pointes, hyperkalaemia, electric shock or patients on anti-dysrhythmic drugs, as per request of the Human Research Ethics Council.

Unlike the animal testing phase, no incisions could be made for the purpose of the testing and thus the only way to take measurements was as the prototype arterial line is inserted into the artery. Thus, the prototype took measurements over time, from the point at which the proximal end of the arterial line entered the patient's skin, to the point where it was located in the patient's artery. This resulted in two sets of data per patient: one with the impedance magnitude over time and the other with the impedance phase over time.

Judging from the animal testing, a theoretical expected model was derived. The expected model (seen in Figure 11-1) illustrates that one would expect

there to be a series of high-level impedance magnitudes (referred to as $|Z|_H$ and illustrated as the high level values on Figure 11-1) as measurements taken in between the skin and the lumen of the artery. These high level measurements may vary depending on what tissue types are encountered in between the skin and the artery, but should remain substantially higher than the impedance of the blood inside the artery. In a discussion with Dr. A Rocher (the assisting anaesthesiologist in the clinical trials), it was mentioned that the two main tissue types to be encountered are subcutaneous tissue and fat tissue. The high level values in Figure 11-1 are thus separated according to those two tissue types. Based on the results from the animal testing, these high level values should vary between 1 k Ω and 10 k Ω , with the fat tissue closer to the artery having a higher moisture content and thus a lower expected impedance magnitude. The model then illustrates that once measurements are taken inside the lumen, a series of low-level impedance magnitudes (referred to as $|Z|_L$ and illustrated as the low level blood values on Figure 11-1) would be measured and it would stay there as long as the proximal tip of the needle stays in the artery. These low level values correspond solely to the blood impedance magnitude and, based on the results from the animal testing, should range between 0,4 k Ω and 1,2 k Ω .

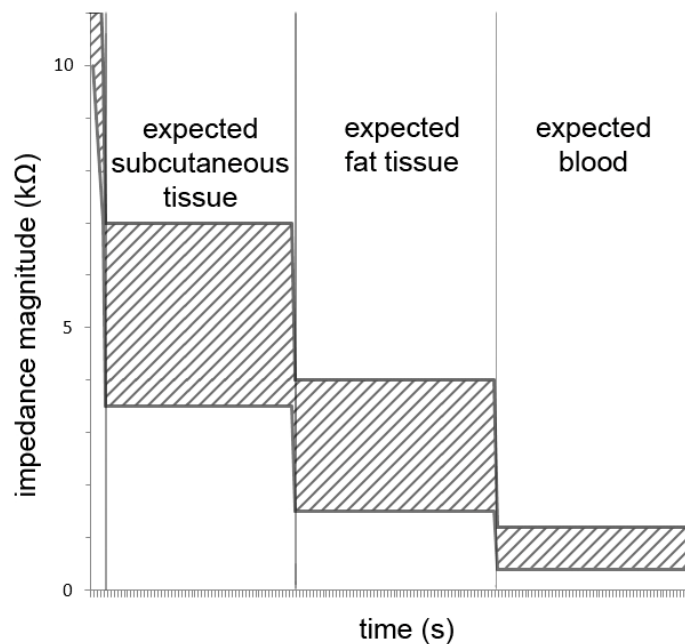


Figure 11-1: Theoretical expected model, showing impedance magnitude over time

No reasonable model could be created for the impedance phase, due to the unpredictable nature of the phase measured during the animal testing.

However, these tests would verify if there is a more predictable pattern in the phases of living human tissue.

The success of the clinical trials would be evaluated based on the usability of the prototype designed and in the measurements taken of the human tissue encountered in the path of the proximal tip of the arterial line. If the measurements showed consistent trends predicted by the expected model, the experiments would be deemed successful. If this were the case, a theoretical threshold value (referred to as $|Z|_T$) between the high level impedance magnitude and the low level impedance magnitude would be established. This value of $|Z|_T$ is determined by analysing at which value of $|Z|_T$ the probability of the $|Z|_L$ going over $|Z|_T$ is lowest, as well as where the probability of the $|Z|_H$ going below $|Z|_T$ is lowest. Thus, $|Z|_T$ is determined by:

$$\min_{|Z|_T \in \mathbb{R}} (P[(|Z|_T > |Z|_H) \cap (|Z|_T < |Z|_L)]) \quad (11-1)$$

This minimization problem was performed on each of the test subjects, in order to find the optimal value of $|Z|_T$ for each subject. After this, the values of $|Z|_T$ were compared between subjects and the variation between these values were analysed to determine whether or not the values found for $|Z|_T$ were feasible.

An identical approach would be used to determine a threshold value for the impedance phase, if the phase results indicated that it could be possible to discern between blood tissue and other biological tissue utilizing the impedance phase.

11.2. Experimental procedure

The clinical trials were done in Tygerberg Hospital, on patients who have given consent and do not fall under the afore mentioned exclusion criteria. These patients received medical treatment which included the administration of an arterial line, regardless of the clinical studies.

The arterial lines were only administered to patients who had already been anaesthetised, as the insertion of arterial lines on conscious patients would require local anaesthetics at the point of insertion. The use of local anaesthetics would be undesirable as it was assumed that the chemical compound of local anaesthetics could contaminate the measurements taken after being absorbed into the target tissue. Subjects were thus anaesthetized before the administration of the arterial line.

The modified arterial lines described in Chapter 10 were gas sterilized prior to the day of testing. The exterior of the electronic setup was cleaned by hand with a fine cloth dipped in ethanol in between tests.

Prior to insertion, the electronics were connected to the modified arterial line prototype and the electronics switched on. A test reading was taken by

switching the device to "Record" mode. Visual feedback, by means of the RGB LED indicated whether or not the device was functioning as intended. If this was the case, the insertion of the arterial line prototype was initiated.

The medical practitioner administering the arterial line was instructed to inform the author holding the electronics when he started the insertion process and at this stage, the author set the device to record and started taking time measurements. Once the medical practitioner observed a pulsatile blood return in the chamber at the distal end of the arterial catheter prototype, the time measurements were stopped, but recording continued until the EEPROM in the device was full and the device stopped recording.

Once this was done, the author and the medical practitioner evaluated if the arterial catheter was successfully placed. In the case it was, the medical practitioner removed the needle from the arterial catheter and the author disconnected the electronics from the arterial catheter prototype. The cannula remained inside the patient until the medical procedure was completed, as is common medical practice, while the needle (with the silver wire) was disposed of, as in common practice. In the case in which the medical practitioner was unsuccessful in placing the arterial catheter, the arterial catheter was removed, the data recorded was erased and the arterial catheter was reinserted, while recording was reinitiated, as described in the previous paragraph.

Afterwards, the author connected the electronics to a PC and transferred the data recorded from the device to the PC, using the Return function described in Chapter 10. This data was stored in a spreadsheet for future analysis, while the data was cleared from the prototype device. The device was then cleaned, as mentioned above, and be ready for the next test.

11.3. Results and conclusion

The results gathered from the clinical trials were informative and mostly positive. As an initial study, ten arterial catheter prototypes were produced and ten patients were approached for testing, of which all ten gave their consent for the testing.

The first thing that was noted during the testing was that the recording window programmed into the electronics was too small and would thus not record the entire travel of the proximal tip of the arterial catheter into the subject and it is because of this that the first two test subjects did not produce results as hoped for. The first set of results showed only high-level impedance data, with some variation in the high level values, while the second set of results showed only low-level impedance data. After these two tests, the code for the device was modified for a much larger recording window. The initial setup would record 256 measurements over a window of 2 seconds (128 Hz), while the altered setup would record 256 measurements over a window of 12 seconds (21,3 Hz). This new time

window was decided based upon the recommendation of the medical practitioners inserting the arterial catheters during these tests.

After these modifications were applied, the prototype functioned better, taking measurements of the entire insertion process, with results shown below in Figures 11-2 to 11-8. However, on the fifth test subject, an arterial catheter was broken, as the cannula deformed due to the thick skin of the patient. This unfortunately cost one prototype arterial catheter. Thus, due to the first two sets of data being recorded over too small of a time window and the loss of a prototype arterial catheter, a total of seven sets of data were obtained which illustrate the measurements under ideal circumstances. Below are seven figures, illustrating the impedance magnitude over time in each of the patients.

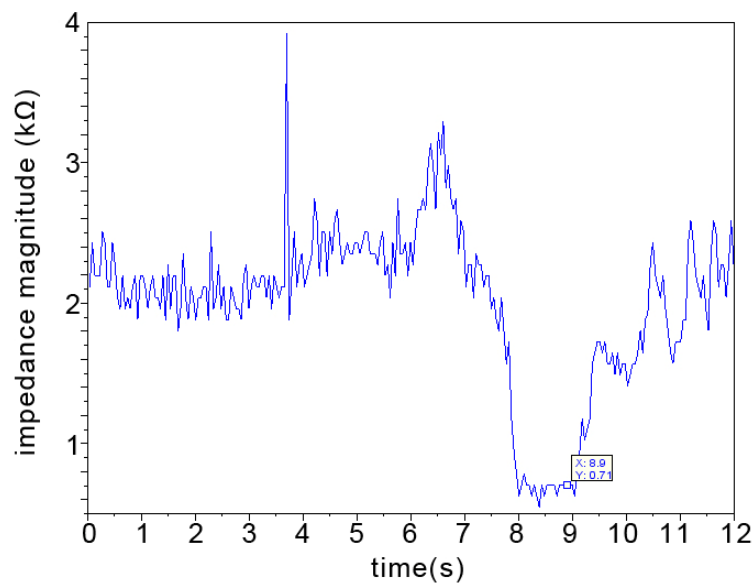


Figure 11-2: Graph illustrating the impedance magnitude over time in subject 3

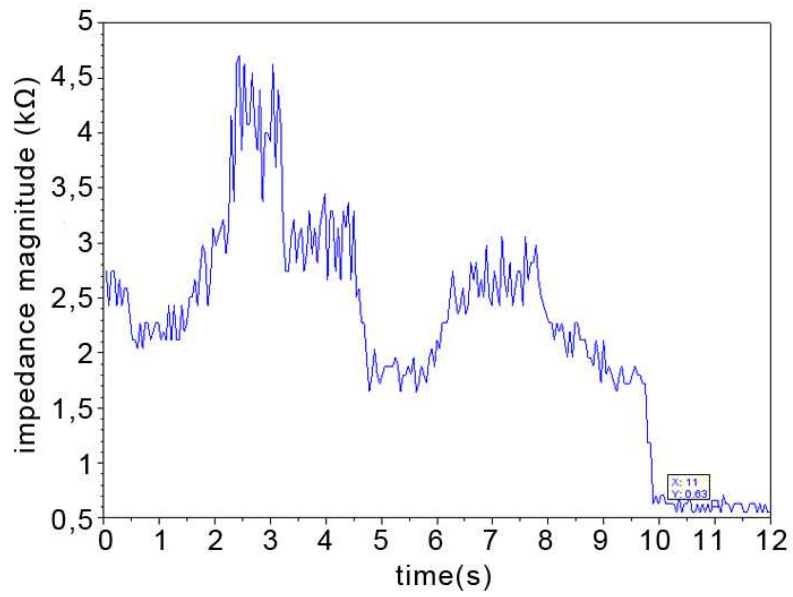


Figure 11-3: Graph illustrating the impedance magnitude over time in subject 4

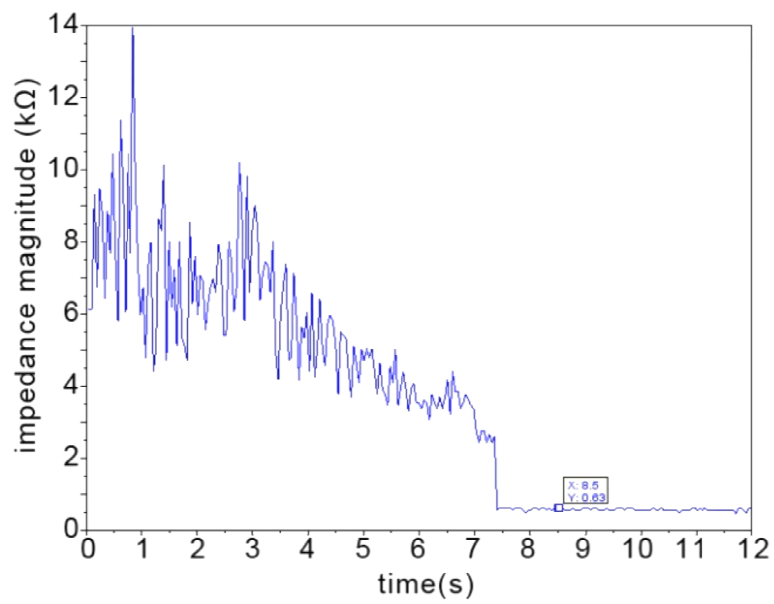


Figure 11-4: Graph illustrating the impedance magnitude over time in subject 6

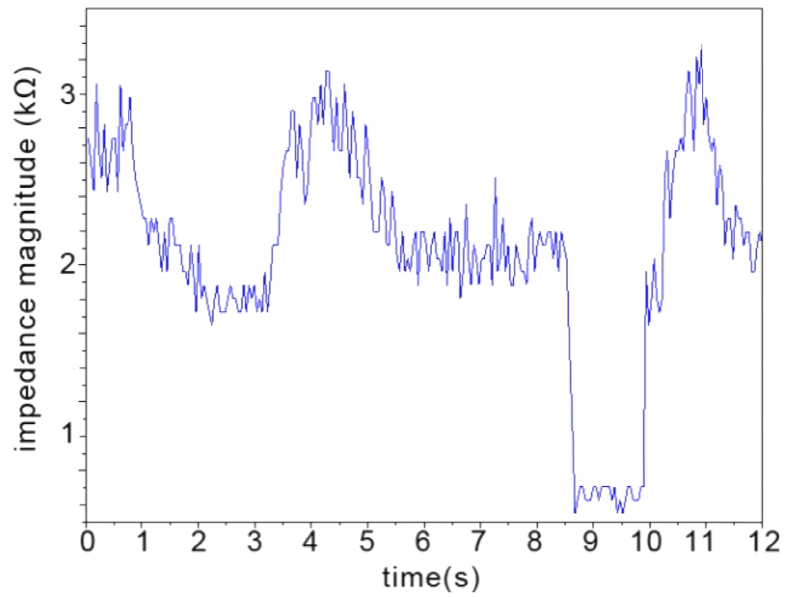


Figure 11-5: Graph illustrating the impedance magnitude over time in subject 7

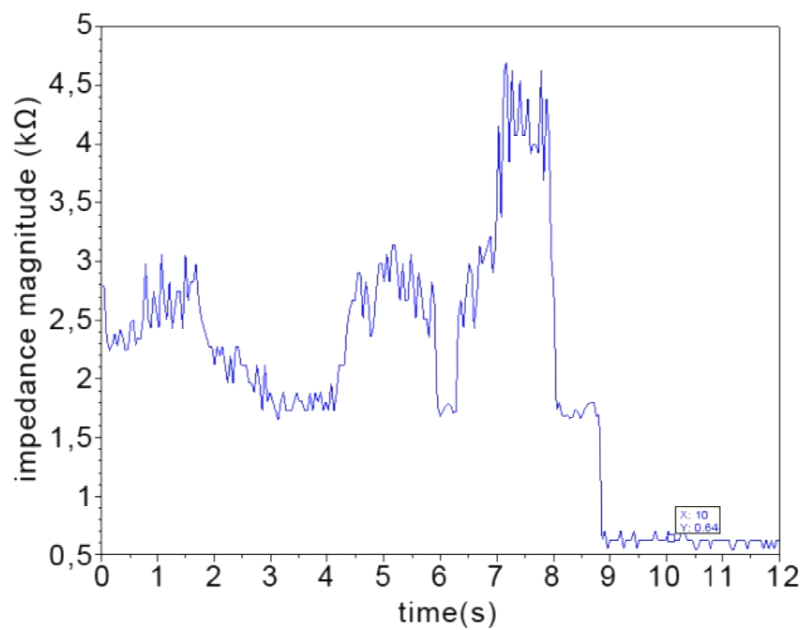


Figure 11-6: Graph illustrating the impedance magnitude over time in subject 8

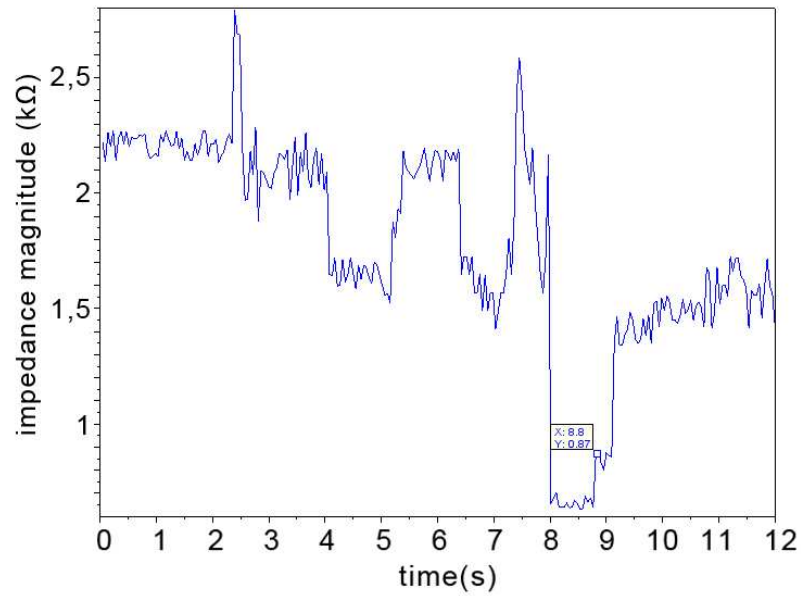


Figure 11-7: Graph illustrating the impedance magnitude over time in subject 9

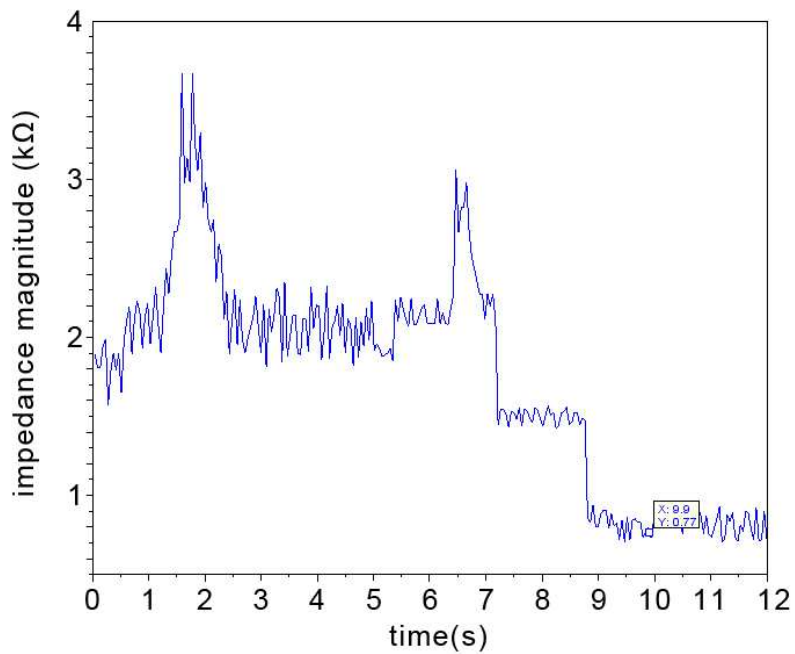


Figure 11-8: Graph illustrating the impedance magnitude over time in subject 10

Figures 11-2 to 11-8 all illustrate the impedance magnitude over the 12 second recording window described previously, while Figures A.4-1 to A.4-7 show the impedance phase over the same time window. Figures 11-2, 11-5 and 11-7 show cases where the practitioner pushed the prototype

arterial catheter through the artery, while Figures 11-3, 11-4, 11-6 and 11-8 show cases where the placement was done without having to pierce through both ends of the artery. The forms of placement were explained by the practitioner after the procedure and was noted when the data was being processed. The data markers on the graphs indicate at which time (correlating to the measurements) the pulsatile blood return was observed. In the case of Figure 11-5, no pulsatile blood return was noted, due to abnormally low blood pressure in the patient. These data markers thus indicate that the low impedance levels noticed in these graphs represent the impedance measurements of blood. It was thus concluded that these low level impedance measurements are an indicator for successful catheterization.

Comparing these results to the expected model, it appears that the clear difference between the low level impedance and the high level impedance is present. Figures 11-9 and 11-10 below show the overlaid model shown in Figure 11-1 and the results seen in Figures 11-2 and 11-3, respectively.

It can be clearly noticed that the difference between the impedance magnitude of blood and other bodily tissue behaved as expected. It can also be noted that the impedance magnitude value for the subcutaneous tissue is a lot lower than expected, as it appears to behave similarly to the fat tissue. The fat tissue impedance magnitude correlates well with the expected model, as does the blood impedance magnitude. Judging from Figures 11-2 to 11-10, it can be seen that the impedance magnitude of the different tissue between the skin and the lumen of the artery are difficult to distinguish, while it is very simple to distinguish between these tissue types and blood.

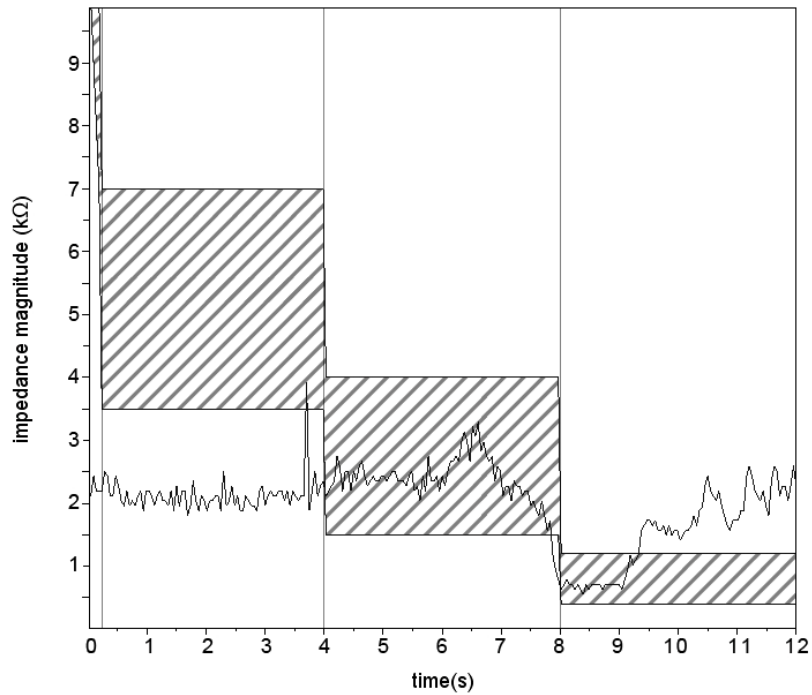


Figure 11-9: Expected model overlaid with impedance magnitude over time of subject 3

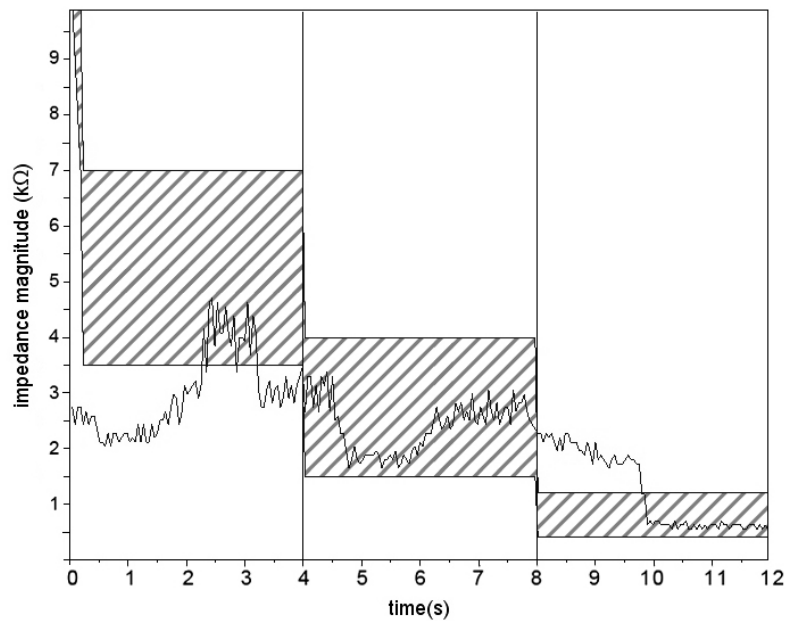


Figure 11-10: Expected model overlaid with impedance magnitude over time of subject 4

From the confirmation of the pulsatile blood return, the knowledge of the way in which the proximal tip interacted with the lumen of the artery and the

similarities between the theoretical expected model and the graphs that were obtained from the tests, it can be seen that the system behaved as expected, with regards to the impedance magnitude. This conclusion was made based on:

- The repeated evident difference between an apparent low-level impedance and an apparent high-level impedance, as seen in the expected theoretical model.
- The pulsatile blood return was measured shortly after the system measured the low-level impedance, implying that the low level impedance magnitudes indicate placement in blood and thus successful catheterization.
- The low level impedance was found to remain at a low-level state in cases where the prototype arterial catheter was not pushed straight through the artery wall, while the low level impedance state tended to revert to a high level state in cases where the prototype arterial catheter did pierce straight through the artery.

From Figures 11-2 to 11-10, it is possible to see that there is a clear threshold between the high-level impedance magnitude and the low-level impedance magnitude and, based on inspection, it would appear that this threshold's value would be similar in all of the subjects.

Taking the data that was measured and splitting it between the high-level impedance magnitudes ($|Z|_H$) and the low-level impedance magnitudes ($|Z|_L$), these two data sets were used to find the optimal value for the threshold between these two data sets ($|Z|_T$). The probability analysis was run using values of $|Z|_T$ from 0,6 k Ω and 1,9 k Ω . The tables that illustrate the probabilities of values of $|Z|_T$ being greater than $|Z|_H$ and lower than $|Z|_L$ can be found in Appendix A.4. An extract of the results can be seen in Table 11-1 below, which illustrates the probability of varying values of $|Z|_T$ being both smaller than values in $|Z|_L$ and larger than values in $|Z|_H$ in the data sets of each test. It also shows the average probability taken over the 7 tests. The results obtained indicate that the optimal value for $|Z|_T$ is between (and including) 1,2 and 1,3 k Ω , as seen in Table A.4-3, showing a 99,41% chance of accurately determining in which impedance category the measured impedance is, with the threshold between the two categories at the calculated value of $|Z|_T$.

Table 11-1: Extract of combined probability table

$ Z _T$ (k Ω)	Test 1	Test 2	Test 3	Test 4	Test 5	Test 6	Test 7	Average
0,9	0,219	0,044	0,000	0,036	0,000	0,000	0,070	0,053
0,95	0,156	0,044	0,000	0,036	0,000	0,000	0,000	0,034
1	0,156	0,044	0,000	0,036	0,000	0,000	0,000	0,034
1,05	0,129	0,044	0,000	0,036	0,000	0,000	0,000	0,030
1,1	0,129	0,044	0,000	0,036	0,000	0,000	0,000	0,030
1,15	0,103	0,044	0,006	0,000	0,000	0,000	0,000	0,022
1,2	0,022	0,013	0,006	0,000	0,000	0,000	0,000	0,006
1,25	0,022	0,013	0,006	0,000	0,000	0,000	0,000	0,006
1,3	0,022	0,013	0,006	0,000	0,000	0,000	0,000	0,006
1,35	0,022	0,013	0,006	0,000	0,000	0,013	0,000	0,008
1,4	0,022	0,013	0,006	0,000	0,000	0,039	0,000	0,011
1,45	0,027	0,013	0,006	0,000	0,000	0,079	0,043	0,024
1,5	0,040	0,013	0,006	0,000	0,000	0,144	0,080	0,040
1,55	0,040	0,013	0,006	0,000	0,000	0,192	0,155	0,058
1,6	0,080	0,013	0,006	0,004	0,000	0,279	0,187	0,081
1,65	0,111	0,038	0,006	0,013	0,005	0,367	0,193	0,105

The information about the impedance phase was unfortunately not as successful. Figures A.4-1 to A.4-7 all indicate highly erratic phase measurements that do not correlate with the movement of the arterial catheter in the body of the subjects. All of these figures show a great degree of variation in the impedance phase, with numerous high and low spikes. Furthermore, there seems to be no indication of successful placement in the artery based solely on the impedance phase. It would thus seem that the impedance phase measurements, when viewed independently, add no useful information regarding the catheterization process.

Using the impedance phase and the impedance magnitude values from the first subject, a graph was generated, depicting the resistance and the reactance of the tissue over time. Figure 11-11 illustrates these plots, as well as the original plot seen in Figure 11-2. It can be seen that in most cases, the reactance is significantly lower than the resistance of the biological tissue, though there are a few cases where the resistance lowers and the reactance heightens. Near the 3 second mark, there is a case where the reactance of the tissue is higher than the resistance of the tissue. The cause for these anomalies is uncertain.

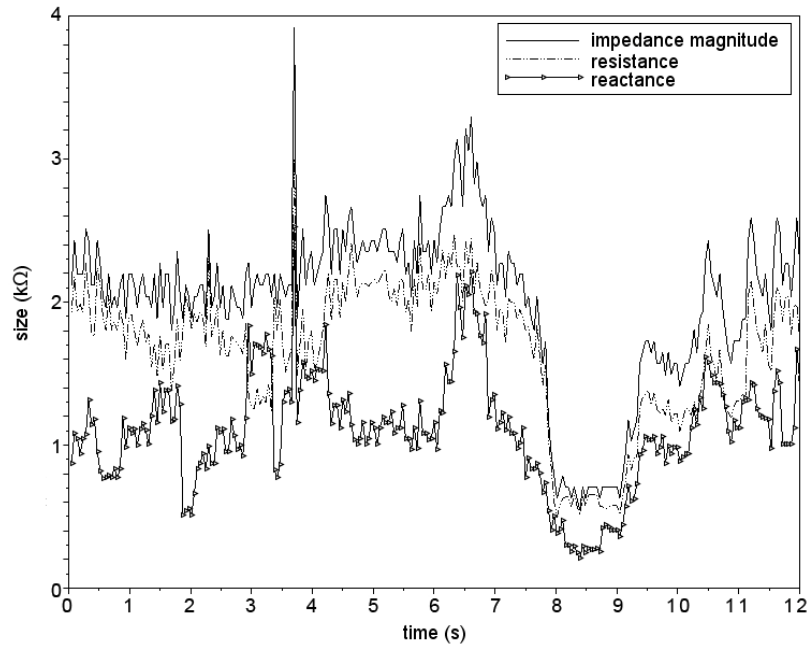
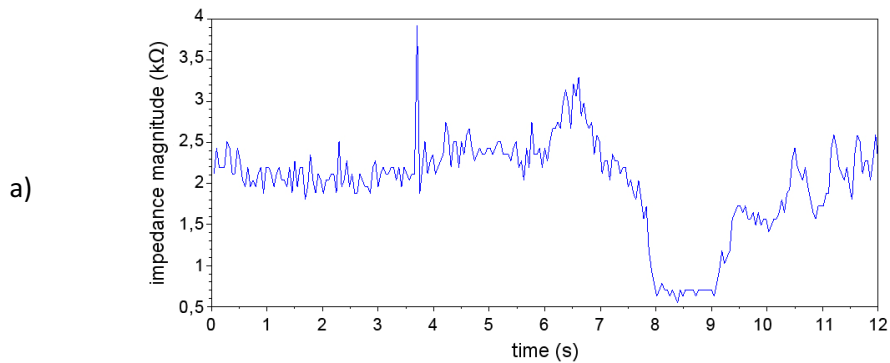


Figure 11-11: Graph showing resistance, reactance and impedance magnitude

Based on the information gathered from the impedance magnitude, a running average window algorithm was developed and tested, using the data gathered during the clinical tests. The algorithm calculated a running average, based on the n 'th measurement and its surrounding measurements. This was tested with a window width of 3, 5 and 7 on the results show in Figure 11-2 and the results of the different window sizes can be seen in Figure 11-12 below.



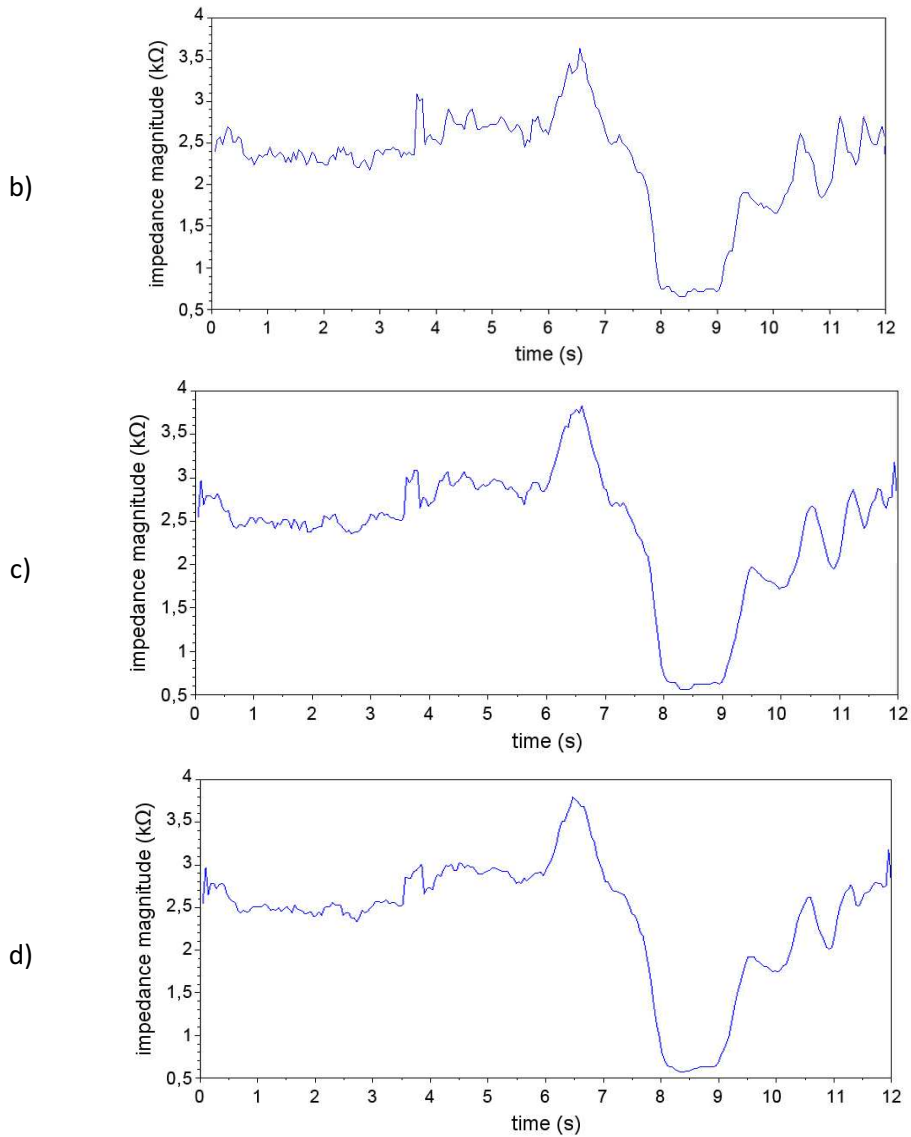


Figure 11-12: Running window average, with different window sizes (a: original, b: $W = 3$, c: $W = 5$, d: $W = 7$)

Figure 11-12 indicates that, as expected, a large portion of noise is cancelled out of the signal by the running average window, at the expense of losing some detail in the graphs. It can be seen, however, that even at a $W = 5$, a considerable amount of detail in the graphs is retained, while at $W = 7$ some of these details are lost.

In each of these cases, the crossover point from $|Z|_H$ to $|Z|_L$ was observed, using $1,25 \text{ k}\Omega$ as the value for $|Z|_T$ (based on the results shown in Table A.4-3 and Table 11-1). Observations were made as to the change in accuracy around the crossover points, which would be the most important points in the data. Any loss in accuracy would be undesirable, while the noise cancelling attributes of this algorithm are desired. Figure 11-13

illustrates the four plots seen in Figure 11-12, now overlaid, zoomed in to the crossover point and a line indicating the value of $|Z|_T$.

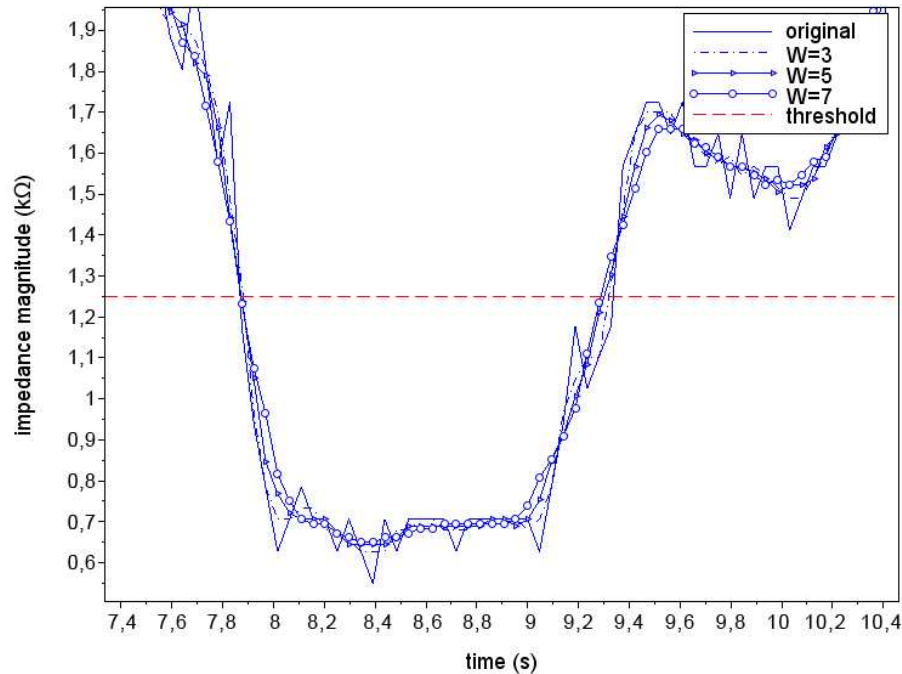


Figure 11-12: Overlaid graph of plots at crossover point

Figure 11-12 indicates that the crossover point accuracy is not adversely affected by the use of the running average window algorithm, while the algorithm is capable of removing noise spikes which could otherwise be seen as incorrect crossover points. Thus, utilizing this algorithm in the completed device would be recommended.

Finally, in order to determine if using the threshold value is an accurate method to judge if catheterization is successful, Figures 11-2 to 11-8 were investigated with the calculated threshold value ($|Z|_T = 1,25 \text{ k}\Omega$, as described above). The locations where the plots crossed the threshold value with a negative gradient represented the points at which the threshold method would declare the catheterization successful. These points were then compared to the actual points where catheterization was completed successfully, in order to judge the accuracy of the method. It was found that the threshold method identified successful catheterization correctly in every case examined, proving that this method is suitable for the device.

It can be said that the clinical trials were successful. Despite the impedance phase contributing very little constructive information, the impedance magnitude data is very promising. The data gathered from the clinical tests indicate that it is highly possible to determine whether or not the proximal

tip of the arterial catheter is within a patient's arterial bloodstream, which is required for the guidance of the device. The feedback from the anaesthesiologists who were using the device were mainly interest in the device and end-product, although there was some concern regarding the size of the device. It was stressed by one of the practitioners that the conductors connecting the prototype arterial catheter with the electronics box was hindering, due to the tension caused by the wires, which reduced the tactile feel of insertion. Additionally, the positioning of these wires made it more difficult to observe the pulsatile blood return from the angle of operation. The latter would not be a problem in the final design, granted that the device would work as intended, but the former stresses the need for a much smaller final device. The main improvement thus required for the prototype used would be to drastically minimize the design, mirroring the concept chosen for the final design, in Chapter 5.

12. Potential future work

Based on the positive results of the clinical trials, it can be seen that the impedance guided intra-arterial catheter is a viable and promising design. However, further work should be done before it could become a commercial product. The two main modifications that would need to be done would be:

- Minimize the design
- Conduct a final session of clinical tests

To effectively minimize the design, it would be recommended to use an impedance measuring IC, such as the AD5933 [41]. This surface mounted chip requires very little additional components, operates at low voltages (2,7 - 5 V) and works with high accuracy. This IC can measure between 1 k Ω and 10 M Ω , and can create an excitation frequency of up to 100 kHz. This IC, in conjunction with the processing chip from the Arduino Mega 2560 (used in the clinical trial prototype) and the recommended precision voltage regulator (the ADR395 [42]) would be the main components of a theoretical final design.

The ATmega2560 has an 8 MHz variant, which has a lower input voltage requirement (1,8 - 5,5 V) and has the dimensions illustrated in Table 12-1, depending on which package is used.

Table 12-1: ATmega2560 package dimensions

Package	Width (mm)	Length (mm)	Height (mm)
100A	16,00	16,00	1,20
100C1	9,00	9,00	1,20

Furthermore, the AD5933 has the maximum dimensions of 6,50 mm x 8,20 mm x 2,00 mm. The ADR395 has maximum dimensions of 2,9 mm x 2,8 mm x 1,0 mm. It is thus clear that the final design can thus be reduced to a much smaller size, based on the dimensions of the main components required. The low voltage requirements of the system would allow button-type batteries to be used, further minimizing the design.

Surface mounted LEDs can be used for visual feedback, with a range of colours to depict the difference impedance levels measured. However, care should be taken in the selection of colours, as to remain visible to users who suffer from colour blindness.

Additionally, housing for all of the electronics will have to be developed. This housing should adhere to the specifications mentioned in Chapter 4. Furthermore, careful consideration should be taken when designing the interface between the housing and the arterial catheter, with regards to the positioning (and possibly the visibility) of the pulsatile blood return chamber and plug, located at the distal end of the arterial catheter. Additionally, it would be recommended to design this housing to interface with one specific brand of arterial catheters, as the structure of these devices usually varies between manufacturers.

If the design of the device were to be furthered, it would be recommended that the cannula of the device be developed by a company currently manufacturing arterial catheters, in order to embed the silver electrodes into the cannula material during the manufacturing of the cannula, as in the original concept. It will also be ideal to place at least two electrodes in the cannula, allowing one to serve as the ground, removing the ground electrode from the arterial catheter's needle, as described in Chapter 5. Due to the nature of the cannula, it is of the utmost importance to ensure that (in case the silver electrodes are embedded into the cannula as suggested) the exposed tips of the electrodes on the proximal end of the cannula are secure in the cannula and will not loosen or break during insertion, removal or the time spent inside the lumen. Testing will have to be done to determine whether or not the embedded silver electrodes are safe for prolonged use.

Once the device has been finalized, a final session of clinical trials would be recommended. These final clinical trials would be used to determine if the final device functions as intended and to perform a practical functionality study on the device. Additionally, statistics should be gathered on the first placement success rate of the device, to conclude whether or not the device has a positive impact in the medical profession.

If these final clinical trials were to prove successful and interest in the device is high enough, the next suggested course of action would be to patent the device and to move forward to a mass production and marketing stage.

13. Conclusion

This project, the design of an impedance guided intra-arterial catheter, had the goal of designing a device which could be guided into a patient's artery by means of measuring and utilizing the changing levels of impedance in human tissue.

The need for such a device arose from cases where accurate placement could not be done by 'blind' insertion and where repeated inaccurate placement would cause trauma for the patient. Additionally, it would serve as a smaller and cheaper alternative to ultrasonic guidance.

Studies were done in terms of the nature of existing arterial catheters and current methods of guidance, along with research based on electrical impedance, the effect of electricity on the human body, electrical qualities of biological tissue and the required physiology of the human body. Additionally, studies were done on other methods of impedance guidance in the medical field. All of these studies were done in order to aid in the design of the described device.

Using the studies mentioned, as well as meetings with two doctors (Prof PR Fourie and Prof AR Coetzee), a series of specifications were developed for the device, in order to function properly. While most of the technical specifications were derived from the studies, the majority of the usability and interface specifications were developed with the aid of the two doctors.

From the abovementioned specifications, several concepts were generated and evaluated. From the concepts generated, a preliminary device was designed, for the purpose of early testing. This device was meant to evaluate the ideas behind the concept chosen. This was evaluated by measuring *in vitro* tissue samples, to both determine the prototype's capability to measure tissue impedance and to validate the concept used. Additionally, the prototype would be used to measure the impedance of these tissue samples, in order to determine if these tissue types could be identified using only their impedance.

Using this preliminary prototype design, a series of experiments were conducted, with the aim of both validating the effectiveness of the concept chosen, as well as gathering data regarding biological tissue impedance. These tests were conducted on samples of fat, skeletal muscle, aorta, blood and skin. The skeletal muscle, fat and aorta results indicated that the impedance phase was erratic and would not serve well for discerning between tissue types, whereas the impedance magnitude results showed more promising results, with distinct patterns between the three types, as well as showing the expected frequency dependant behaviour. It was thus concluded that the concept was functioning as intended and that it could be possible to use the different levels of tissue impedance for guidance.

With the success of the preliminary testing, the design of the prototype was furthered, in preparation for the next phase of experimentation; animal testing. While the electronic design of this next iteration remained the same as the

previous prototype, the mechanical design was altered. For these experiments, a single electrode was wrapped helically around the cannula, while being fixed and insulated by a nontoxic resin applied around the electrode. This allowed only the proximal tip of the electrode to be exposed and thus conductive. The distal end of this electrode was connected to the electronic apparatus. A second wire, connected to the needle of the arterial catheter was also connected to the electronics, allowing the needle to serve as the grounded electrode for the experimentation. This design was a step forward in the design process and would allow the animal testing phase to give both valuable data concerning living biological tissue, as well as further testing the viability of the concept being developed.

The animal testing was successful, despite numerous setbacks. The goals for the animal testing phase were to gather data regarding in vivo measurements of living biological tissue, with the aim of determining whether or not there would be a noticeable difference between the different tissue types, as well as testing how the developed concept functions with in vivo testing. It was found that the concept functioned as intended, however it proved difficult to measure thin samples (such as arterial walls) due to the distance between the two electrodes. In terms of impedance results, it was found that there was a moderate measured difference between arterial blood tissue and skeletal muscle tissue. The fat tissue measured indicated a large level of variance in the fat tissue, which seemed to be linked to the moisture content of the fat tissue. The lowest measurements of fat tissue seemed to be on the same impedance level as skeletal muscle tissue, while the highest measurements of fat tissue (the driest fat tissue) was on the same level as the dermis and epidermis layers of the skin. The results still indicated that one could determine whether or not the proximal tip of the arterial catheter was successfully placed inside the artery, due to the low level impedance measured in the arterial blood, which deemed the experiments successful.

The next step was to develop the next iteration of the concept, one which would be used for clinical trials and would thus have to be of such a standard that it could be used on living humans. Several changes had to be made, both to the electronics and the mechanical aspect of the concept. The oscilloscope, signal generator and laptop were removed in favour of a microprocessor and ICs, all contained in a remote box which would be connected to the prototype arterial catheter. The electrode placement used in the animal testing phase would not be acceptable in human testing, due to the dangers of the electrodes breaking off. Thus, an alternative design was used, which was safer for human testing and easier to manufacture by a single person. The design used was to run an insulated electrode through the centre of the needle and then loop it back from the proximal tip of the needle, back to the distal end, outside the needle, but under the cannula. The cannula would thus fix the position of the electrode until the needle is removed. This proximal tip of the electrode has its insulation scraped off at the tip, allowing that section to be conductive. This, along with the needle thus serves as the two electrodes.

The clinical tests were set up with the goal to prove that the prototype could successfully measure the impedance of human tissue and that these impedance values of the human tissue could be used to distinguish between

tissue types and thus predict when the proximal tip of the arterial catheter is successfully placed inside the artery. Unfortunately, the tests showed that the impedance phase was highly erratic and unpredictable, which would suggest that the impedance phase could not be used for guidance. However, the impedance magnitude measurements produced positive results, showing a distinct difference between blood tissue and the intermediary tissue.

The successful placement of the arterial catheter was confirmed with the pulsatile blood return and the time measurements for this blood return correlated with the low-level impedance measurements recorded by the device, indicating that the low-level impedance measurements were in fact blood measurements. This behaviour was noted in every successful test conducted and, after statistical analysis of the data, a threshold value to differentiate between the high level intermediary tissue impedances and the low level blood tissue impedance. From this data, a suggested running average window algorithm was developed, in order to reduce noise in the measurements. Thus, despite the unsatisfactory results gained from the impedance phase data, it was proven that the concept of the impedance guided intra-arterial catheter is a plausible design and bodes well for the potential future of the device.

In conclusion, it can be said that this thesis has proven that the concepts generated for the impedance guided intra-arterial catheter are viable concepts and that it is possible to guide an arterial catheter based on the impedance levels of biological tissue. Furthermore, this thesis includes suggestions on how to further this concept, to the point where this concept could become a finalized product for use in a medical setting. If this is the case, the author of this project firmly believes that the addition of the impedance guided intra-arterial catheter would be a valuable addition to the medical world.

14. References

- [1] Johnson, K, 2004, Arterial line, version 1.4 [online]
- [2] Ramakrishnan, N., Clermont, G., 1999, Placement and management of arterial catheters [online]
- [3] Sanderson, H, 2007, Arterial line insertion, version 1.0 [online]
- [4] Gregory Thompson, E., 2011, Angioplasty for heart attack and unstable angina [online]
- [5] Enderlene, J., Blanchard, S., Bronzino, J., Introduction to biomedical engineering, 2nd Edition
- [6] Curtis, J., Klykken, P., 2008, A comparative assessment of three common catheter materials [online]
- [7] Sechrist, K.R., 1993, Arterial catheter complications and management problems [online]
- [8] Lai, S.Y., 2011, Sutures and needles [online]
- [9] Lefrant, J.Y., *et al.*, 1998, Pulsed doppler ultrasonography guidance for catheterization of the subclavian vein: a randomized study [online]
- [10] Sachdeva, B., Abreo, K., Temporary catheter placement - Understanding the procedure [online]
- [11] Clermont, G., *et al.*, 2011, Arterial catheterization techniques for invasive monitoring [online]
- [12] Shiloh, A.L., Savel, R.H., Paulin, L.M., Eisen, L.A., 2011, Ultrasound-guided catheterization of the radial artery: a systematic review and meta-analysis of randomized controlled trials [online]
- [13] Rothschild, J.M., Ultrasound Guidance of central vein catheterization [online]
- [14] Seldinger, S.I., 1953, Actaradiologica 39, Catheter replacement of the needle in percutaneous arteriography; a new technique
- [15] Arrow International, 2007, Arterial catheterization sets, product sheet [online]
- Available at: <http://www.arrowintl.com/documents/pdf/literature/eng-sac-c0507.pdf>
- [16] Mangar, D., Thrush, D.N., Connell, G.R., Downs, J.B., 1993, Direct or modified Seldinger guide wire-directed technique for arterial catheter insertion [online]

- [17] Srejjic, U., Wenker, O.C., 2003, "A-Line" or "Intra-arterial catheters", The Internet Journal of Health, Volume 3 Number 1
- [18] Becker, D.E., 2001, Arterial catheter insertion. AACN Procedure Manual for Critical Care, 4th Edition
- [19] Hambley, A.R., Electrical engineering: Principles and applications, Third Edition
- [20] Joseph C.J., 1997, Safety for electronic hobbyists. Popular Electronics [online]
- [21] Zitzewitz, P.W., Robert N.F., 1995, Merrill Physics, principles and problems.
- [22] Grey, H., 1918, Anatomy of the human body, 20th Edition
- [23] Marieb, E.N., 1995, Human anatomy and physiology, 3rd Edition
- [24] Miklavčič, D., Pavšelj, N., Electric properties of tissues [online]
- [25] Peyman, A., Gabriel, C., 2005, Dielectric properties of tissues, WHO Workshop on Dosimetry of RF Fields [online]
- [26] Skin effect and biological impedance analysis [online]
- Available at:
http://www.rifevideos.com/pdf/skin_effect_and_bio_electrical_impedance_analysis.pdf
- [27] Geddes, L.A., Baker, L.E., 1967, The specific resistance of biological material - A compendium of data for the biomedical engineer and physiologist [online]
- [28] Malmivuo, J., Plonsey, R., 1995, Bioelectromagnetism - Principles and applications of bioelectric and biomagnetic fields [online]
- [29] Cheney, M., Isaacson, D., Newell, J.C., 1999, Electrical impedance tomography [online]
- [30] Kauppinen, P., Hyttinen, J., Malmivuo, J., 2006, Sensitivity distribution visualizations of impedance tomography measurement strategies [online]
- [31] Takafumi, U., *et al.*, 2004, Catheter with puncture sensor [online]
- [32] Zhang, B., *et al.*, 2006, Compatibility of porcine and human interleukin 2: implications for xenotransplantation. [online]
- [33] Cooper, D.K.C., Kemp, E., Plat, J.L., White, D.J.G., 1997, Xenotransplantation: The transplantation of organs and tissue between species
- [34] Arduino Corporation, Arduino Mega2560, datasheet [online]

Available at: <http://www.jameco.com/Jameco/Products/ProdDS/2121113.pdf>

[35] Atmel Corporation, 2012. 8-Bit Atmel microcontroller with 64k/128k/256k bytes in-system programmable flash, datasheet [online]

Available at: <http://www.atmel.com/Images/doc2549.pdf>

[36] Intersil, 2001. ICL8038 Precision waveform generator/voltage controlled oscillator, datasheet [online]

Available at:

<http://www.intersil.com/content/dam/Intersil/documents/fn28/fn2864.pdf>

[37] Analog Devices, 1997. AD741 Low cost, high accuracy op amps, datasheet [online]

Available at: http://classes.soe.ucsc.edu/ee070/Winter02/DataSheet_AD741.pdf

[38] Fairchild Semiconductors, 2012. LM78XX 3 terminal 1 A positive voltage regulator, datasheet [online]

Available at: <http://www.fairchildsemi.com/ds/LM/LM7805.pdf>

[39] National Semiconductors, 1995. LM79XX 3 terminal negative regulators, datasheet [online]

Available at: <http://www.hep.upenn.edu/SNO/dag/parts/lm7915.pdf>

[40] National Semiconductors, 2009. LM136-2.5 reference diode, datasheet [online]

Available at: <http://www.ti.com/lit/ds/symlink/lm136-2.5-n.pdf>

[41] Analog Devices, 2011. 1 MSPS, 12-bit Impedance converter, network analyzer, datasheet [online]

Available at: http://www.analog.com/static/imported-files/data_sheets/AD5933.pdf

[42] Analog Devices, 2008. Micropower, low noise precision voltage references with shutdown, datasheet [online]

Available at: http://www.analog.com/static/imported-files/data_sheets/ADR390_391_392_395.pdf

Appendix A: Additional graphs and tables

A.1. Graphs and tables from chapter 7

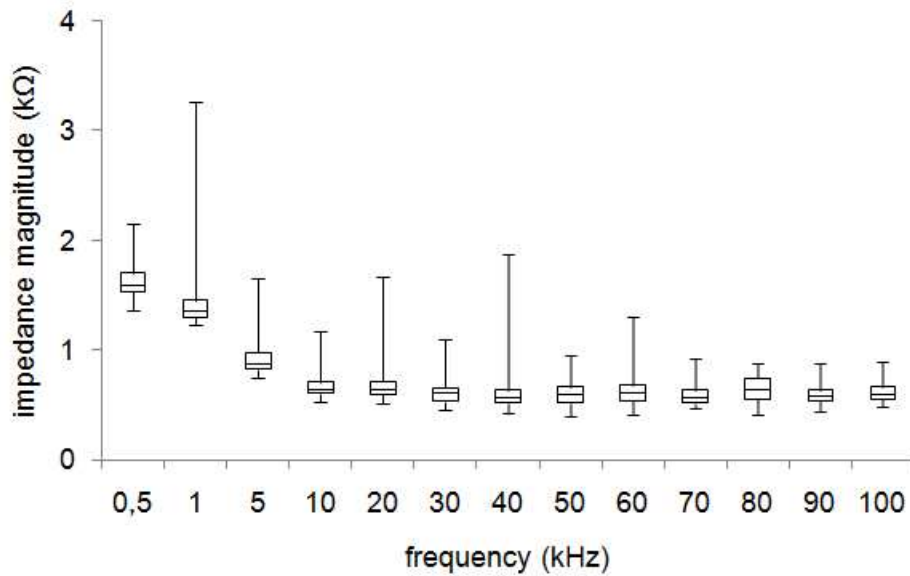


Figure A.1-1: Skeletal muscle tissue impedance magnitude box and whisker chart

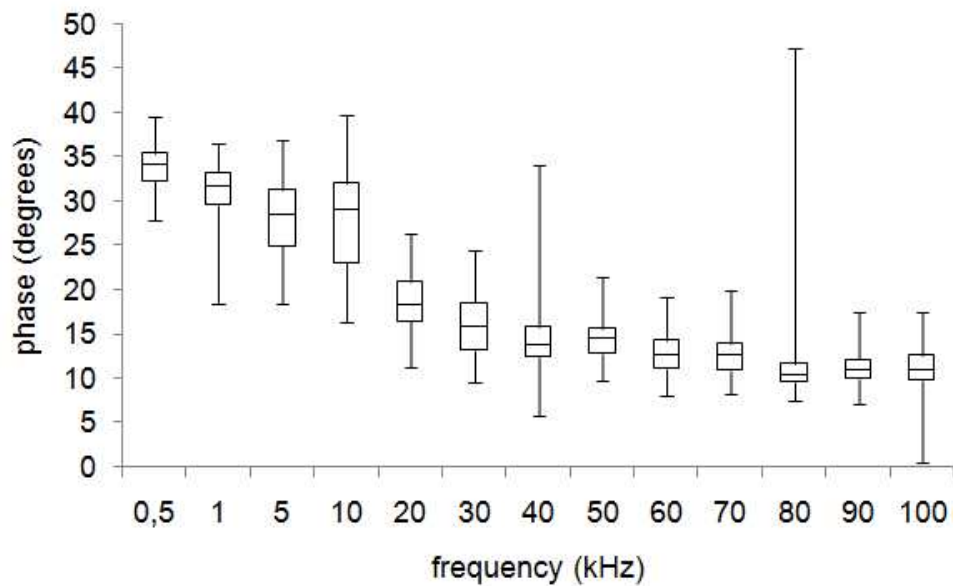


Figure A.1-2: Skeletal muscle tissue impedance phase box and whisker chart

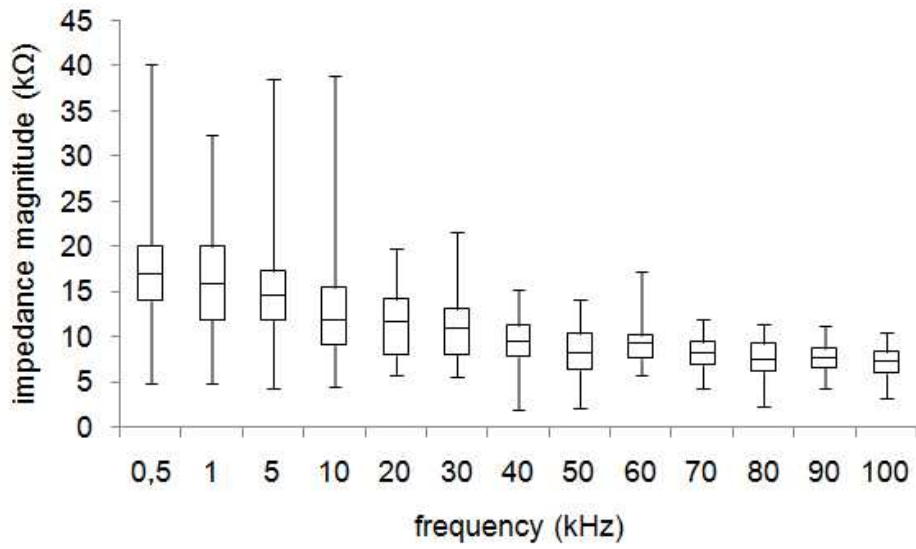


Figure A.1-3: Fat tissue impedance magnitude box and whisker chart

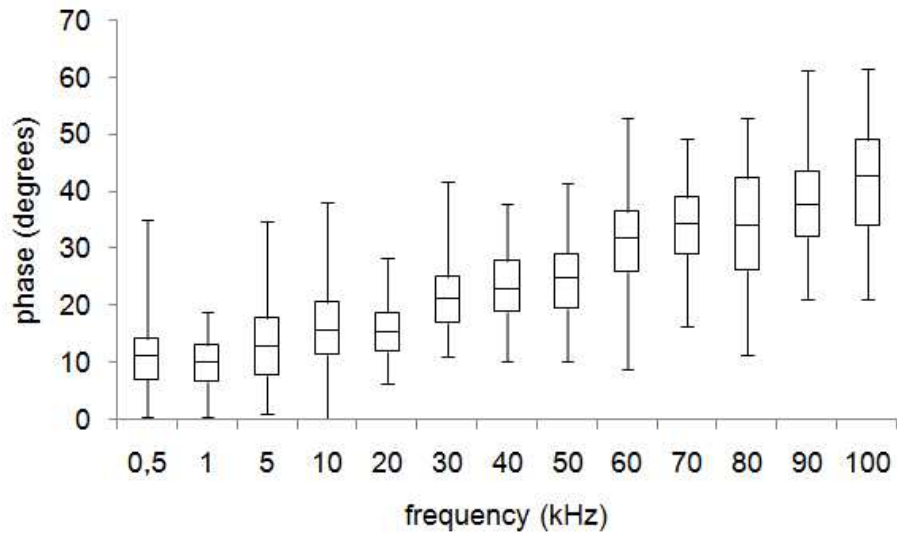


Figure A.1-4: Fat tissue impedance phase box and whisker chart

A.2. Graphs and tables from Chapter 9

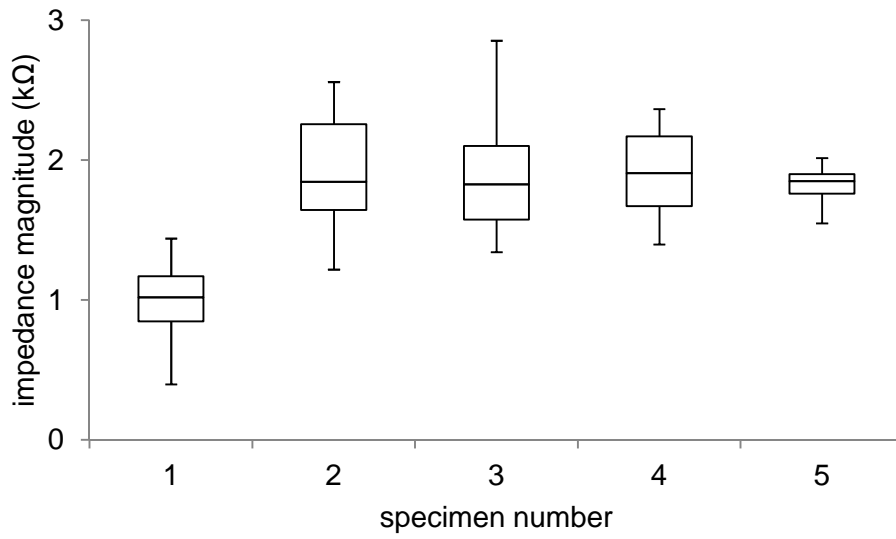


Figure A.2-1: Skeletal muscle impedance magnitude box and whisker plot

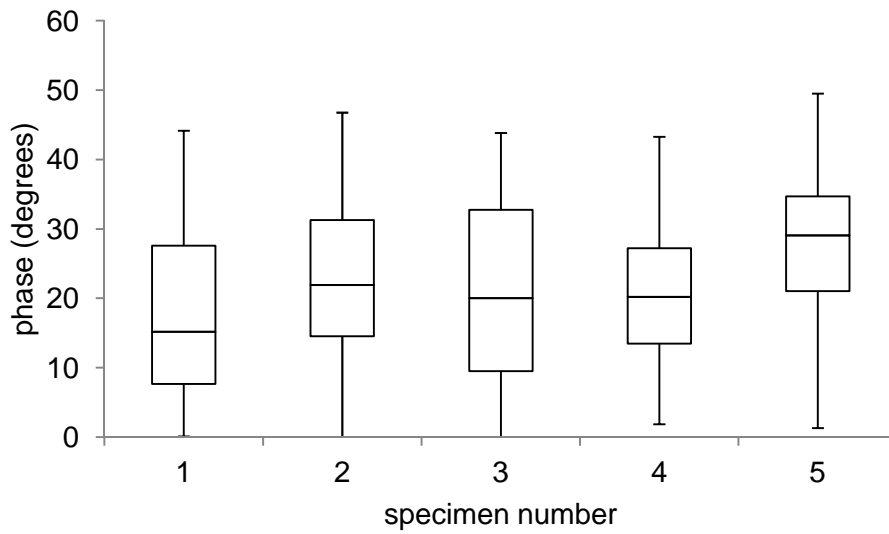


Figure A.2-2: Skeletal muscle impedance phase box and whisker plot

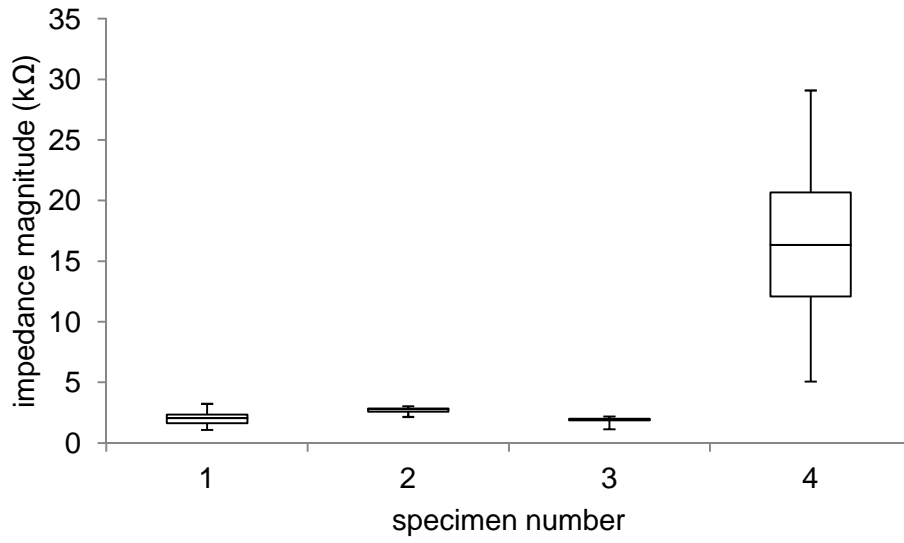


Figure A.2-3: Fat impedance magnitude box and whisker plot

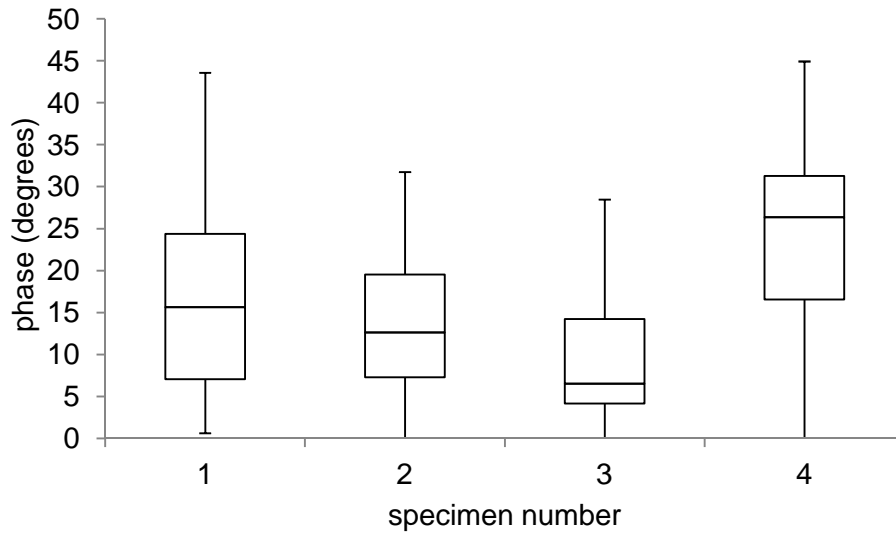


Figure A.2-4: Fat impedance phase box and whisker plot

A.3. Graphs and tables from Chapter 10

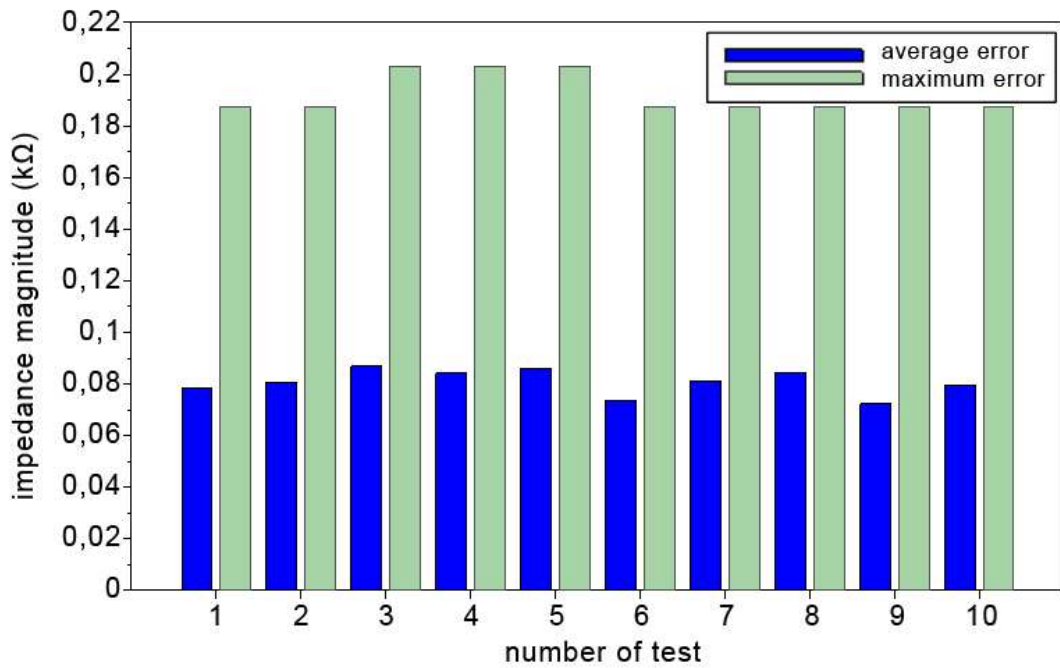


Figure A.3-1: 0,5 kΩ, 0 ° Tests Impedance Magnitude Error Graph

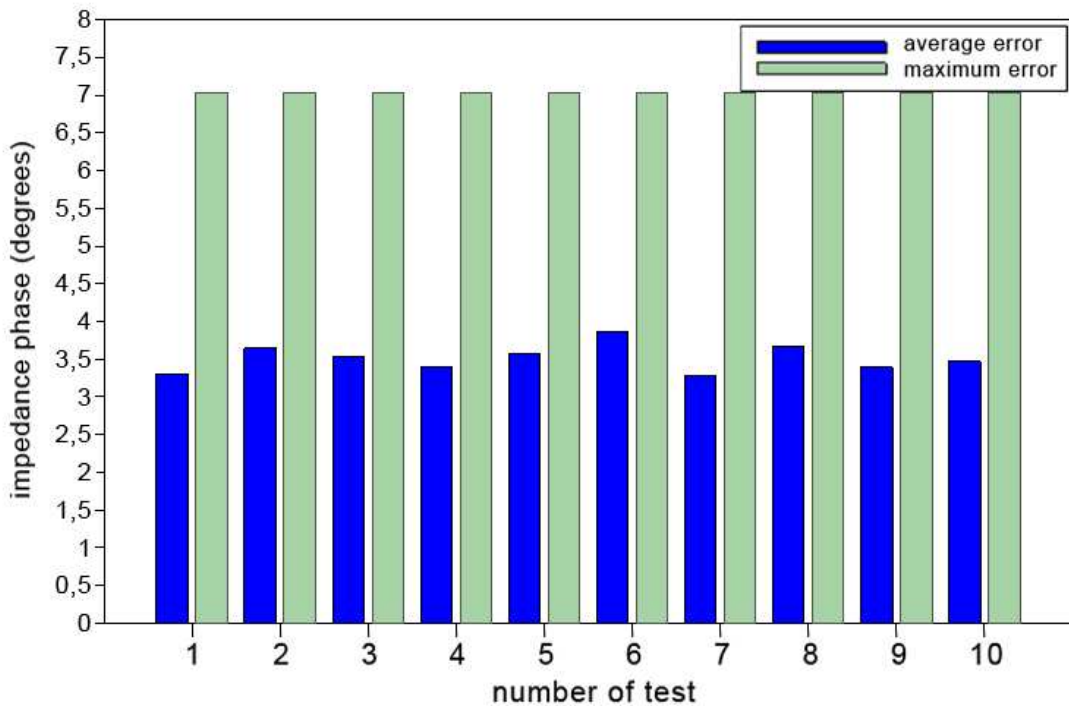


Figure A.3-2: 0,5 kΩ, 0 ° Tests Impedance Phase Error Graph

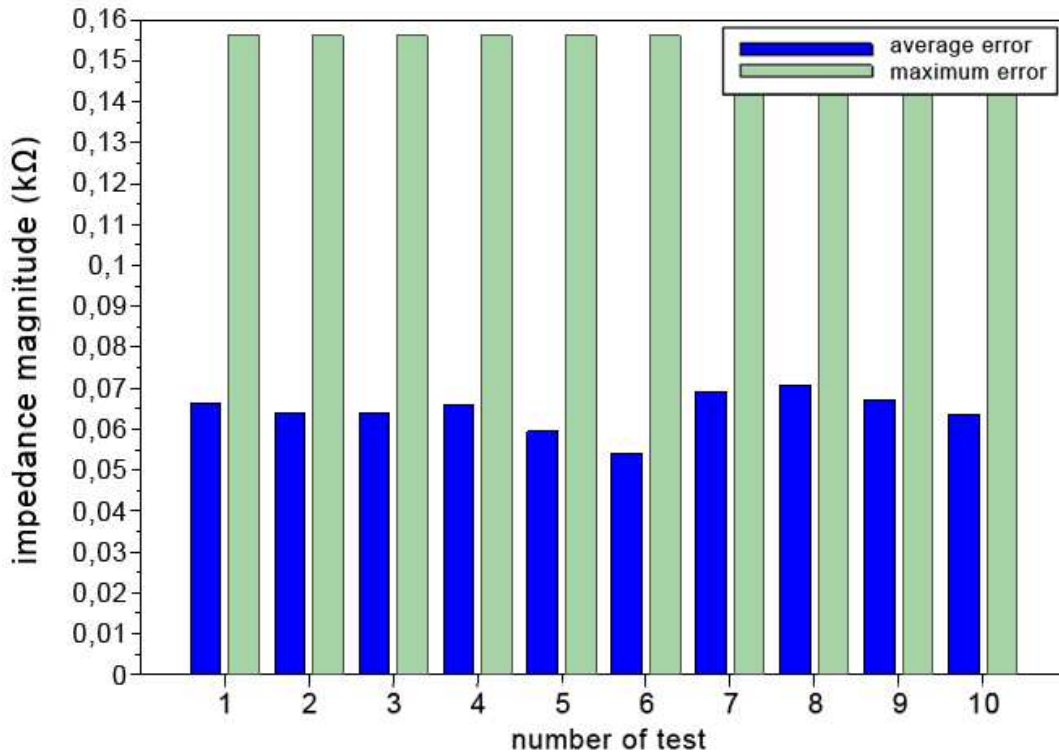
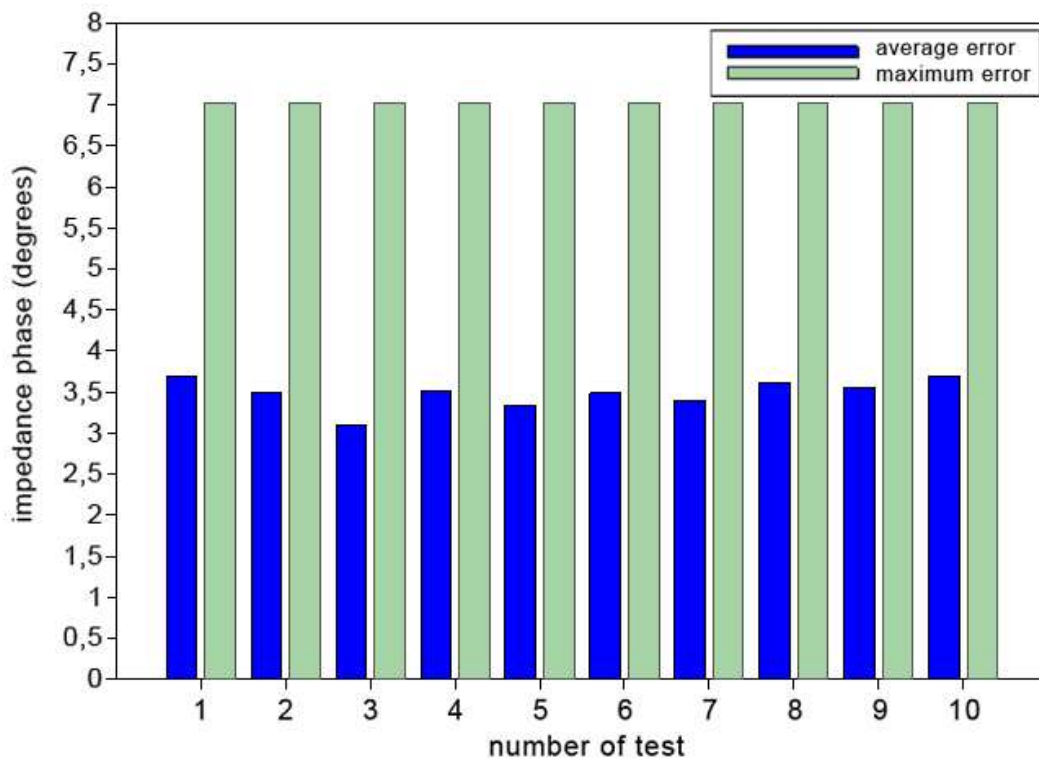


Figure A.3-3: 5 kΩ, 0 ° Tests Impedance Magnitude Error Graph



FigureA.3-4: 5 kΩ, 0 ° Tests Impedance Phase Error Graph

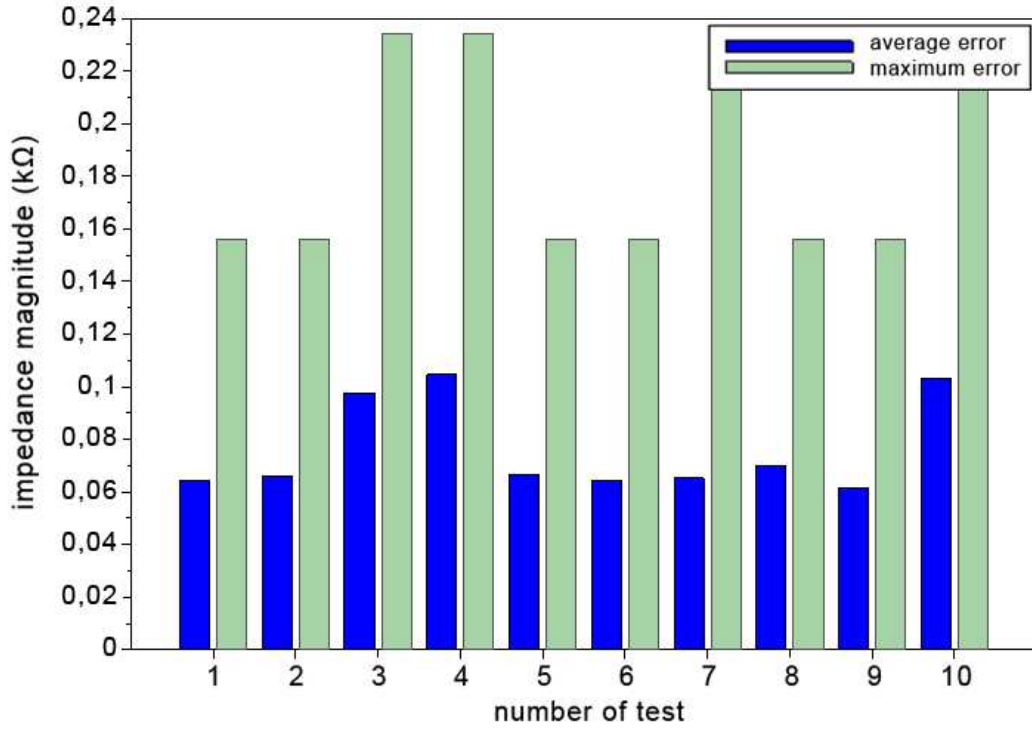


Figure A.3-5: 10 kΩ, 0 ° Tests Impedance Magnitude Error Graph

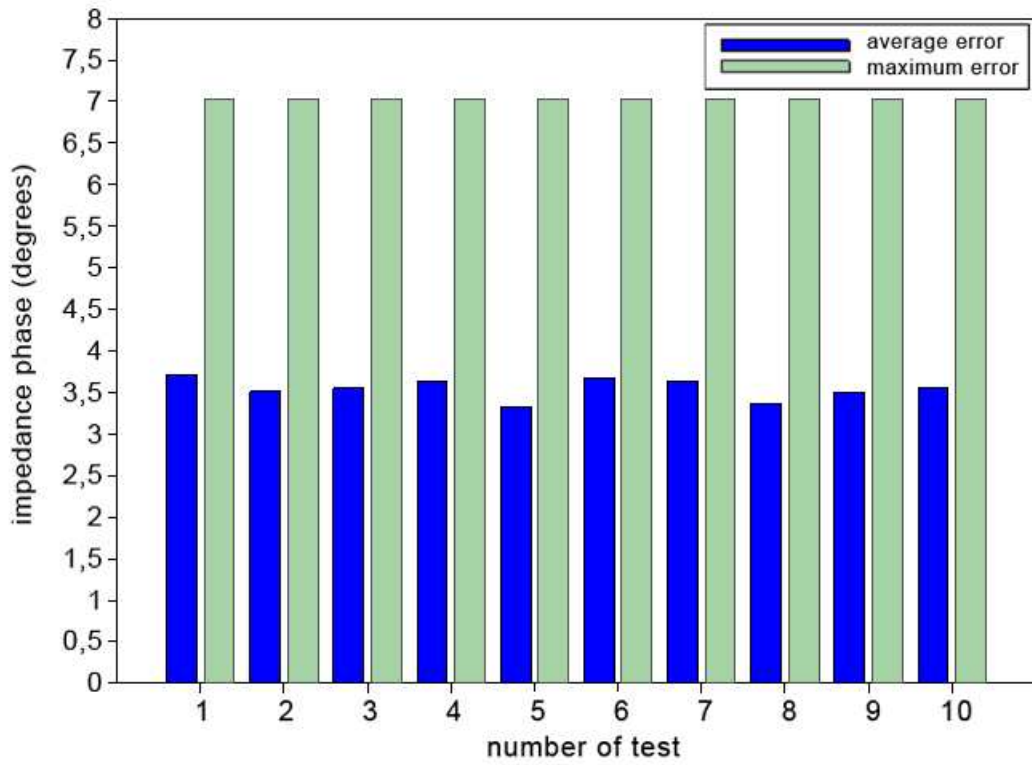


Figure A.3-6: 10 kΩ, 0 ° Tests Impedance Phase Error Graph

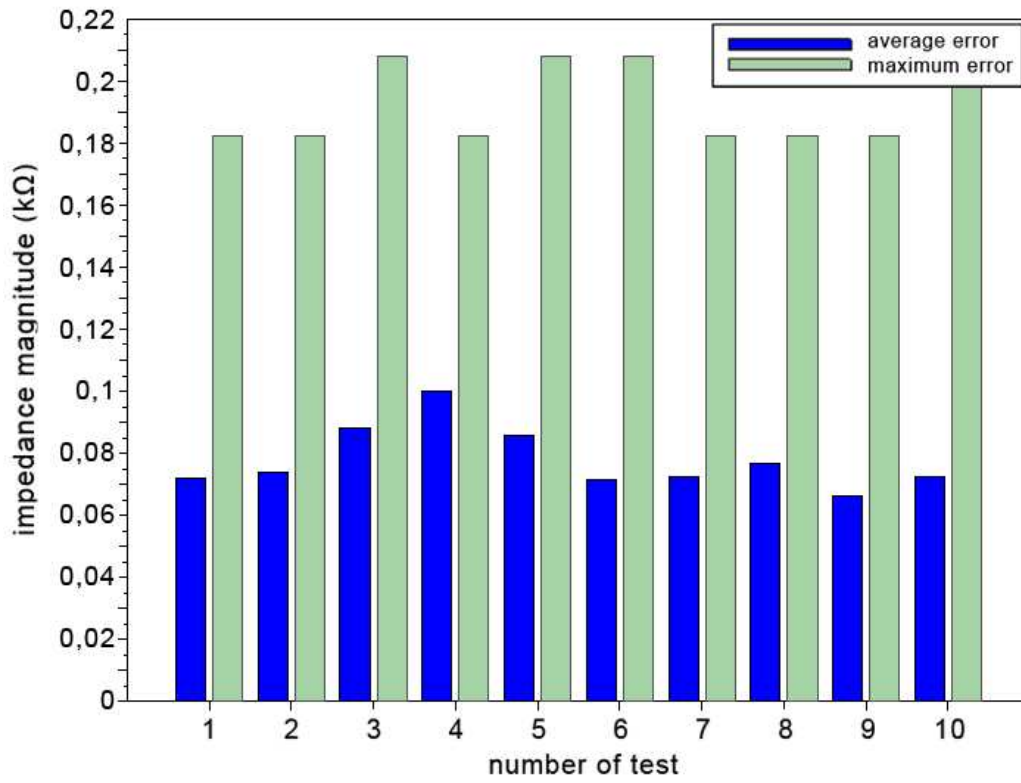


Figure A.3-7: 0,5 kΩ, 30 ° Tests Impedance Magnitude Error Graph

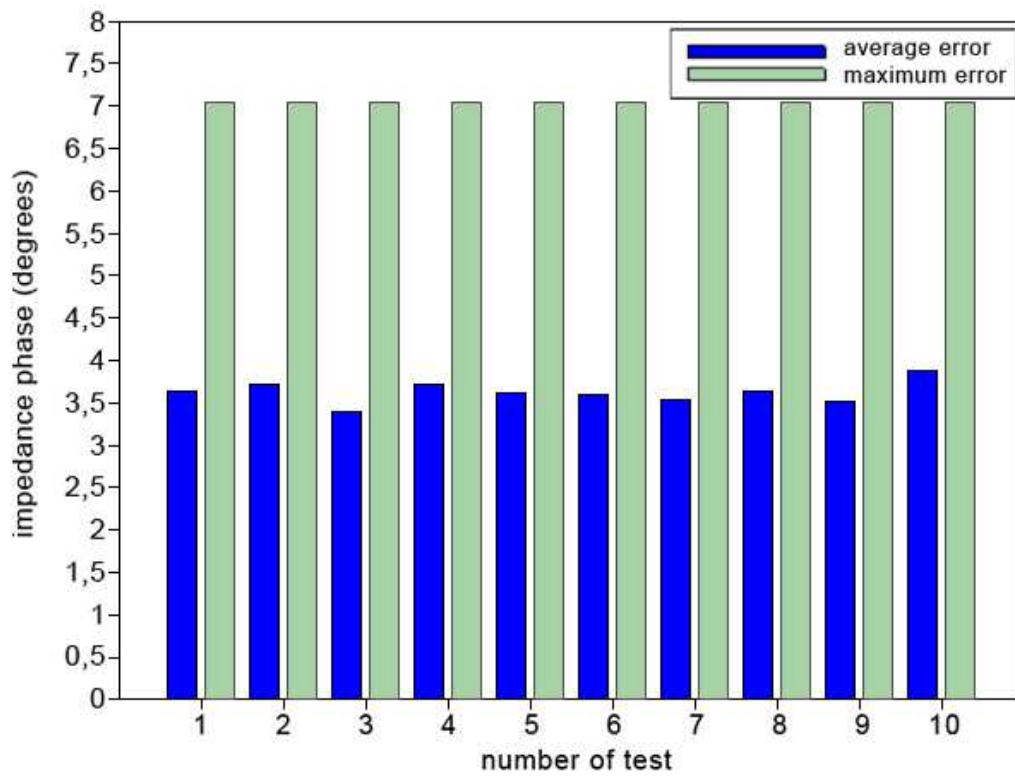


Figure A.3-8: 0,5 kΩ, 30 ° Tests Impedance Phase Error Graph

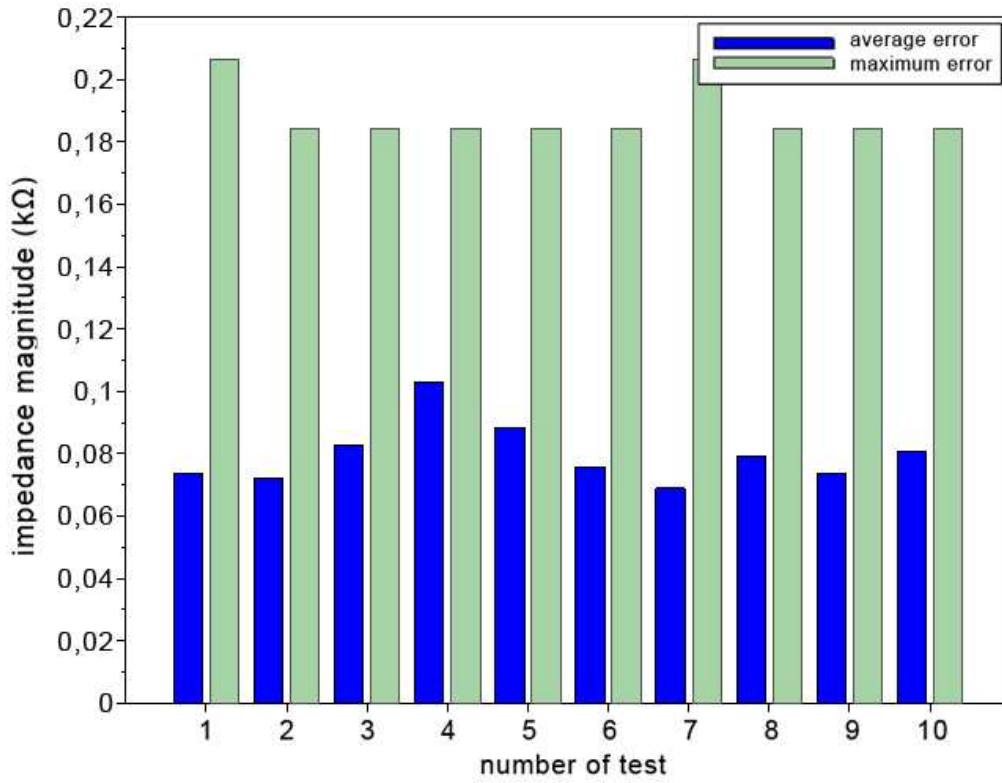


Figure A.3-9: 5 kΩ, 30 ° Tests Impedance Magnitude Error Graph

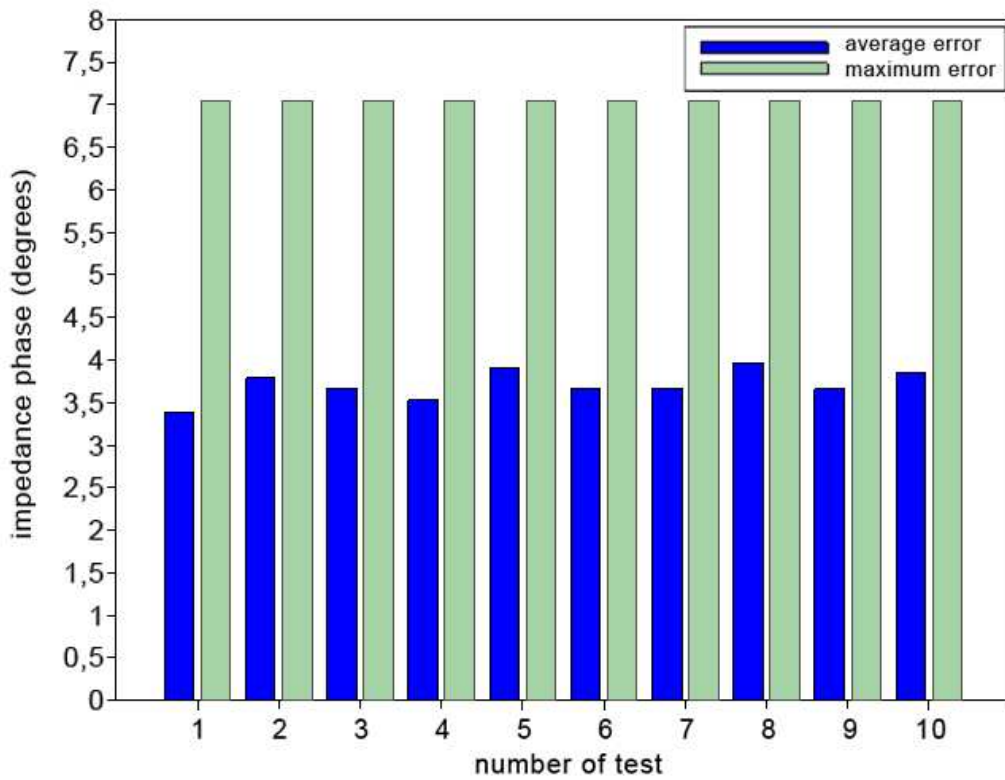


Figure A.3-10: 5 kΩ, 30 ° Tests Impedance Phase Error Graph

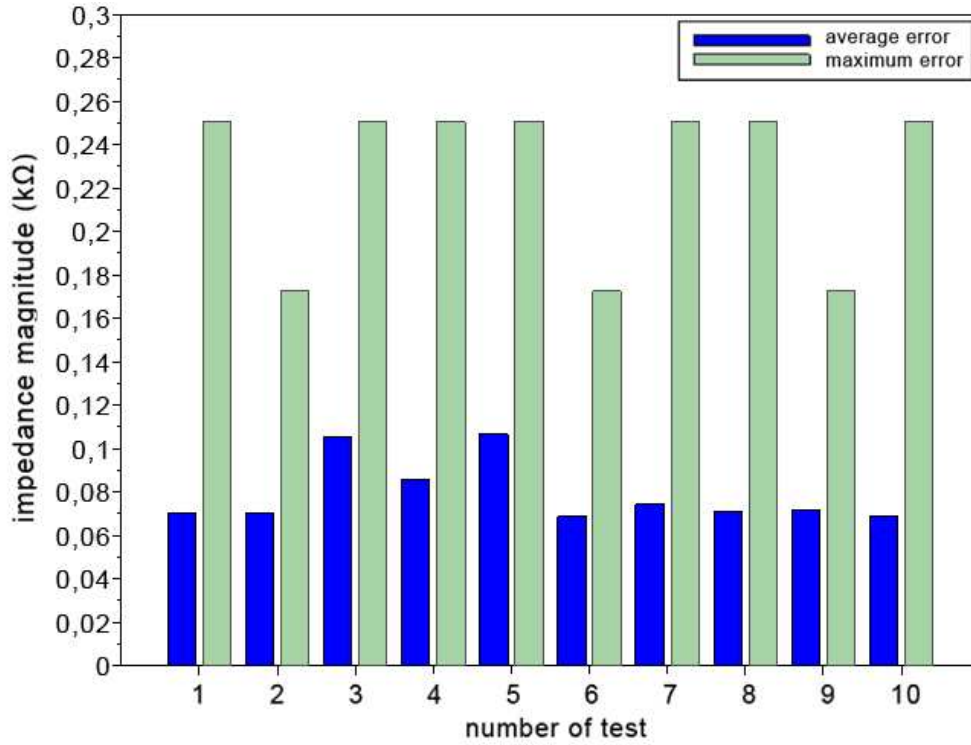


Figure A.3-11: 10 kΩ, 30 ° Tests Impedance Magnitude Error Graph

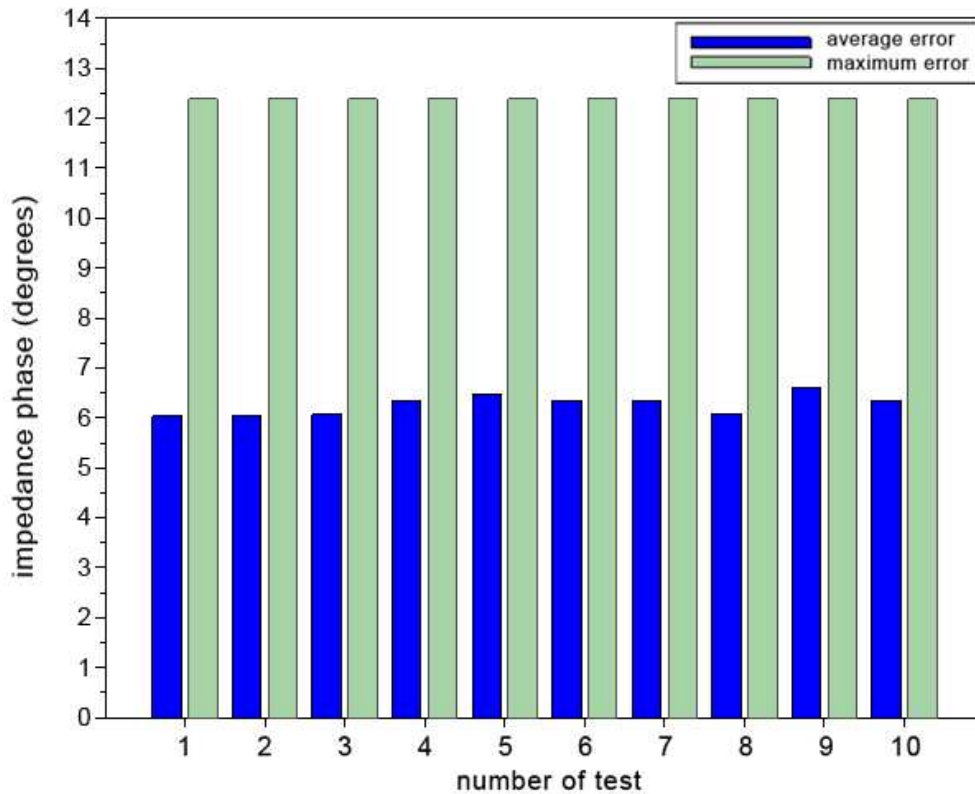


Figure A.3-12: 10 kΩ, 30 ° Tests Impedance Phase Error Graph

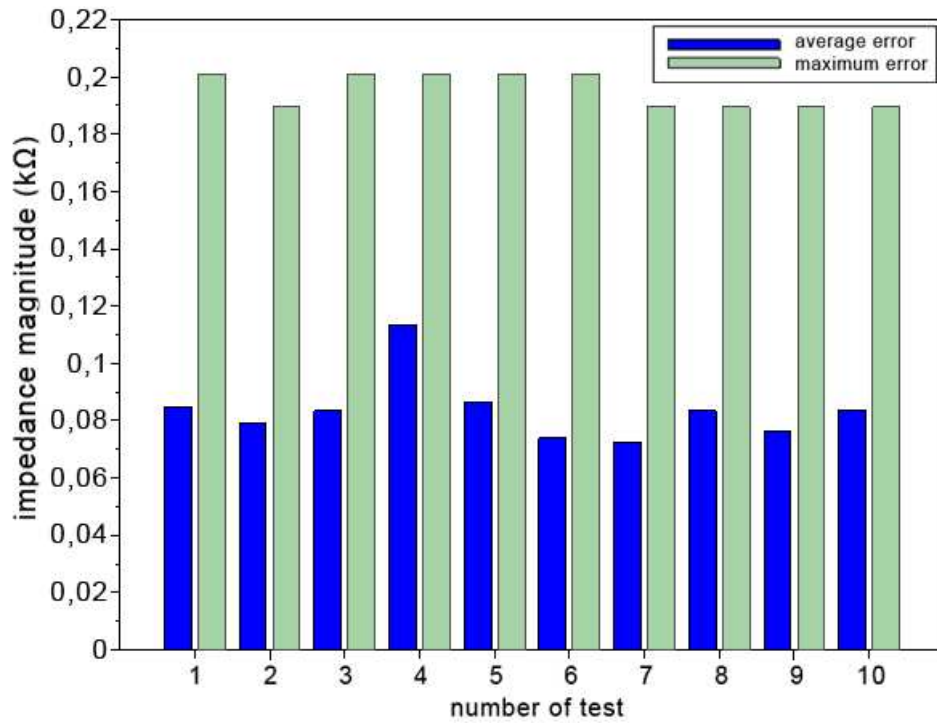


Figure A.3-13: 0,5 kΩ, 60 ° Tests Impedance Magnitude Error Graph

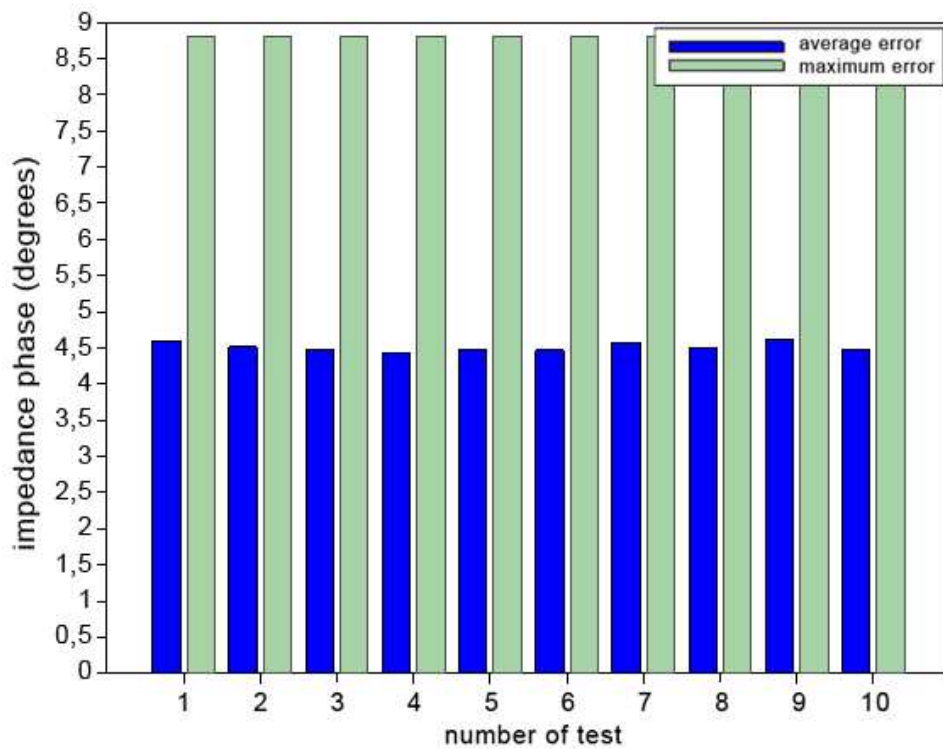


Figure A.3-14: 0,5 kΩ, 60 ° Tests Impedance Phase Error Graph

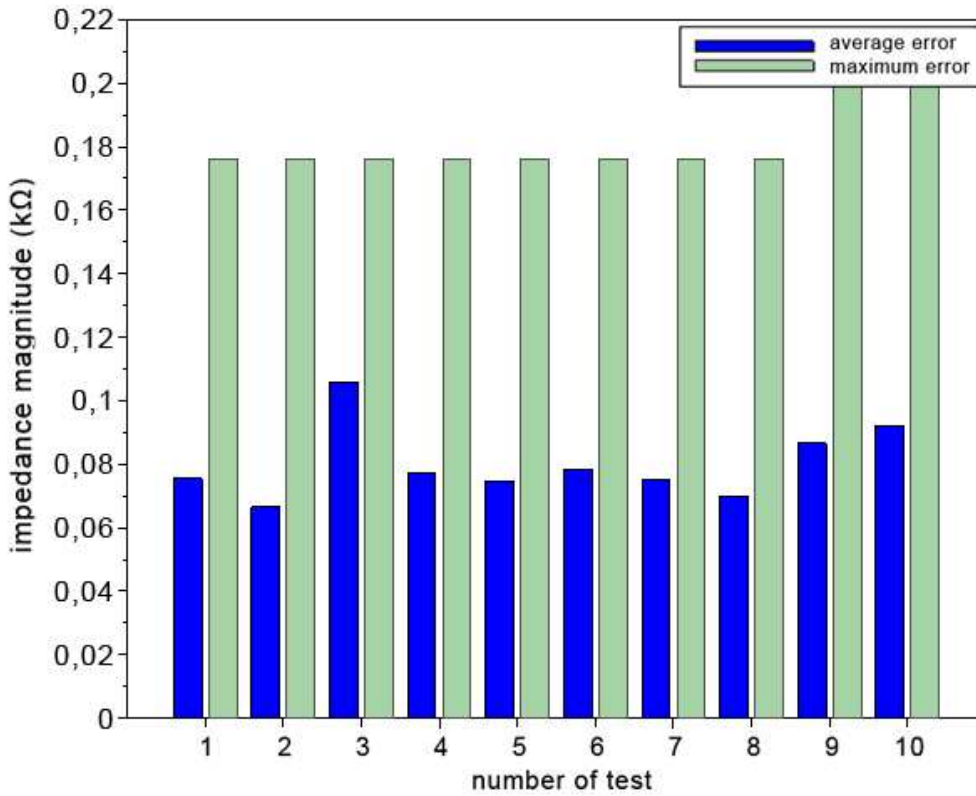
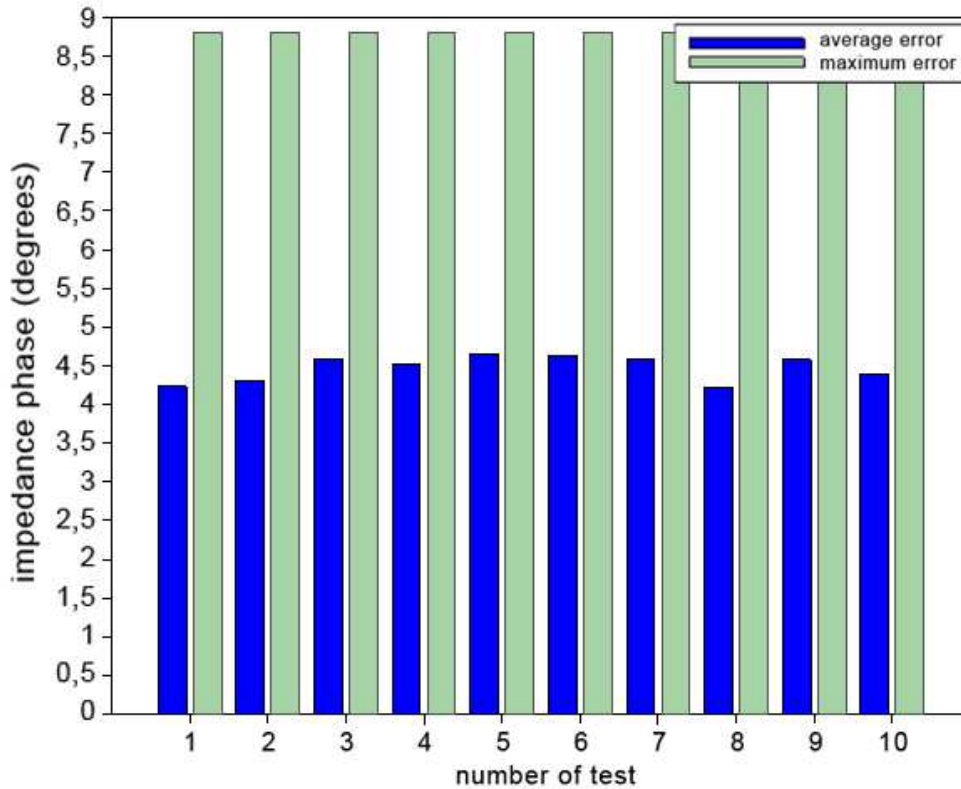


Figure A.3-15: 5 kΩ, 60 ° Tests Impedance Magnitude Error Graph



FigureA.3-16: 5 kΩ, 60 ° Tests Impedance Phase Error Graph

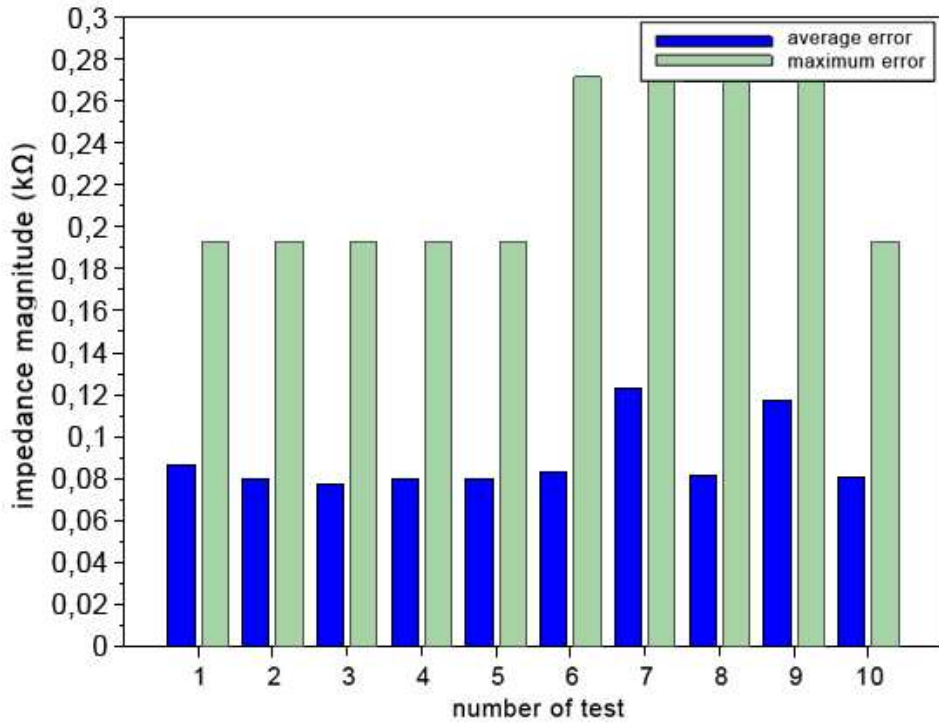
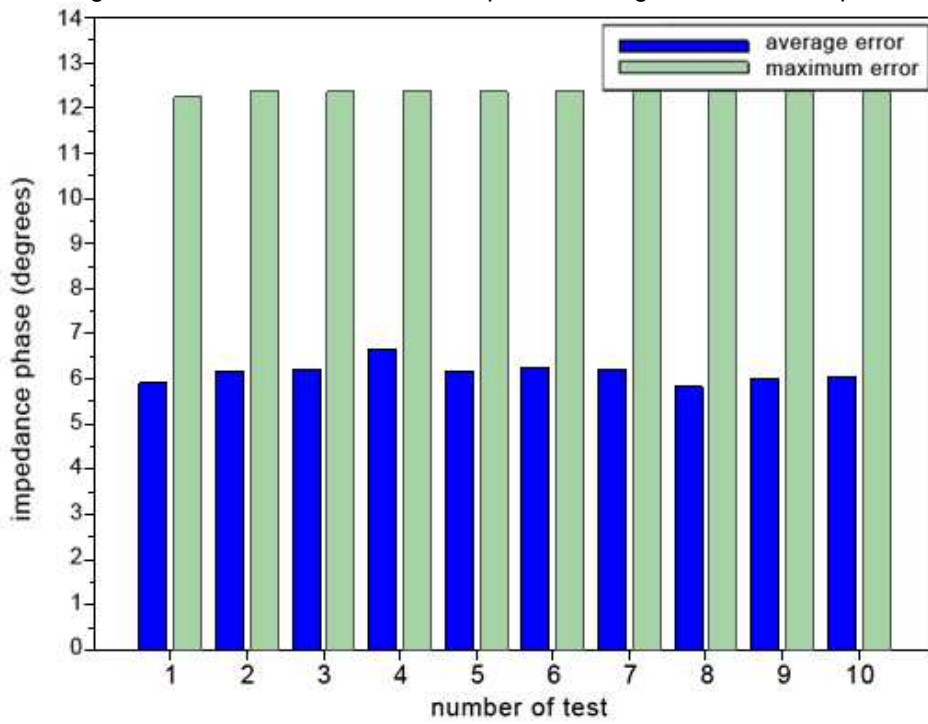


Figure A.3-17: 10 kΩ, 60 ° Tests Impedance Magnitude Error Graph



FigureA.3-18: 10 kΩ, 60 ° Tests Impedance Phase Error Graph

A.4. Graphs and tables from Chapter 11

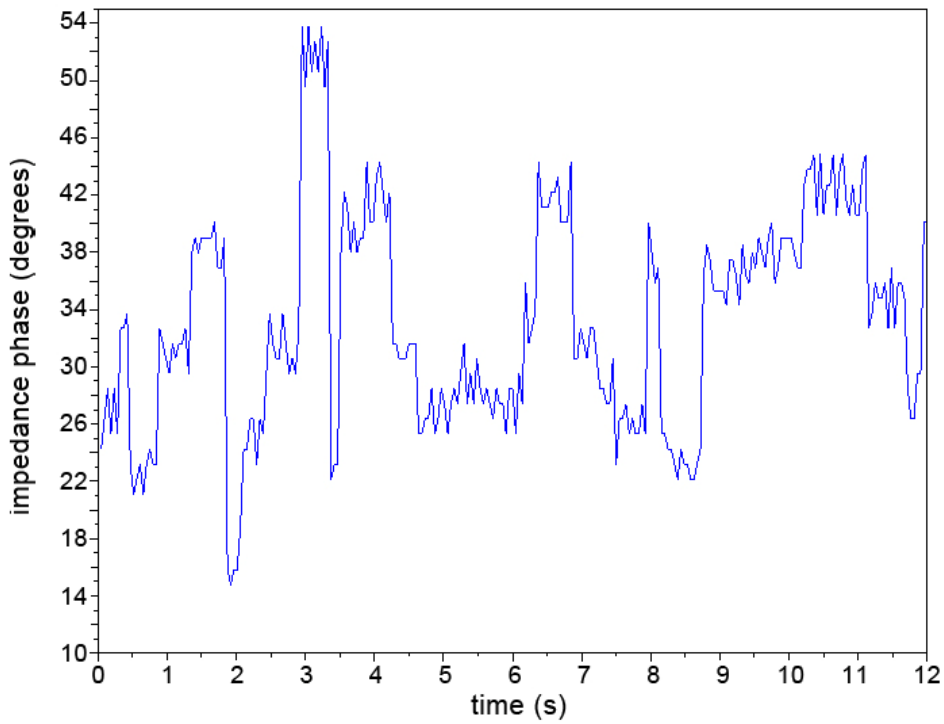


Figure A.4-1: Patient 3 impedance phase over time

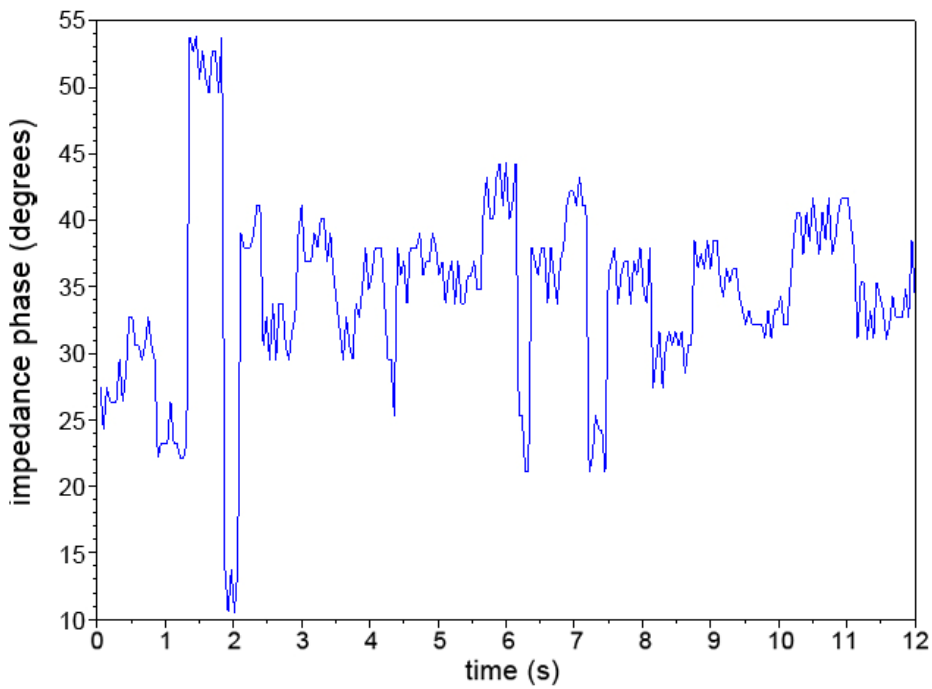


Figure A.4-2: Patient 4 impedance phase over time

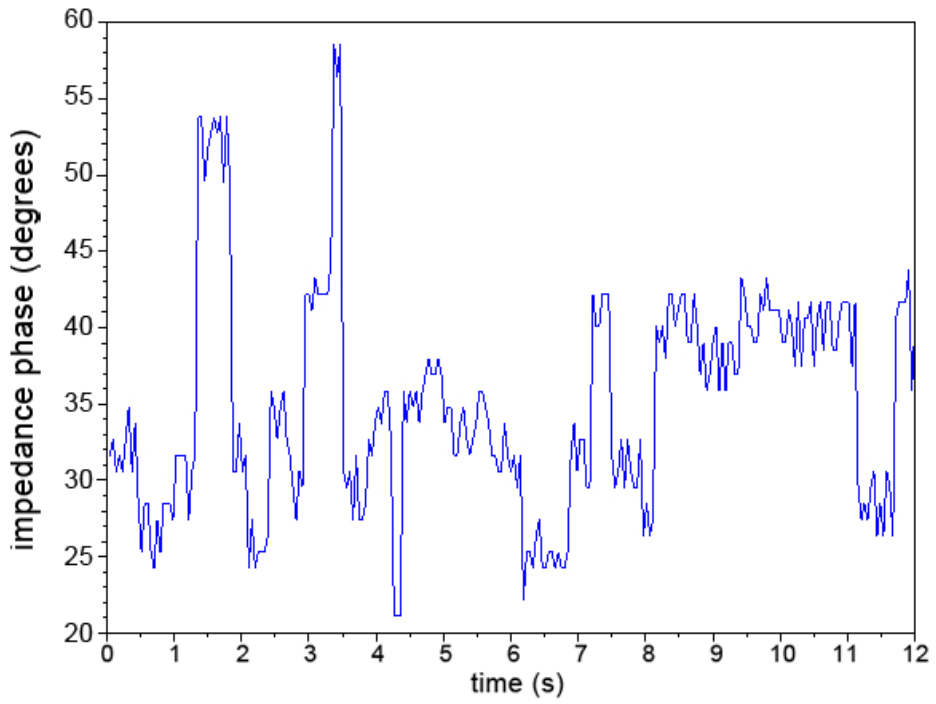


Figure A.4-3: Patient 6 impedance phase over time

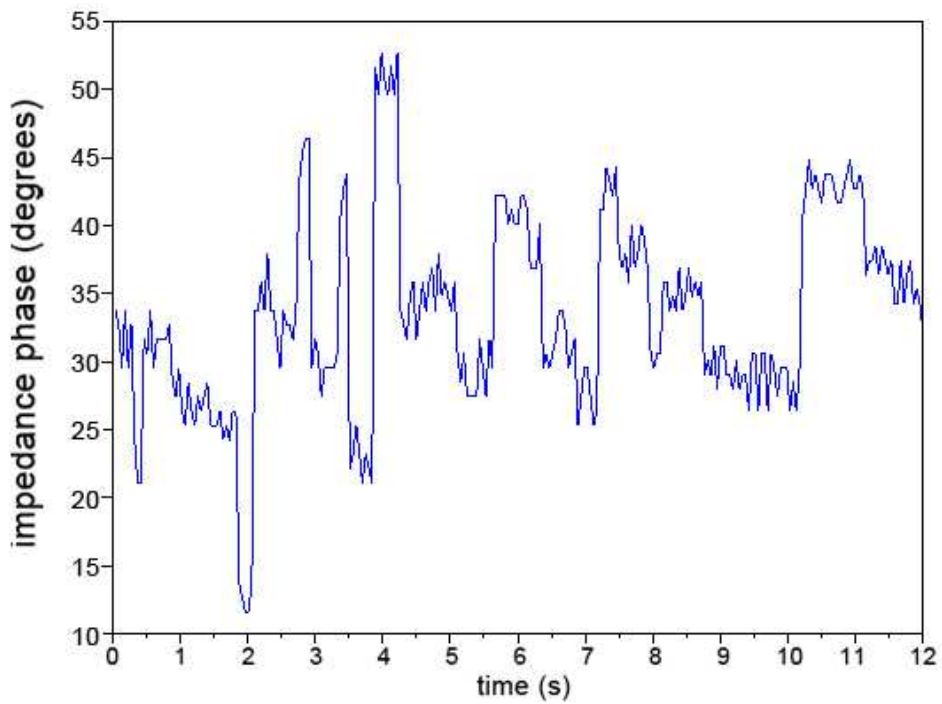


Figure A.4-4: Patient 7 impedance phase over time

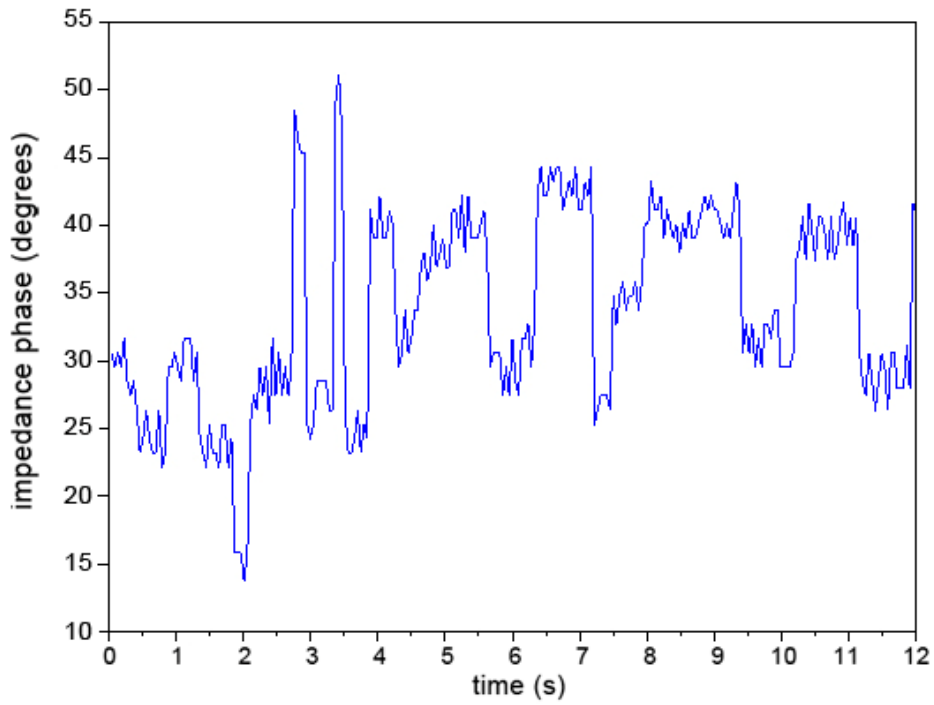


Figure A.4-5: Patient 8 impedance phase over time

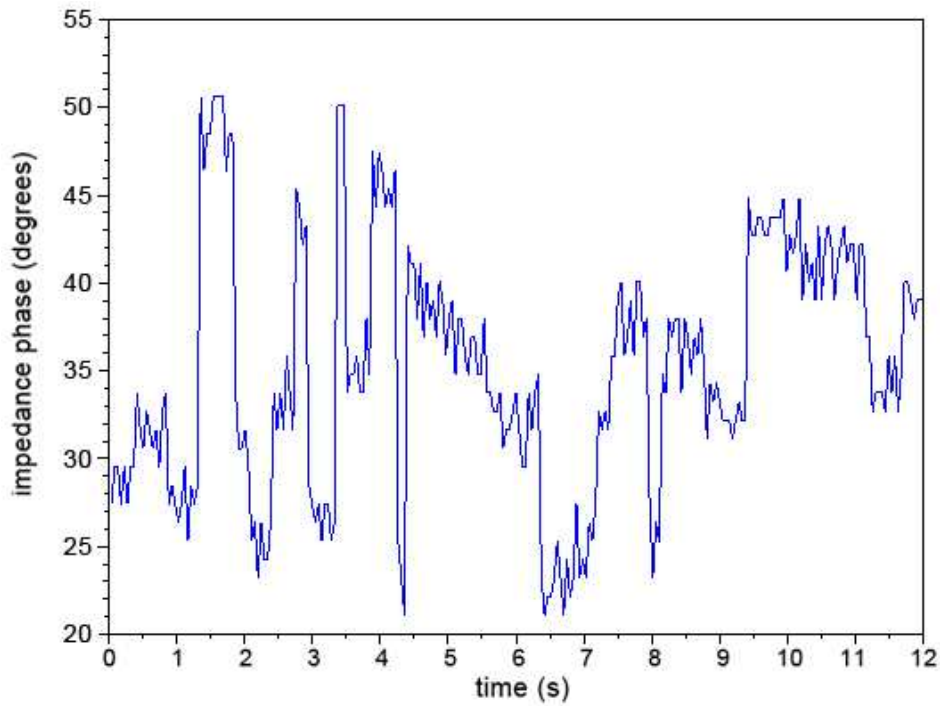


Figure A.4-6: Patient 9 impedance phase over time

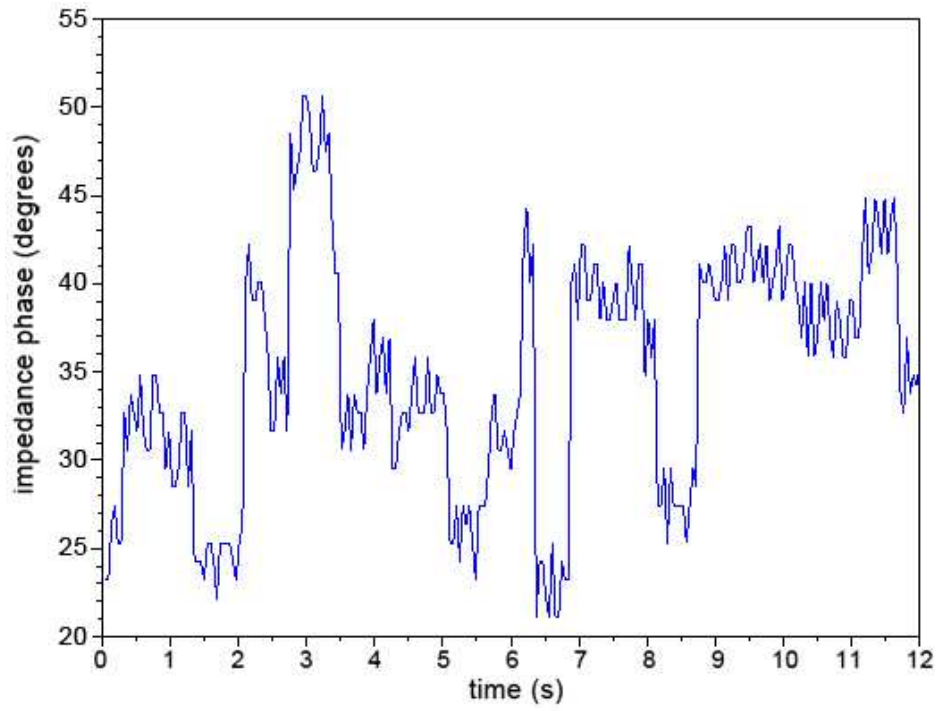


Figure A.4-7: Patient 10 impedance phase over time

Table A.4-1: Probability table of $|Z|_T > |Z|_H$

	Test 1	Test 2	Test 3	Test 4	Test 5	Test 6	Test 7
0,60	0,00	0,00	0,00	0,00	0,00	0,00	0,00
0,65	0,00	0,00	0,00	0,00	0,00	0,00	0,00
0,70	0,00	0,00	0,00	0,00	0,00	0,00	0,00
0,75	0,00	0,00	0,00	0,00	0,00	0,00	0,00
0,80	0,00	0,00	0,00	0,00	0,00	0,00	0,00
0,85	0,00	0,00	0,00	0,00	0,00	0,00	0,00
0,90	0,00	0,00	0,00	0,00	0,00	0,00	0,00
0,95	0,00	0,00	0,00	0,00	0,00	0,00	0,00
1,00	0,00	0,00	0,00	0,00	0,00	0,00	0,00
1,05	0,00	0,00	0,00	0,00	0,00	0,00	0,00
1,10	0,00	0,00	0,00	0,00	0,00	0,00	0,00
1,15	0,01	0,00	0,01	0,00	0,00	0,00	0,00
1,20	0,02	0,01	0,01	0,00	0,00	0,00	0,00
1,25	0,02	0,01	0,01	0,00	0,00	0,00	0,00
1,30	0,02	0,01	0,01	0,00	0,00	0,00	0,00
1,35	0,02	0,01	0,01	0,00	0,00	0,01	0,00
1,40	0,02	0,01	0,01	0,00	0,00	0,04	0,00
1,45	0,03	0,01	0,01	0,00	0,00	0,08	0,04
1,50	0,04	0,01	0,01	0,00	0,00	0,14	0,08
1,55	0,04	0,01	0,01	0,00	0,00	0,19	0,16
1,60	0,08	0,01	0,01	0,00	0,00	0,28	0,19
1,65	0,11	0,04	0,01	0,01	0,01	0,37	0,19
1,70	0,11	0,04	0,01	0,01	0,05	0,41	0,19
1,75	0,14	0,10	0,01	0,07	0,15	0,46	0,19
1,80	0,14	0,10	0,01	0,07	0,19	0,46	0,20
1,85	0,17	0,18	0,01	0,12	0,24	0,47	0,24
1,90	0,23	0,26	0,01	0,19	0,28	0,48	0,32

Table A.4-2: Probability table of $|Z|_T < |Z|_L$

	Test 1	Test 2	Test 3	Test 4	Test 5	Test 6	Test 7
0,60	0,97	0,71	0,84	0,89	1,00	1,00	1,00
0,65	0,78	0,18	0,00	0,50	0,16	0,67	1,00
0,70	0,78	0,18	0,00	0,50	0,16	0,33	1,00
0,75	0,31	0,04	0,00	0,04	0,00	0,29	0,34
0,80	0,22	0,04	0,00	0,04	0,00	0,29	0,28
0,85	0,22	0,04	0,00	0,04	0,00	0,21	0,15
0,90	0,22	0,04	0,00	0,04	0,00	0,00	0,07
0,95	0,16	0,04	0,00	0,04	0,00	0,00	0,00
1,00	0,16	0,04	0,00	0,04	0,00	0,00	0,00
1,05	0,13	0,04	0,00	0,04	0,00	0,00	0,00
1,10	0,13	0,04	0,00	0,04	0,00	0,00	0,00
1,15	0,09	0,04	0,00	0,00	0,00	0,00	0,00
1,20	0,00	0,00	0,00	0,00	0,00	0,00	0,00
1,25	0,00	0,00	0,00	0,00	0,00	0,00	0,00
1,30	0,00	0,00	0,00	0,00	0,00	0,00	0,00
1,35	0,00	0,00	0,00	0,00	0,00	0,00	0,00
1,40	0,00	0,00	0,00	0,00	0,00	0,00	0,00
1,45	0,00	0,00	0,00	0,00	0,00	0,00	0,00
1,50	0,00	0,00	0,00	0,00	0,00	0,00	0,00
1,55	0,00	0,00	0,00	0,00	0,00	0,00	0,00
1,60	0,00	0,00	0,00	0,00	0,00	0,00	0,00
1,65	0,00	0,00	0,00	0,00	0,00	0,00	0,00
1,70	0,00	0,00	0,00	0,00	0,00	0,00	0,00
1,75	0,00	0,00	0,00	0,00	0,00	0,00	0,00
1,80	0,00	0,00	0,00	0,00	0,00	0,00	0,00
1,85	0,00	0,00	0,00	0,00	0,00	0,00	0,00
1,90	0,00	0,00	0,00	0,00	0,00	0,00	0,00

Table A.4-3: Combined probability table, including average probability

	Test 1	Test 2	Test 3	Test 4	Test 5	Test 6	Test 7	Average
0,60	0,97	0,71	0,84	0,89	1,00	1,00	1,00	0,92
0,65	0,78	0,18	0,00	0,50	0,16	0,67	1,00	0,47
0,70	0,78	0,18	0,00	0,50	0,16	0,33	1,00	0,42
0,75	0,31	0,04	0,00	0,04	0,00	0,29	0,34	0,15
0,80	0,22	0,04	0,00	0,04	0,00	0,29	0,28	0,13
0,85	0,22	0,04	0,00	0,04	0,00	0,21	0,15	0,09
0,90	0,22	0,04	0,00	0,04	0,00	0,00	0,07	0,05
0,95	0,16	0,04	0,00	0,04	0,00	0,00	0,00	0,03
1,00	0,16	0,04	0,00	0,04	0,00	0,00	0,00	0,03
1,05	0,13	0,04	0,00	0,04	0,00	0,00	0,00	0,03
1,10	0,13	0,04	0,00	0,04	0,00	0,00	0,00	0,03
1,15	0,10	0,04	0,01	0,00	0,00	0,00	0,00	0,02
1,20	0,02	0,01	0,01	0,00	0,00	0,00	0,00	0,01
1,25	0,02	0,01	0,01	0,00	0,00	0,00	0,00	0,01
1,30	0,02	0,01	0,01	0,00	0,00	0,00	0,00	0,01
1,35	0,02	0,01	0,01	0,00	0,00	0,01	0,00	0,01
1,40	0,02	0,01	0,01	0,00	0,00	0,04	0,00	0,01
1,45	0,03	0,01	0,01	0,00	0,00	0,08	0,04	0,02
1,50	0,04	0,01	0,01	0,00	0,00	0,14	0,08	0,04
1,55	0,04	0,01	0,01	0,00	0,00	0,19	0,16	0,06
1,60	0,08	0,01	0,01	0,00	0,00	0,28	0,19	0,08
1,65	0,11	0,04	0,01	0,01	0,01	0,37	0,19	0,10
1,70	0,11	0,04	0,01	0,01	0,05	0,41	0,19	0,12
1,75	0,14	0,10	0,01	0,07	0,15	0,46	0,19	0,16
1,80	0,14	0,10	0,01	0,07	0,19	0,46	0,20	0,17
1,85	0,17	0,18	0,01	0,12	0,24	0,47	0,24	0,20
1,90	0,23	0,26	0,01	0,19	0,28	0,48	0,32	0,25

Appendix B: Extracts from protocol for animal testing

Background information

This study aims to discover the electrical impedance values of different tissue found in the body. This is done in order to design a device that can guide an arterial catheter into arteries, using the impedance of surrounding tissue. Research needs to be done in order to determine the average tissue impedance of the target tissue types, as well as the standard deviation in those tissue types. Determining what these averages and deviations are and programming it into the device, one will be able to categorize tissue types according to their impedance. With this available, the device being designed will be able to determine what the tissue surrounding it is by simply measuring its impedance. The target tissue types to study will be skeletal muscle, fat, skin, arterial wall and blood, for this experiment.

Scientific Aim(s) of the proposed study/teaching activity

The aim of the procedure is to determine the expected impedance values of different kinds of tissue found in the subject of the procedure. Multiple values must be taken to determine the variance in these values and different tissues, such as arterial wall tissue, muscle tissue, fat and blood must be used to determine if there is a discernable difference in the electrical impedance of the different types of tissue. The procedure has been done on dead tissue, but not yet on living tissue and the potential difference needs to be examined.

Potential benefits of the research findings/teaching activity

Proving that there is a discernable difference in the electrical impedance of different tissue in the body will allow the development of the abovementioned guided arterial catheter device that could be guided through the electrical impedance of adjacent tissue, which would make the placement of arterial catheters easier and less traumatic.

Hypothesis/ Research Question

The hypothesis, formed by experiments on dead tissue, is that there is a difference noted between fat, muscle and arterial wall tissue, especially at certain electrical frequencies. Furthermore, it is believed that the values found in the dead tissue experiments would be marginally higher than those to be found in this procedure. This belief is based on the fact that dead tissue has different physical properties to living tissue, especially cold dead tissue as temperature plays a large role in resistivity and impedance of conductors (including tissue). Additionally, the moisture content and ion concentration of the tissue will differ depending on it being alive or dead. In short, the physical properties (and therefore, electrical properties) of tissue cannot be assumed to be the same for living and dead tissue, thus it is critical for testing to be done on living tissue as well to get a more accurate model of the impedance values of different tissue types.

Justification for the use of sentient animals

Pigs were chosen as they have similar tissue properties to humans and the electrical impedance is to be expected to be close to that found in human tissue. Pig tissue is commonly used as donor tissue with certain operations on humans (xenotransplantation). Additionally, pigs are anatomically similar to humans.

Testing cannot be done on smaller specimen, because the experimental probe needs to be applied to a specimen with tissue sizes that are roughly the same as those of humans.

Refinement

The computing and programming used to measure the impedance values have been refined in order to take measurements at a very fast pace (200 measurements per hour), allowing the procedure to be over quickly. Using a standard oscilloscope without the programming made for this experiment, it would take roughly an hour to generate and process 15 measurements (whereas the refined process automatically does the processing of the data). Additionally, the power source used to induce the electrical impedance is set low enough to produce a weak current that cannot be felt by the animals. Even though the animals are under anaesthetics, the low current will not induce any trauma to the tissue that will be taken measurements of. Finally, only a small incision is required, deep enough to expose the femoral artery.

Experimental procedure(s)

- Animals will be placed under anaesthesia. Anaesthesia will consist of ketamine 2-5 mg/kg given intravenously, thiopentone 2-4 mg/kg intravenously and the trachea will be intubated. The animals will be ventilated with air and oxygen. Anaesthesia will be maintained with halothane administered via the circle breathing circuit. Normal saline will be infused at a rate of 5 ml/kg per hour.
- An incision will be made into the thigh, to expose the femoral artery.
- During this time, the experimental setup will be readied. The Signal Generator will produce a sinusoidal signal with a peak amplitude of 4V at a frequency between 20kHz and 100kHz. The circuit contains a 1k Ω resistor, which will limit the maximum current to 4mA.
- The modified arterial catheter, which is connected to the laptop, will be placed roughly 1-3mm into the tissue to be tested.
- A button will then be pressed on the laptop and a measurement will be taken and recorded (which takes less than a second) and the modified catheter will be removed.
- The last two steps are repeated until a sufficient amount of data per tissue type has been collected. 50 measurements per tissue type is the target and will take no longer than 10 minutes per 50 measurements (with previous tests on dead tissue showing an average of 200 measurements per hour). This is then repeated for different tissue types. 50 measurements was chosen as part of the pilot study, to determine how many samples will be required and how many measurements per sample are required to reach the desired accuracy.
- To measure blood tissue, the catheter will be inserted into the femoral artery and held there while the measurements are taken. The exposed femoral artery is required because measurements of the artery wall are required and because the modified catheter will need to pierce the artery wall to be placed inside the flowing blood.
- Once all measurements are taken, all tools are removed and the procedure will then repeat for the next animal.

Animal caging, care and monitoring

Animals will be collected the day prior to surgery.

The animals will be caged at the Central Animal Research unit at the Faculty of Health Sciences, according to their standard procedures. Regarding the use of

pigs, standard pens will be used at Tygerberg Campus. If any further details are required, Mr Noël Markgraaff will gladly assist where possible.

Department of Physiological Sciences

Private Bag X1, MATIELAND

7602, South Africa

Telephone: +27 21 8083146

Fax: +27 21-8083145

Mr. Noël Markgraaff

(Animalhouse Manager)

Room 2018

Tel.: +27 21 808-3631

e-Mail: N Markgraaff (nrm@sun.ac.za)

Personnel will be of abovementioned authority. There will be one animal per instance, and only overnight detention is necessary.

Humane endpoints

After completion of the experiments, the animals will be euthanized with 20 mmol KCl given intravenously while the animal is still anesthetized. The KCl will stop the heart. This will be monitored by Prof A Coetzee.

Appendix C: Extracts from protocol for clinical testing

Clinical Trials HREC 1 & 2 Protocol

The impedance guided intra-arterial catheter is a newly designed concept, developed to aid the placement of arterial catheters by means of judging the position of the tip of the arterial catheter with the use of the electrical impedance of the surrounding tissue in the human. It is intended to make the placement of arterial catheters easier in conditions when it is difficult to locate the artery of the patient by touch or sight.

It achieves this with the inclusion of a biologically inert electrode along the length of the cannula of the arterial catheter, the addition of a grounding conductor to the needle of the arterial catheter, turning the needle into another electrode and the application of an AC voltage over the two electrodes, introducing a voltage difference at the proximal end of the arterial catheter. Utilizing this AC voltage, one can determine the impedance (the opposition of a system to the presence of an alternating current, or the AC version of electronic resistivity) of the tissue encountered by the proximal end of the arterial catheter. The hypothesis is that different types of human tissue have different impedances and that the impedance guided intra-arterial catheter could thus detect which tissue it is surrounded by, solely on the impedance it detects. If this poses to be true, the practitioner administering the arterial catheter would be able to determine where the arterial catheter is within the patient's body with given feedback from the device.

The motivation for this device is to ease the process of administration of arterial catheters in cases when locating the patient's artery is made difficult due to a variety of conditions. In current medical practice, there are cases where the medical practitioner cannot locate the target artery for the administration of an arterial catheter and this often leads to misplacement of the arterial line, causing trauma for the patient. An arterial catheter which is guided in real time by the impedance of human tissue will aid greatly in locating the artery sought in the procedure.

The justification for these clinical trials is that there has not been any other research surrounding the impedance values of living human tissue. The concept of an impedance guided arterial catheter is a novel one and, thus, the applicable available research surrounding the concept is scarce and inadequate. Therefore, it is necessary to perform experiments to determine the estimate values of different human tissue expected to be encountered by the impedance guided arterial catheter.

Animal testing has been done to determine whether or not the device and the concept work and to discover if the hypothesis of varying impedances for different tissue types was correct. Results from the animal testing were positive, with blood having an impedance magnitude ranging from 0,3 k Ω – 0,7 k Ω , muscle ranging from 0,6 k Ω – 2,8 k Ω and pig fat ranging from 1,5 k Ω – 27 k Ω . Impedance phase found in the tests on animals were scattered and not discernible. During the protocol, no noticeable health implications were detected on the test subjects and the measured impedance levels were different for different tissue types, proving that in living pigs there is a discernible difference in the impedance of different tissue types and that one could use the measured impedance to estimate where the arterial catheter is. With the values mentioned

above, it can be seen that a clear difference was found in the animal testing and that one could distinguish the different tissue types based on the impedance measured. This trend is expected to be present in human tissue as well, due to the similarities between human and pig tissue (an attribute that has allowed for xenotransplantation of pig organs into humans) and, because of this assumption, the research is expected to be feasible and successful.

The objectives for the clinical trials are to record the impedance values of human fat, muscle, skin and blood tissue, from a wide variety of human subjects and to determine if there is a constant discernible difference between the tested tissue types, which will determine if the impedance guided intra-arterial catheter is a viable design or not.

Clinical tests need to be done on humans in order to determine what the impedance levels are for different tissue types in humans and to find whether or not there is still a discernible difference in humans. Furthermore, the tissue impedance variation between human subjects also needs to be recorded, to discover whether or not one can accurately set up a fuzzy logic system for the impedance of human tissue for all humans or whether adjustments to this system need to be made, based on the individual subject's characteristics (such as age, race, gender and weight). Tissue impedances on human subjects thus need to be recorded and stored, to be analysed and processed at a later stage and that information will then be used to create a foundation for the statistical analysis of the expected impedance brackets for tissue types. The main tissue types that need to be tested for are blood, skeletal muscle, arterial wall and fat tissue, as these are the commonly expected tissue types.

The experimental procedure will involve a setup, comprising of a modified arterial catheter, which has a biologically inert material (such as gold or silver), in the shape of a thread, embedded into the cannula of the arterial catheter, with the proximal tip exposed over 0,5 mm will act as an electrode, which will be exposed to the tissue of the subject. The needle of the arterial catheter and the above mentioned electrode will both be connected to an electronic device, which will produce a 0 V-5 V sinusoidal wave at a frequency of 30 kHz, with a reference resistor of 1,2 k Ω . The setup is powered by an internal 18 V battery pack. The electronic device also contains a micro processing unit which will analyse the incoming signal and interpret the data, give feedback to the user and store the data gathered for analysing after the procedure. The setup will produce an absolute maximum current of 4,16 mA (assuming 0 impedance from the tested tissue), but a more realistic maximum would be estimated at 3,33 mA (assuming a 0,3 k Ω impedance found in blood, where the value mentioned is the lowest found impedance in the animal testing session). The maximum current expected in the patient's muscles is estimated at 2,27 mA (assuming a 1 k Ω impedance found in muscle, where the value mentioned is the lowest found muscle impedance in the animal testing). The setup includes several voltage regulators, which will not allow the voltage to go over the maximum voltage used to calculate the maximum current. With a fixed minimum resistance (due to the inclusion of a reference resistor) and the voltage regulators keeping the maximum voltage in check, the maximum current is thus also regulated, due to Ohm's Law ($V=IR$). If the voltage regulators were to fail, it would break the circuit, halting the current leading to the patient.

Before the procedure, the catheter will be modified as explained above. Once it is done, it will be gas sterilized as done in practice by the department of health sciences. It will thus be on the same level of sterilization as tools used daily in theatres.

The placement of these catheters is not done for the sake of the project. The clinical circumstances and the medical practitioner in charge decide who requires the placement of an arterial catheter and if the patient gives consent, the catheter will be replaced with the modified arterial catheter described in this protocol. Participants will be given the informed consent forms prior to the procedure and the procedure will then take place, with or without the modified arterial catheter, depending on their choice to participate in the testing or not. Professor André Coetzee, from the Department of Anaesthetics and Critical Care, or one of his colleagues will supervise all of the experimental procedures and be in charge of the placement of the arterial lines. Thus, a doctor will always be present during the experiments.

For the procedure, a medical practitioner will take the device, with the modified arterial catheter and apply it to a patient already requiring an arterial catheter. Before the procedure, the modified arterial catheter will be chemically sterilized as to avoid infection after the procedure. As the modified arterial catheter is to be inserted, the electronics will be switched on and the arterial catheter will then be introduced to the patient's body. Measurements will be taken in real time as the arterial catheter passes through the patient's tissue, until it is located within the bloodstream. Once it has been located, the electronics will be switched off and disconnected from the modified arterial catheter. The needle will then be removed and the cannula will remain inside the patient, as with the procedure when normal arterial catheters are applied. The electronics will be moved away after having been disconnected and the data will be analysed after the procedure. After the procedure, the used modified arterial catheter will be disposed of, while the electronics will be cleaned on the outside and reused for the next test.

The arterial lines in these experiments will only be placed in peripheral arteries and thus radiographic visualizations are not required and will not be used.

The exclusion criteria encompasses declination of consent or patients with any of the following conditions: congenital heart disease, cardiomyopathy, cardiac ischaemia/infarct/unstable angina, Torsade de pointes, hyperkalaemia, electric shock, patients on anti-dysrhythmic.

A sample size of 100 participants was chosen. Sample size was chosen at 100 to form a wide basis for statistical analysis, while still adhering to financial constraints. Because no previous studies in human tissue impedance have been done, there is no statistical background on which to base the sample size. Thus, a sample size of 100 has been chosen for the pilot study and if it proves to be insufficient, further studies will be conducted.

Ethical considerations have been taken with the risks involved in the procedure, which are the risk of infection from the apparatus and the risk of the application of the electrical current to the patient. The risk of infection is countered by the sterilization of the arterial catheter before the procedure, as mentioned above. High electrical currents are harmful to human tissue and could, in the worst of cases, cause ventricular fibrillation. The myocardium is most sensitive to electrical frequencies between 30-100 Hz and at that frequency, currents over 100 mA can trigger ventricular fibrillation. Currents between 10mA and 20mA can cause muscle spasms, currents over 5 mA are received as painful and currents over 1 mA can be felt (*Zitzewitz, Paul W., Neff, Robert F. Merrill Physics, Principles and Problems. New York: Glencoe McGraw-Hill, 1995*). For this reason, the absolute maximum current is kept below 5mA. Additionally, the needle of the modified arterial catheter is grounded, to draw all current towards it and thus not allowing the current to move through adjacent tissue and vital organs through the bloodstream.

The eventual benefits of the success of this protocol include the data required for the statistical analysis of the impedance in human tissue. If that data is favourable, it could allow for the classification of tissue types at a fixed frequency by measurement of its impedance. This, in turn, will lead to the proof of concept of the impedance guided intra-arterial catheter and will allow for future development of the concept.